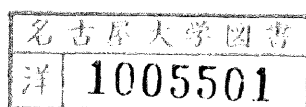


**Studies on the Formation and Structure of Lignin  
in Tree Xylem by Microautoradiography**



**Kazuhiko Fukushima**

**Faculty of Agriculture  
Nagoya University**

**1990**

**Studies on the Formation and Structure of Lignin in Tree  
Xylem by Microautoradiography**

**Contents**

	page
<b>1. Introduction</b>	1
<b>2. Materials and Methods</b>	6
2.1. Plant materials	6
2.2. Syntheses of radio-labeled precursors of lignin	6
2.3. Administration of labeled precursors	14
2.4. Radioassay	16
2.5. Quantitative analysis of oxidation products	17
2.6. Microautoradiography	17
<b>3. Formation and Structure of Lignin in Gymnosperms</b>	19
3.1. Pine	19
3.2. Pine compression wood	35
3.3. Gingko	47
<b>4. Formation and Structure of Lignin in Angiosperms</b>	63
4.1. Magnolia	63
4.2. Lilac	77
4.3. Beech	80
4.4. Poplar	82
<b>5. Summary</b>	88
<b>References</b>	90
<b>Acknowledgment</b>	93

## CHAPTER 1

### Introduction

Many approaches have been employed to elucidate the structure of wood lignin. Most studies dealt with isolated lignins and utilized a number of different physical and chemical degradative methods. These methods provided important basic information on the structure of isolated lignin. However, these have afforded only limited information on the topochemical nature of lignin. So the structure of protolignin in the cell wall is still an open question. Lignin is heterogeneous with respect to its macromolecular structure, morphological location and association with carbohydrates in its native state. This information is lost during its isolation from the cell wall. It is impossible to obtain a lignin sample which can be unambiguously considered to represent whole protolignin. In addition, it is impossible to depolymerize lignin quantitatively into monomeric or oligomeric building units by any known degradative methods. Therefore, it is very difficult to investigate the macromolecular structure of protolignin in the cell wall.

More detailed information about the macromolecular structure of protolignin can only be obtained by suitable non-degradative analyses, such as ultraviolet (UV) microscopic photometry<sup>1-3</sup>), bromination-SEM<sup>4</sup>) and TEM-EDXA<sup>5</sup>), solid state NMR<sup>6-8</sup>), Raman spectroscopy<sup>9,10</sup>) and radiotracer methods<sup>11-17</sup>). Many researchers have attempted to overcome the difficulties encountered in investigation of structure of protolignin in the cell wall by employing these methods.

Gymnosperm lignin is believed to consist of almost guaiacylpropane units. However, there are significant differences in reactivity and physical properties of protolignins found in the compound middle lamella and the secondary wall. According to the chemical characterization of tissue

fractions corresponding to compound middle lamella and secondary wall of black spruce tracheids by Whiting and Goring<sup>18)</sup>, the secondary wall lignin contains 1.7 times as much methoxyl per C<sub>9</sub> as the compound middle lamella lignin, indicating a substantial proportion of *p*-hydroxyphenylpropane moieties in the compound middle lamella. On the other hand, the compound middle lamella fraction of spruce normal wood gave only a small amount of *p*-hydroxybenzaldehyde by alkaline nitrobenzene oxidation<sup>19)</sup>. Interestingly, most compression wood in gymnosperms gave considerable amount of *p*-hydroxybenzaldehyde by the oxidation. However, *p*-hydroxyphenylpropane units in lignin can not be estimated quantitatively by degradative methods<sup>20,21)</sup>. Therefore, it is expected that *p*-hydroxyphenylpropane units exist also in normal wood. It is very important to know the localization of this units in cell wall and to elucidate the difference in localization of this units between the normal wood and the compression wood.

Hardwood lignins are considered to consist mainly of syringylpropane units and guaiacylpropane units, and the ratios of syringyl- to guaiacylpropane units vary in different morphological regions of white birch (Betula papyrifera Marsh.). This was shown by UV-microscopy<sup>1-3)</sup> and by bromination-TEM-EDXA<sup>5)</sup>, and by chemical characterization of various tissue fractions<sup>22-24)</sup>. However, most papers dealing with hardwood lignin do not pay much attention to *p*-hydroxyphenylpropane units in the lignin. This is because most hardwood lignin give a small amount of compounds derived from *p*-hydroxyphenylpropane units by oxidative degradation. However, this does not provide conclusive proof that *p*-hydroxyphenylpropane unit is not one of the important building stones of hardwood lignin as in the case of gymnosperm wood lignin.

Among various non-degradative methods for analysis of lignin, the radiotracer method has been shown to be a promising approach to understanding of structure of protolignin in the cell wall<sup>21)</sup>. Radio-labeled precursors of lignin biosynthesis can be prepared by replacement of either

a specific hydrogen or carbon of the precursor with  $^3\text{H}$  or  $^{14}\text{C}$  respectively. If it is possible to label selectively the specific structural units of lignin with radioisotope, their exact location in plant cell wall will be detected by microautoradiography. The process of deposition of lignin in the cell wall can be visualized by taking a microautoradiograph of a cross section of the newly formed xylem. The newly formed xylem contains cell walls of every stage of differentiation, and the incorporation of activity into the specific morphological region indicates the deposition of lignin. Therefore, it is possible to deduce the architecture of protolignin in the cell wall from the integral of the incorporated activity from cambium to matured region determined by image analysis of the microautoradiogram. Thus, a combination of selective labeling of lignin structural unit and visualization of their distribution in differentiating cell wall by high resolution microautoradiography provides a useful method for investigation of formation process of macromolecular protolignin.

Among several methods of selective labeling tested, feeding the labeled ferulic acid or sinapic acid in the dark to a sprout of eucalyptus<sup>16)</sup> or to a poplar shoot<sup>17)</sup> was found to be promising. Localization of syringyl and guaiacyl lignin selectively labeled by this method in newly formed poplar xylem was visualized by microautoradiography<sup>17)</sup>. However, the selectivity of labeling by feeding these acids in the dark was not satisfactory, because interconversions between guaiacyl and syringyl units involved in the course of lignin biosynthesis are suppressed incompletely<sup>17)</sup>. Besides these cinnamic acids, monolignol glucosides are considered to be more efficient lignin precursors. This is because:

- i) Monolignol glucosides (*p*-glucocoumaryl alcohol, coniferin and syringin) occur naturally in the cambial sap of gymnosperms and angiosperms<sup>25,26)</sup>;
- ii) Cinnamyl alcohol-glucosyl transferases<sup>27)</sup> and  $\beta$ -glucosidases<sup>28)</sup> are widely distributed in the plant kingdom even though in the species in which these glucosides were not yet detected in the lignifying tissues;

iii) These glucosides are suitable for feeding the differentiating xylem because of their considerable solubility in water.

In this work, three kinds of radioactive monolignol glucosides, *p*-glucocoumaryl alcohol, coniferin and syringin, were used as the precursors of *p*-hydroxyphenyl, guaiacyl and syringyl lignin respectively.

It has been shown that the three kinds of lignin building stones distribute heterogeneously in the cell wall, and the degree of condensation in guaiacyl- or *p*-hydroxyphenyl lignin differs with respect to their location in the cell wall. The amounts of condensed units in lignin were estimated by several methods. But the values varied with investigating methods. This is perhaps due to the fact that most studies have dealt with the isolated lignin samples which represent only a part of lignin in wood.

Terashima et al.<sup>13)</sup> showed by radio-tracer method that the amount of condensed structures in the lignin formed at an early stage of cell wall differentiation was larger than that in the lignin formed at a late stage. In this study, ferulic acid labeled with <sup>3</sup>H at position C-5 of aromatic ring was used as a lignin precursor and the amount of removed <sup>3</sup>H during the formation of condensed structure at this position was determined. Tomimura et al.<sup>15)</sup> showed that the removal of <sup>3</sup>H at position 2 or 6 of guaiacyl nucleus was less than 2 and 4% respectively indicating the very low degree of condensation at these positions.

It is possible to visualize the heterogeneous distribution of the condensed structures and non-condensed structures by employing suitable precursors labeled at a specific position of aromatic ring and by visualizing their removal by microautoradiography. In this work, coniferin-[arom. ring-5-<sup>3</sup>H] and *p*-glucocoumaryl alcohol-[arom. ring-3-<sup>3</sup>H] were administered to the differentiating xylem of various trees and the localization of incorporated radioactivities in the cell

wall were compared with those administered with coniferin-[arom. ring-2-<sup>3</sup>H] or p-glucocoumaryl alcohol-[arom. ring-2-<sup>3</sup>H].

Hemicellulose is considered to play an important role in lignification of cell wall. Lignin carbohydrate complex (LCC) has been isolated from ball milled wood by Björkman<sup>29)</sup>, and several kinds of lignin-carbohydrate bonds have been proposed by chemical analysis of the low molecular LCC fraction<sup>30)</sup>. In addition, it was shown that the degree of condensation of lignin varies with the kind of carbohydrate<sup>31)</sup> in which gel the polymerization of lignols proceeds. These suggest that hemicellulose may affect the heterogeneity in formation of lignin. In this work, the process of deposition of hemicellulose was also visualized by microautoradiography and was compared with the process of deposition of lignin.

In this thesis, the macromolecular structure of protolignin in the tree cell wall was discussed based on its formation in differentiating xylem. The main approach is the combination of selective radio-labeling of specific structural moiety of protolignin and visualization of their distribution in differentiating cell wall by microautoradiography.

## CHAPTER 2

### Materials and Methods

#### 2.1. Plant Materials

Two year old shoots were obtained in late June or early July from Pinus thunbergii Parl., Ginkgo biloba L., Magnolia kobus DC., Syringa vulgaris L. and Populus Maximowiczii X Populus berolinensis grown on the campus of Nagoya University and from Fagus crenata Blume grown on the experimental forest of Nagoya University. These shoots were grown vertically. Two year old shoots containing compression wood was also obtained from the same tree of Pinus thunbergii Parl. and Ginkgo biloba L..

#### 2.2. Syntheses of radio-labeled precursors of lignin

p-Coumaric acid-[arom. ring-2-<sup>3</sup>H] (H-a, Fig. 1.) was synthesized from p-hydroxybenzaldehyde-[arom. ring-2-<sup>3</sup>H] and malonic acid. p-Hydroxybenzaldehyde-[arom. ring-2-<sup>3</sup>H] was synthesized as follows (Fig. 2.): 2-bromo-4-hydroxybenzaldehyde (670mg) synthesized<sup>32,33)</sup> from m-bromoaniline (Tokyo Kasei Kogyo Co., Ltd. Tokyo) was dissolved in absolute methanol (0.8ml); dimethyl sulfite (0.4 ml) and a drop of methanol saturated with hydrogen chloride were added and the solution was refluxed for 90 min; after cooling, the solution was neutralized with sodium methoxide in methanol and evaporated to dryness; the residue was extracted with petroleum ether and recrystallization from petroleum ether gave 2-bromo-4-hydroxybenzaldehyde dimethyl acetal (620mg) ; to a stirred cold solution of 2-bromo-4-hydroxybenzaldehyde dimethyl acetal (500mg) in dry ether (12ml) was slowly added a solution of butyllithium in n-hexane (15%, 2.2ml) at -50 °C under nitrogen; the reaction mixture was maintained at -20 °C for 1 hr, and tritium water (0.22ml, about 3.7x10<sup>9</sup>Bq, New England Nuclear, Mass., U.S.A.) was added and warmed for 1 hr

under reflux; then water (10ml) was added and acidified to pH 2 with dilute hydrochloric acid; the whole mixture was extracted with ether. After the evaporation of ether, the residue was dissolved in a small amount of methanol, and hydrochloric acid was added to a turbid point and heated for 5 min at 50°C. The cooled mixture was extracted with ether. The ether solution was evaporated and the residue was purified by silica gel column chromatography employing a mixture of n-hexane: ethyl acetate (4:1 v/v) as a developer to give 135mg (about  $2.0 \times 10^8$  Bq) of *p*-hydroxybenzaldehyde-[arom. ring-2- $^3$ H].

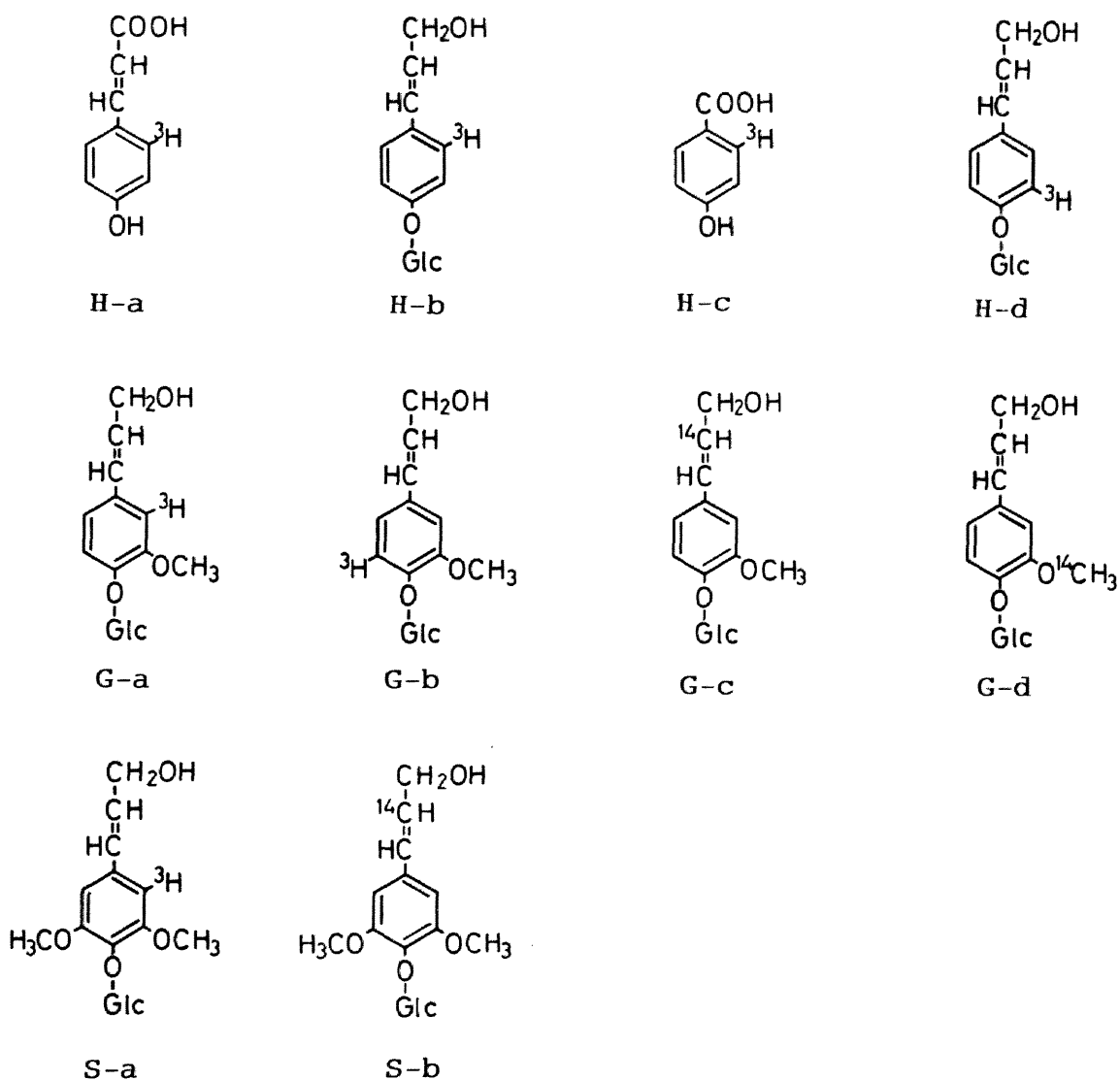


Fig. 1. Labeled precursors synthesized for this study.

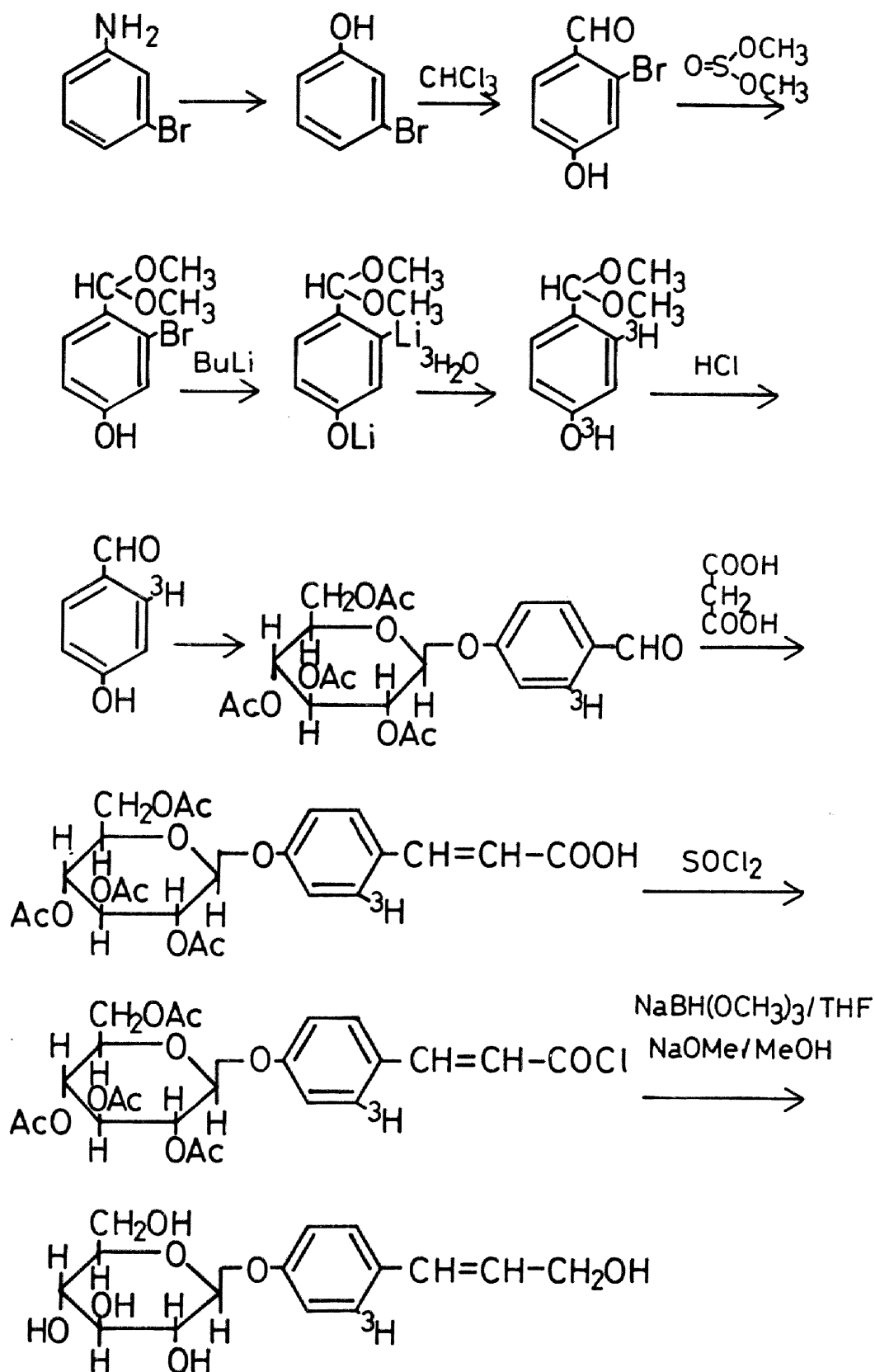


Fig. 2. Synthesis of p-glucocoumaryl alcohol-[arom. ring-2-<sup>3</sup>H]

Then the tritiated aldehyde (24mg) and malonic acid (22mg) were condensed in anhydrous pyridine (0.2ml) and piperidine (1 drop) at 80°C for 4 hours to give *p*-coumaric acid-[arom. ring-2-<sup>3</sup>H] (34mg, about 3.3x10<sup>7</sup>Bq).

*p*-Glucocoumaryl alcohol-[arom. ring-2-<sup>3</sup>H] (H-b, Fig. 1.) was synthesized from *p*-hydroxybenzaldehyde-[arom. ring-2-<sup>3</sup>H] (Fig. 2). According to the method described by Kratzl and Billek<sup>34</sup>), the *p*-hydroxybenzaldehyde (50mg) was converted to tetra-O-acetyl-β-D-glucoside (118mg), which was condensed with malonic acid (30mg) to give tetra-O-acetyl-glucocoumaric acid (110mg). The acid chloride obtained by treating the acid (110mg) with thionyl chloride was reduced by sodium trimethoxyborohydride to give the corresponding alcohol<sup>35</sup>). Deacetylation with sodium methoxide gave crude *p*-glucocoumaryl alcohol labeled with <sup>3</sup>H at position 2 of the aromatic ring. This was purified by silica gel column chromatography employing a mixture of acetone : ethyl acetate : water (10:10:1 v/v/v) as a developer to give 31mg (1.4x10<sup>7</sup> Bq) of *p*-glucocoumaryl alcohol-[arom. ring-2-<sup>3</sup>H].

*p*-Hydroxybenzoic acid-[arom. ring-2-<sup>3</sup>H] (H-c, Fig. 1.) was synthesized from *p*-hydroxybenzaldehyde-[arom. ring-2-<sup>3</sup>H] according to the method described by Pearl<sup>36</sup>). The aldehyde (10mg) was dissolved in aqueous sodium hydroxide (10% w/w, 0.18ml) and silver oxide (10mg) was added and stirred for 10 min (60 °C). After cooling, sulfur dioxide gas was bubbled into the mixture (2 min.). Then the mixture was acidified with dil. HCl to pH 2. The mixture was extracted with ether (1mlx3) and evaporation of ether gave *p*-hydroxybenzoic acid-[arom. ring-2-<sup>3</sup>H] (12mg, 8.9x10<sup>6</sup>Bq).

*p*-Glucocoumaryl alcohol-[arom. ring-3-<sup>3</sup>H] (H-d, Fig. 1.) was synthesized from *p*-hydroxybenzaldehyde-[arom. ring-3-<sup>3</sup>H] by the same method as that for *p*-glucocoumaryl alcohol-[arom. ring-2-<sup>3</sup>H]. *p*-Hydroxybenzaldehyde-[arom. ring-3-<sup>3</sup>H] was synthesized as follows: 3-iodo-4-hydroxybenzaldehyde (1.8g) was dissolved in absolute methanol (2ml); dimethyl sulfite (1ml)

and two drops of methanol saturated with hydrogen chloride were added and the solution was refluxed for 90 min; after cooling, the solution was neutralized with sodium methoxide in methanol and evaporated to dryness; the residue was extracted with petroleum ether and evaporation of the petroleum ether gave 3-iodo-4-hydroxybenzaldehyde dimethyl acetal as an oil (1.5g); to a stirred cold solution of 3-iodo-4-hydroxybenzaldehyde dimethyl acetal (560mg) in ether (10ml) was slowly added a solution of butyllithium in n-hexane (15%, 4.4ml) at  $-50^{\circ}\text{C}$  under nitrogen; the reaction mixture was maintained at room temperature for 1 hr, and after cooling ( $-20^{\circ}\text{C}$ ), tritium water (0.2ml,  $7.4 \times 10^9 \text{Bq}$ , New England Nuclear, Mass., U.S.A.) was added and warmed for 1 hr under reflux; then water (10ml) was added and acidified to pH 2 with dilute hydrochloric acid; the whole mixture was extracted with ether. After the evaporation of ether, the residue was dissolved in a small amount of methanol and hydrochloric acid was added to a turbid point and heated for 5 min at  $60^{\circ}\text{C}$ . The cooled mixture was extracted with ether. The ether solution was evaporated and the residue was purified by silica gel column chromatography employing a mixture of benzene : chloroform (5:1 v/v) as a developer to give 120mg (about  $2.6 \times 10^8 \text{Bq}$ ) of p-hydroxybenzaldehyde-[arom. ring-3- $^3\text{H}$ ].

**Coniferin-[arom. ring-2- $^3\text{H}$ ] (G-a, Fig. 1.)** was synthesized from vanillin-[arom. ring-2- $^3\text{H}$ ]<sup>11)</sup>. According to the method described by Kratzl and Billek<sup>34)</sup>, the vanillin (107mg) was converted to tetra-O-acetyl- $\beta$ -D-glucoside (216mg), which was condensed with malonic acid (63mg) to give tetra-O-acetyl glucoferulic acid (250mg). The acid chloride obtained by treating the acid (250mg) with thionyl chloride was reduced by sodium trimethoxyborohydride to give the corresponding alcohol<sup>35)</sup>. Deacetylation with sodium methoxide gave crude coniferin labeled with  $^3\text{H}$  at position 2 of the aromatic ring. This was purified by silica gel column chromatography employing a mixture of acetone : ethyl acetate : water (10:10:1 v/v/v) as a developer to give 84.5 mg ( $2.7 \times 10^7 \text{Bq}$ ) of coniferin-[arom. ring-2- $^3\text{H}$ ]. This label has

been shown to be fairly stable during dehydropolymerization in differentiating xylem except that about 2% was lost due to formation of bond at this position<sup>14)</sup>.

**Coniferin-[arom. ring-5-<sup>3</sup>H]** (G-b, Fig. 1.) was synthesized from vanillin-[arom. ring-5-<sup>3</sup>H]<sup>13)</sup>. According to the method described by Kratzl and Billek<sup>34)</sup>, the vanillin (107mg) was converted to tetra-O-acetyl- $\beta$ -D-glucoside (239mg), which was condensed with malonic acid (58mg) to give tetra-O-acetyl glucoferulic acid (240mg). The acid chloride obtained by treating the acid (240mg) with thionyl chloride was reduced by sodium trimethoxyborohydride to give the corresponding alcohol<sup>35)</sup>. Deacetylation with sodium methoxide gave crude coniferin labeled with <sup>3</sup>H at position 5 of the aromatic ring. This was purified by silica gel column chromatography employing a mixture of acetone : ethyl acetate : water (10:10:1 v/v/v) as a developer to give 93mg (5.8x10<sup>7</sup>Bq) of coniferin-[arom. ring-5-<sup>3</sup>H].

**Coniferin-[ $\beta$ -<sup>14</sup>C]** (G-c, Fig. 1.) was synthesized from tetra-O-acetyl-glucovanillin and malonic acid-[2-<sup>14</sup>C] (Fig. 3). According to the method described by Kratzl and Billek<sup>34)</sup>, the glucoside (400mg) and malonic acid-[2-<sup>14</sup>C] (90mg, corresponding to 9.3x10<sup>6</sup>Bq, New England Nuclear, Mass., U.S.A.) were condensed in anhydrous pyridine (0.4ml) and piperidine (1 drop) at 100°C for 2 hours to give 2,3,4,6-tetra-O-acetyl-glucoferulic acid-[ $\beta$ -<sup>14</sup>C] (372mg). The acid chloride obtained by treating the acid with thionyl chloride was reduced with sodium trimethoxyborohydride to give the corresponding alcohol by the method described by Fuchs<sup>35)</sup>. Deacetylation with sodium methoxide gave coniferin-[ $\beta$ -<sup>14</sup>C] (207mg, 5.4x10<sup>6</sup>Bq).

**Coniferin-[OMe-<sup>14</sup>C]** (G-d, Fig. 1.) was synthesized from tetra-O-acetyl-glucovanillin-[OMe-<sup>14</sup>C] by the same methods as that described for coniferin-[ $\beta$ -<sup>14</sup>C]. Tetra-O-acetyl-glucovanillin-[OMe-<sup>14</sup>C] was synthesized as follows: 4-(tetra-O-acetyl- $\beta$ -D-glucosyl)-protocatechualdehyde<sup>37)</sup> (140mg) was dissolved in methyl ethyl ketone (3ml); potassium carbonate

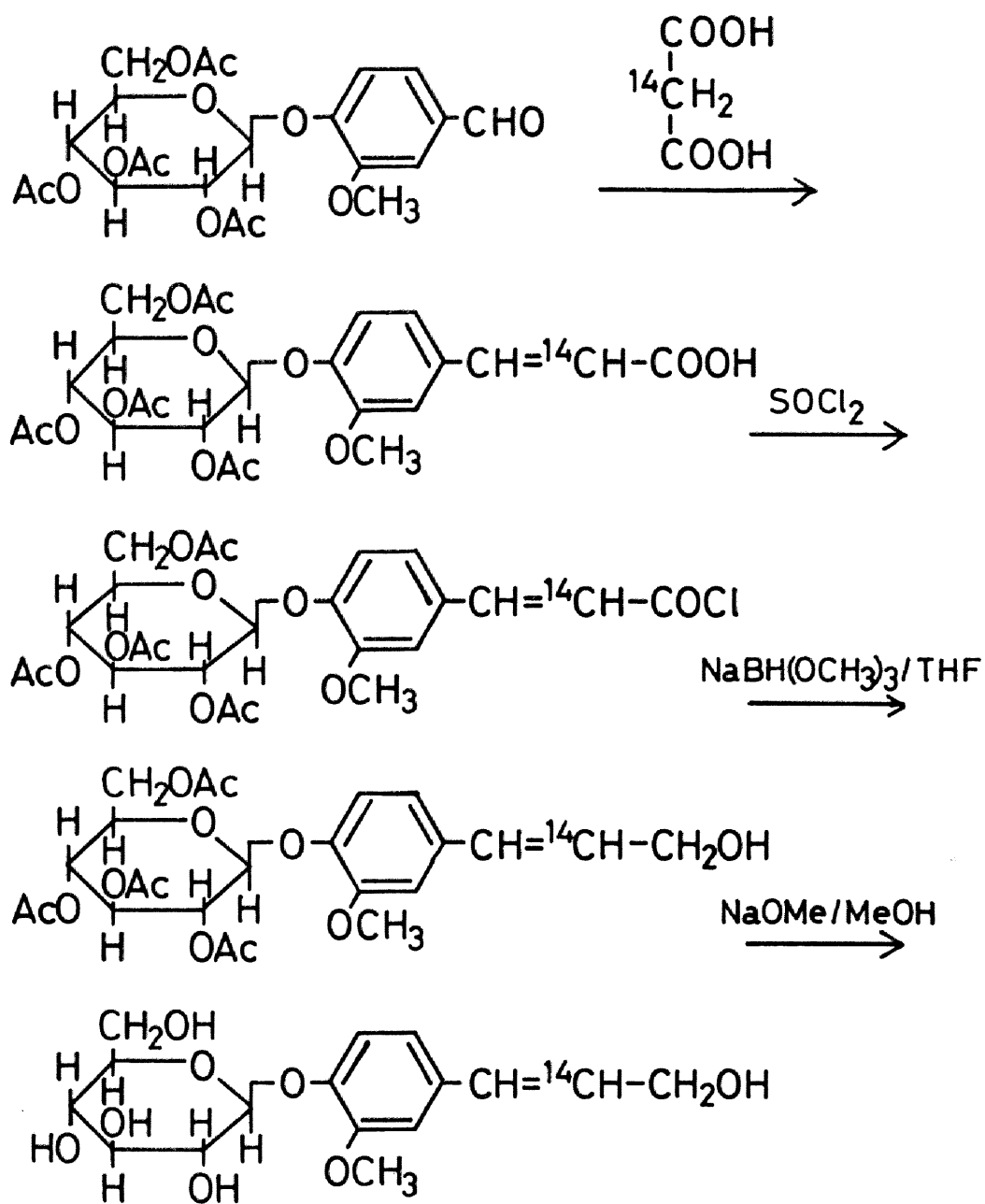


Fig. 3. Synthesis of coniferin- $[\beta -^{14}\text{C}]$

(43mg) and methyl iodide- $[^{14}\text{C}]$  (50mg,  $3.7 \times 10^7 \text{Bq}$ , New England Nuclear, Mass., U.S.A.) were added, and the solution was left for 4 hours at room temperature and heated ( $60^\circ \text{C}$ ) for 4 hours; after cooling, the reaction mixture was filtrated; the filtrate was evaporated and the residue was recrystallized from methanol to give tetra-O-acetyl-glucovanillin- $[\text{OMe-}^{14}\text{C}]$  (140mg, about  $1.6 \times 10^7 \text{Bq}$ ).

**Syringin-[arom. ring-2- $^3\text{H}$ ] (S-a, Fig. 1.)** was synthesized from syringaldehyde-[arom. ring-2- $^3\text{H}$ ]<sup>16)</sup>. According to the method described by Kratzl and Billek<sup>34)</sup>, the syringaldehyde (80mg) was converted to tetra-O-acetyl- $\beta$ -D-glucoside (177mg), which was condensed with malonic acid (40mg) to give tetra-O-acetyl glucosinapic acid (160mg). The acid chloride obtained by treating the acid (160mg) with thionyl chloride was reduced by sodium trimethoxyborohydride to give the corresponding alcohol<sup>35)</sup>. Deacetylation with sodium methoxide gave crude syringin labeled with  $^3\text{H}$  at position 2 of the aromatic ring. This was purified by silica gel column chromatography employing a mixture of acetone : ethyl acetate : water (10:10:1 v/v/v) as a developer to give 50 mg ( $2.0 \times 10^7 \text{Bq}$ ) of syringin-[arom. ring-2- $^3\text{H}$ ]. This label will also be fairly stable during dehydropolymerization in differentiating xylem as observed in guaiacyl analog<sup>14)</sup>.

**Syringin- $[\beta -^{14}\text{C}]$  (S-b, Fig. 1.)** was synthesized from tetra-O-acetyl-glucosyringaldehyde and malonic acid- $[2-^{14}\text{C}]$ . According to the method described by Kratzl and Billek<sup>34)</sup>, the glucoside (425mg) and malonic acid- $[2-^{14}\text{C}]$  (92mg, corresponding to  $9.3 \times 10^6 \text{Bq}$ , New England Nuclear, Mass., U.S.A.) were condensed in anhydrous pyridine (2.0ml) and piperidine (1 drop) at  $100^\circ \text{C}$  for 2 hours to give 2,3,4,6-tetra-O-acetyl-glucosinapic acid- $[\beta -^{14}\text{C}]$  (400mg). The acid chloride obtained by treating the acid with thionyl chloride was reduced with sodium trimethoxyborohydride to give the corresponding alcohol by the method described by Fuchs<sup>35)</sup>. Deacetylation with sodium methoxide gave syringin- $[\beta -^{14}\text{C}]$  (199mg,  $5.1 \times 10^6 \text{Bq}$ ).

### 2.3. Administration of labeled precursors

A V-shaped groove, 2mm wide and 5mm long, was made in circumferential direction on a cut shoot (normal wood, about 5-8cm length) with a razor blade. The bottom of the groove reached to the differentiating xylem as shown in Fig. 4. Fine grass wool was packed in the groove. The inclined shoot of pine was divided into upper part (opposite wood) and under part (compression wood) with a knife and a V-shaped groove was made in the same way. A solution of labeled precursor of lignin or hemicellulose was added dropwise to the groove and metabolized for 3 hours. The list of labeled precursors administered to various plant materials was shown in Table 1.

A drop of 3% glutaraldehyde in phosphate buffer ( $1/15M$   $KH_2PO_4$  :  $1/15M$   $Na_2HPO_4$  = 3:7) was added to the groove, and a small block of xylem tissue near the groove was cut and fixed again in 3% glutaraldehyde overnight in the refrigerator (Fig. 4). A part of the xylem tissue was dehydrated through a graded ethanol series by a conventional method, and embedded in epoxy resin prepared by mixing Quetol 812 (100g, Nissin EM Co. Ltd. Tokyo), MNA (89g, Nissin EM Co. Ltd. Tokyo) and DMP-30 (1.7g, Nissin EM Co. Ltd. Tokyo) (Fig. 4).

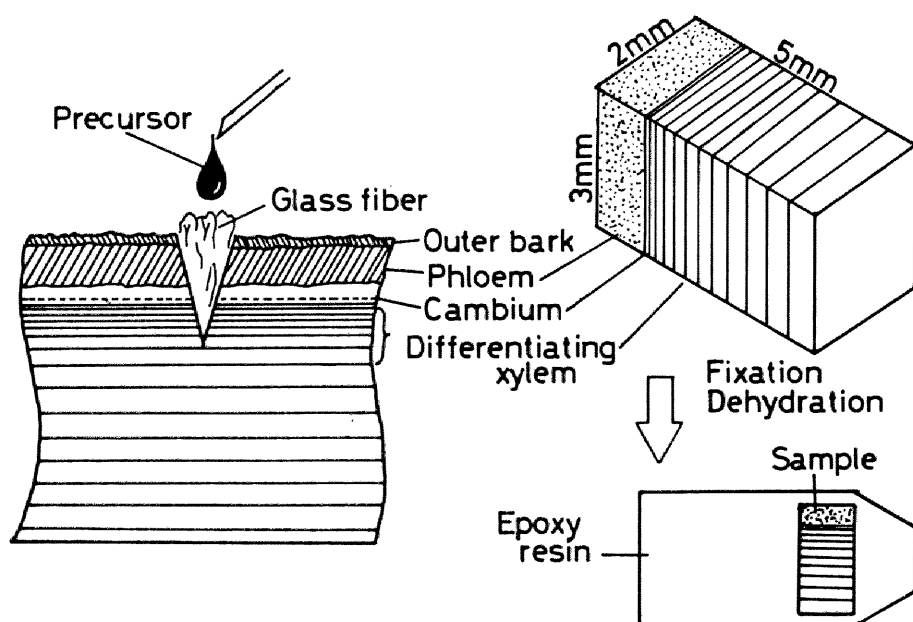


Fig. 4. Administration of labeled precursors.

Table 1

Amounts of radioactivity of labeled precursors administered to various plants

Plant materials	Amount of labeled precursors administered ( $10^5$ Bq)										
	H-a*	H-b	H-c	H-d	G-a	G-b	G-c	G-d	S-a	S-b	UDP-GA
Pine ( <u>P. thunbergii</u> )	5.5	4.3	---	---	3.1	6.2	0.26	---	2.8	---	0.73
Pine opposite and compression wood	---	3.0	---	---	1.9	3.0	---	---	1.9	---	---
Ginkgo ( <u>G. biloba</u> )	---	3.7	---	3.7	3.7	3.7	---	3.7	2.8	---	---
Magnolia ( <u>M. kobus</u> )	---	4.3	---	---	3.1	---	0.26	---	2.8	0.26	0.73
Lilac ( <u>S. vulgaris</u> )	---	4.3	---	---	3.1	---	---	---	2.8	---	---
Beech ( <u>F. crenata</u> )	---	4.3	---	---	3.1	---	---	---	2.8	---	---
Poplar ( <u>P. Maximowiczii</u> <u>P. berolinensis</u> )	---	4.3	3.7	---	3.1	---	---	---	2.8	---	0.73

\* H-a:p-coumaric acid-[a.r.-2- $^3$ H], H-b:p-glucocoumaryl alcohol-[a.r.-2- $^3$ H],  
H-c:p-hydroxybenzoic acid-[a.r.-2- $^3$ H], H-d:p-glucocoumaryl alcohol-[a.r.-3- $^3$ H],  
G-a:coniferin-[a.r.-2- $^3$ H], G-b:coniferin-[a.r.-5- $^3$ H], G-c:coniferin-[ $\beta$ - $^{14}$ C],  
G-d:coniferin-[OMe- $^{14}$ C], S-a:syringin-[a.r.-2- $^3$ H], S-b:syringin-[ $\beta$ - $^{14}$ C].  
UDP-GA: UDP-glucuronic acid-[glucuronyl-U- $^{14}$ C] (New England Nuclear, Mass,  
U.S.A.)

Another part of the tissue was used for radioassay.

#### 2.4. Radioassay

A part of the xylem tissue obtained from the same shoot of magnolia or pine used for the microautoradiography was milled (80 mesh) and extracted thoroughly with ethanol-benzene and hot water. The dried wood meal (20mg) was heated with 2N sodium hydroxide (300  $\mu$ l) and nitrobenzene (20  $\mu$ l) in a stainless steel bomb containing a small steel ball with shaking at 170 °C for 2 hours. The cooled mixture was centrifuged and the supernatant was extracted with ether (3x3 ml). The aqueous layer was acidified to pH 3, and extracted again with ether (3x3 ml). Dried ether solution was evaporated, and oxidation products were separated by silica gel thin layer chromatography (20x20 cm) employing a mixture of n-hexane-isoamyl alcohol-acetic acid (400:64:1 v/v/v) as a developer. p-Hydroxybenzaldehyde, vanillin and syringaldehyde were extracted from the gel with methanol. The specific radioactivity of the aldehydes in methanol were determined by a liquid scintillation spectrometer. The amounts of these compounds were determined by ultraviolet spectrophotometry of the methanol extracts.

Oxidation products of ginkgo wood were examined by high performance liquid chromatography (HPLC) according to the previous paper<sup>38</sup>). Three ml aliquot of the combined 10ml ether extract (Fraction E, Fig. 26.) was evaporated to dryness, and the residue was dissolved in dioxane (50  $\mu$ l) containing 3,5-dihydroxybenzoic acid (0.50mg) as an internal standard. An aliquot (10  $\mu$ l) of the solution was applied to the HPLC system (Shimazu LC-6A) with a Unisil Pack 5C-18 column (6 x 300 mm) and a UV-detector (280 nm). The gradient elution program was as follows: 12% acetonitrile containing 0.1% phosphoric acid for the first 30min, followed by a linear gradient from 20% to 50% another solution (30% acetonitrile containing 0.1% phosphoric acid) for the next 20 min. The radioactivity of each fraction were determined by a scintillation counting method. A and C fractions (Fig. 26.)

were subjected to combustion by the sample oxidizer (Aloka ASC 113) to give  $^3\text{H}_2\text{O}$ , and the radioactivities were determined by a liquid scintillation spectrometer (Beckman LC 3801).

## 2.5. Quantitative analysis of oxidation products

The alkaline nitrobenzene oxidation products of pine normal, pine opposite, pine compression, magnolia and ginkgo wood were separated by HPLC and the amounts of the aromatic aldehydes and acids were determined by a UV detector as the same procedures described in 2.4. L-Tyrosine (Wako Pure Chem. Ind. Osaka) and egg albumin (Katayama Chem. Co. Tokyo) were also subjected to alkaline nitrobenzene oxidation and products were examined by the same procedures.

## 2.6. Microautoradiography

The tissues embedded in epoxy resin were trimmed as shown in Fig. 5.. Two- $\mu\text{m}$ -thick transverse sections were cut on a Reichert-Jung Supercut 2050 microtome equipped with a glass knife from the embedded segment of xylem tissue (Fig. 5). Only the sections of pine normal wood were cut on a Sorval JB-4 microtome. They were mounted on glass slides and covered with Kodak AR-10 stripping film. The glass slides were stored in a refrigerator for 1 month - 1 year. They were developed with Kodak D-19 (20 °C, 7 min.) and fixed with Fuji Fix (20 °C, 10 min.). The sections were stained with toluidine blue O, and the sections of beech were stained with safranin O. Photomicrographs were taken with ZEISS photomicroscope III using with Fuji MINICOPY film. The analysis of silver grain distributions in the photomicrographs were made with the aid of ZEISS IBAS 1 image analyzer. Silver grains per cell or per 100  $\mu\text{m}$  cell wall were counted in several series of tracheids, fiber and vessel which were ordered from cambium to old xylem in a radial direction. The average numbers of silver grains were shown in Fig. 8, 12, 18, 31, 39 and 40. A polarization microscope Olympus POS was used for observation of secondary wall formation.

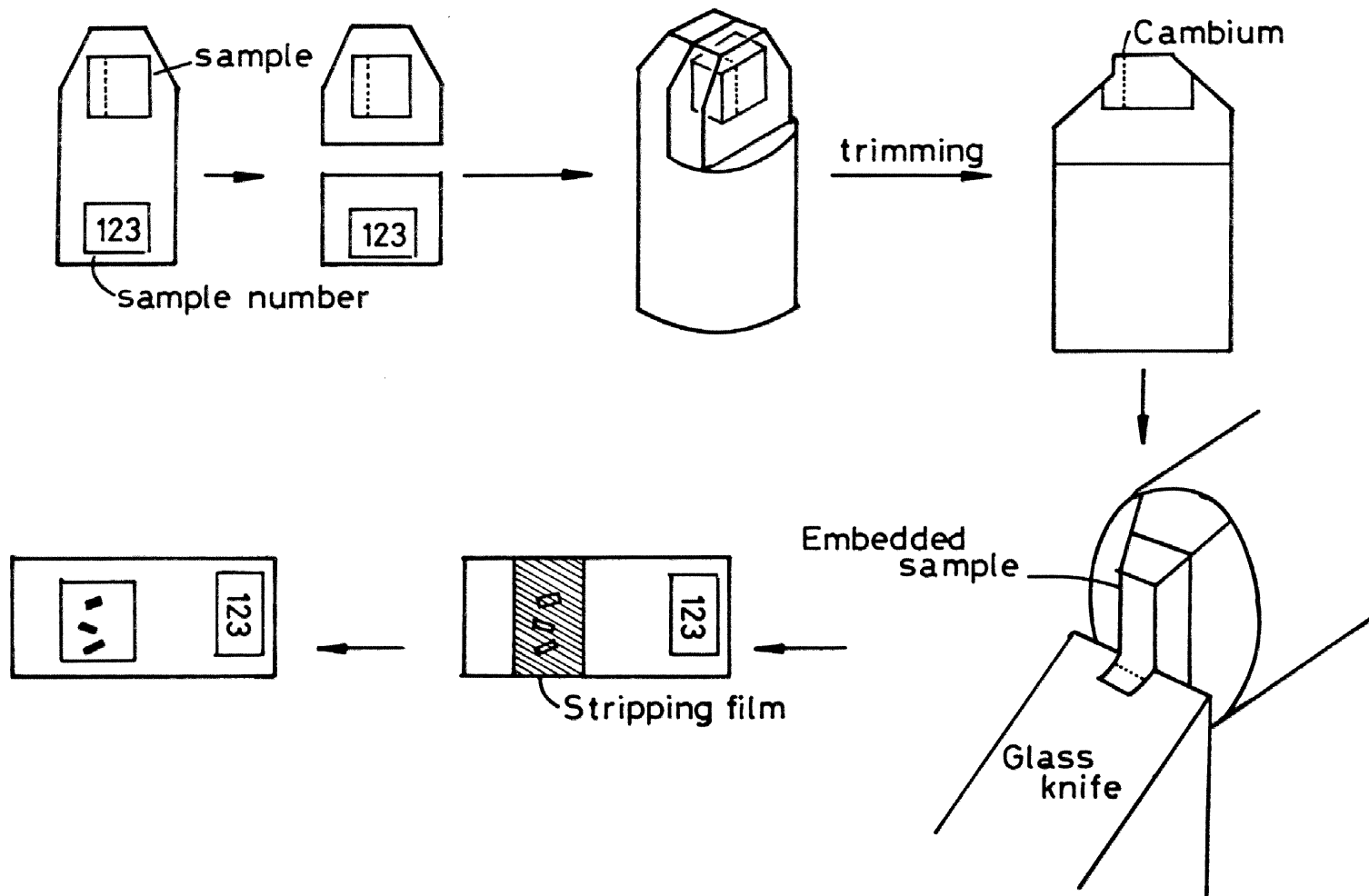


Fig. 5. Prerparation of transverse sections for microautoradiography.

## CHAPTER 3

### Formation and Structure of Lignin in Gymnosperms

#### 3.1. Pine

The newly formed xylem of pine contains cell walls of every stages of differentiation, and the incorporation of radioactivity into the specific morphological region corresponds to the deposition of lignin or carbohydrates at a particular differentiation stage. Therefore, it is possible to deduce the architecture of cell wall from the integral of incorporated activity from the early stage in cambium to the late stage in matured region.

This chapter deals with the process of deposition of  $^{14}\text{C}$ -labeled carbohydrates and lignin into the differentiating xylem of pine (*Pinus thunbergii* Parl.) visualized by microautoradiography to examine the architecture of the cell wall. The process of lignification was further examined by selective labeling of each units of lignin macromolecule. Labeled precursors used for this study were shown in **Fig. 6**.

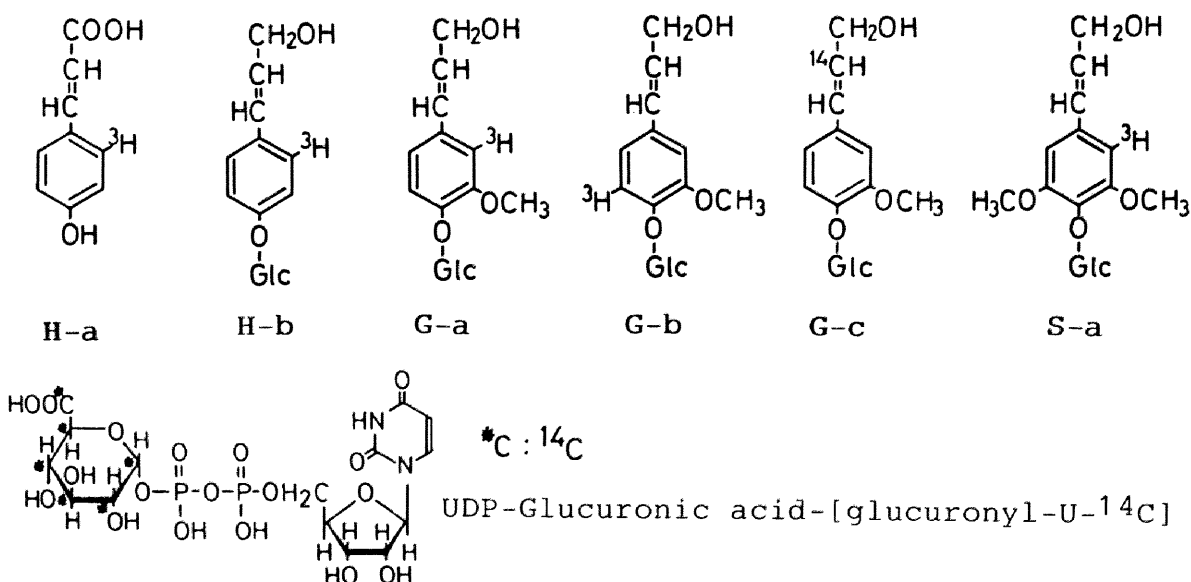


**Fig. 6.** Precursors used for labeling of pine lignin and carbohydrate.

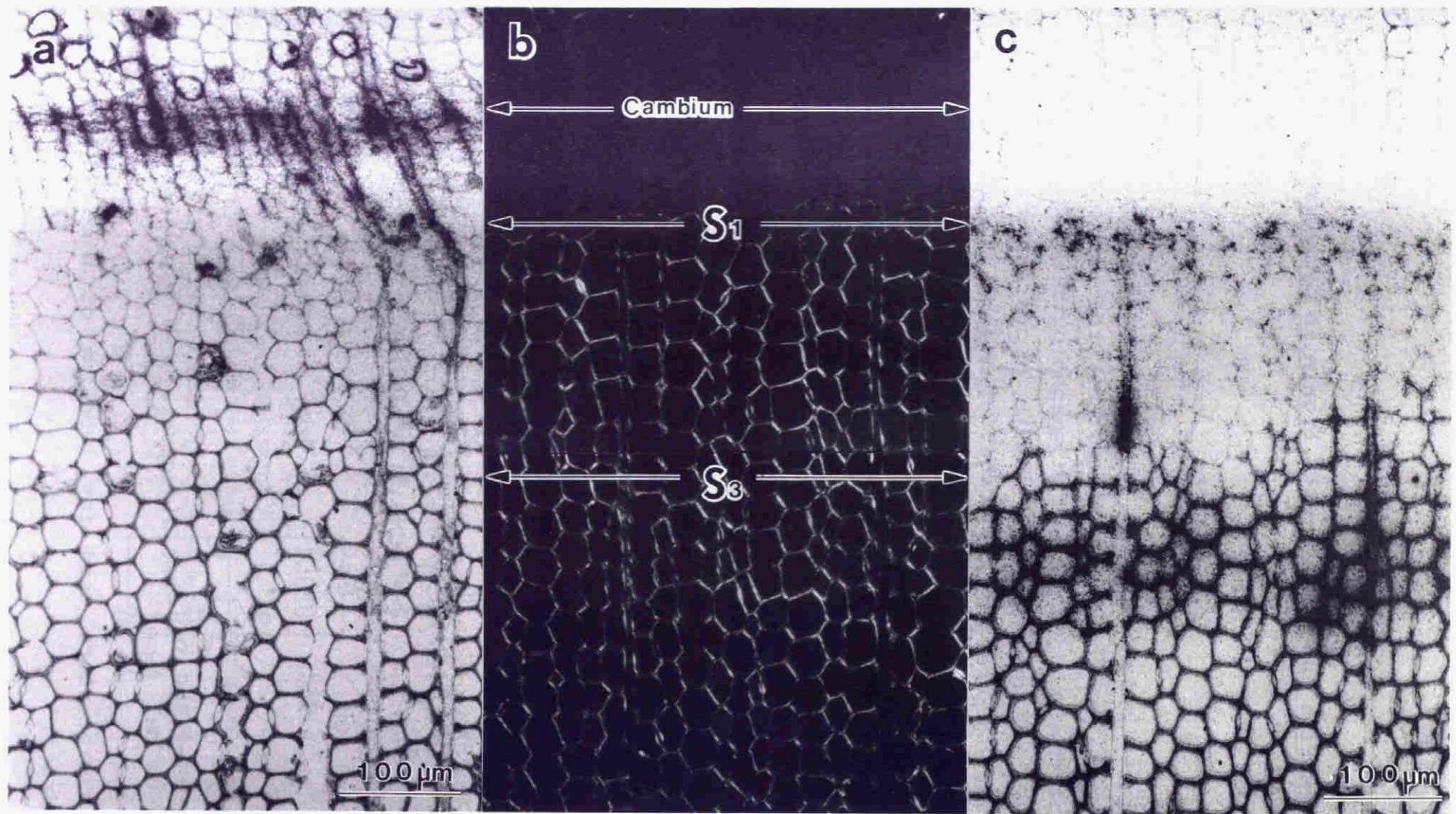


**Fig. 7a:** Microautoradiograph of differentiating xylem of pine administered with UDP-glucuronic acid-[glucuronyl- $U-^{14}C$ ] indicating deposition of pectin and hemicellulose, **b:** Polarization micrograph of the same section as c indicating deposition of cellulose microfibrils in the secondary wall. **c:** Microautoradiograph of differentiating xylem of pine administered with coniferin-[ $\beta-^{14}C$ ].

### Visualization of deposition of carbohydrates

UDP-glucuronic acid is known to be a precursor of pectin and xylan<sup>39)</sup>. When UDP-glucuronic acid-[glucuronyl-U-<sup>14</sup>C] was administered to the growing stem of pine, the radioactivity was incorporated mainly into the cell walls in the earliest stage of xylem differentiation in the cambium as shown in **Fig. 7a**. This incorporation is due to the deposition of pectic substances which mainly consists of partially methylated polymer of galacturonic acid derived from glucuronic acid by epimerase. The fact that the incorporation is greater in radial cell walls than in tangential walls indicates that the former is expanding more rapidly than the latter. The distribution of silver grains shown in **Fig. 8**. indicates that a small part of the activity was incorporated also at later stages between the start of S<sub>1</sub> formation and S<sub>3</sub> formation. This is due to the deposition of xylan in which the activity is distributed in xylose residues derived from glucuronic acid by decarboxylase and also in 4-O-methylglucuronyl residues.

Deposition of cellulose microfibrils was detected by observation of the tissue section under a polarization microscope as shown in **Fig. 7b**. and **Fig. 9**. Microfibrils in the outer and inner layer of secondary wall (S<sub>1</sub> and S<sub>3</sub>) are bright and those in the middle layer (S<sub>2</sub>) are dark.

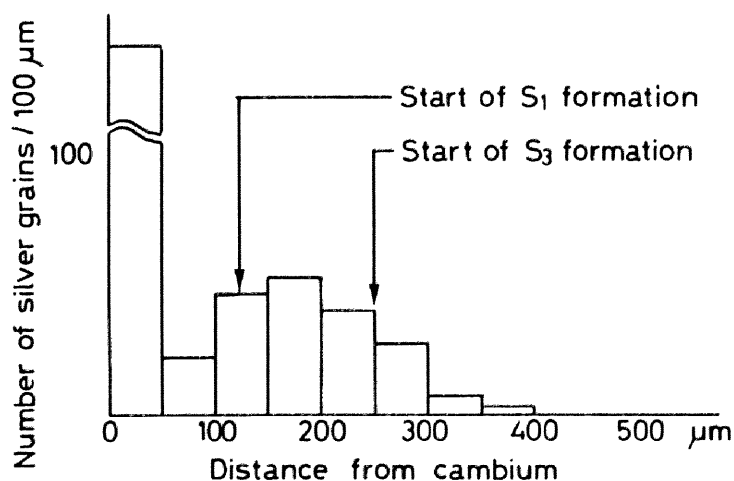


**Fig. 8.** Distribution of silver grains in microautoradiogram of differentiating xylem of pine administered with UDP-glucuronic acid-[glucuronyl-U-<sup>14</sup>C].

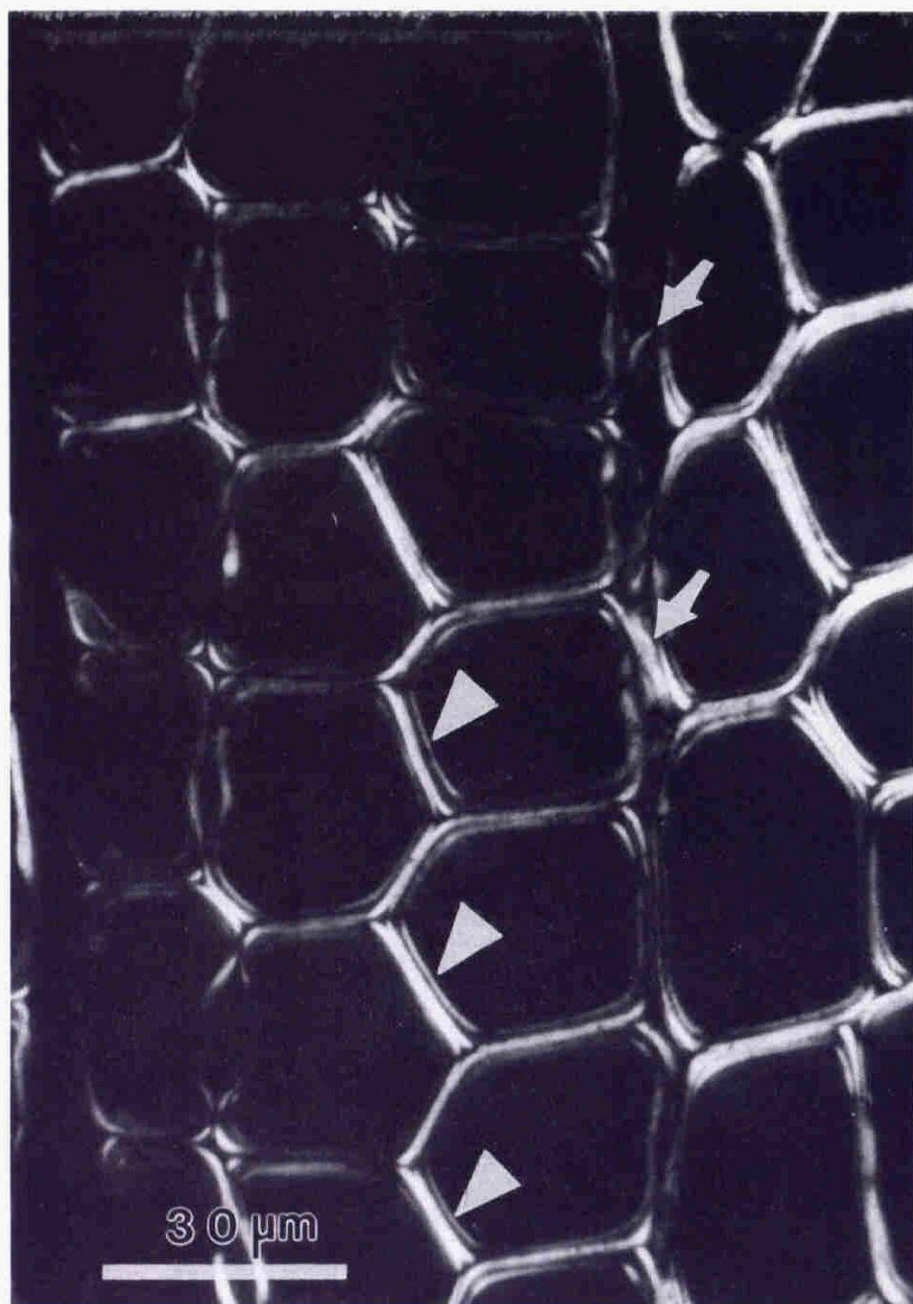


**Fig. 9.** Enlarged polarization photomicrograph of the same section as Fig. 7b and 7c indicating cellulose microfibrils in  $S_1$  and  $S_3$  (arrow head) and  $S_2$  in tangential wall of ray cell (arrow).

### Visualization of formation of lignin

Coniferin is usually found in the cambial sap of gymnosperm trees, and specific labeling of protolignin is effected by the administration of labeled coniferin<sup>40,41</sup>). Incorporation of radioactivity from coniferin- $[\beta\text{-}^{14}\text{C}]$  shown in **Fig. 7c.** indicates deposition of lignin. Microautoradiogram of tissue section labeled by the higher beta energy emitter  $^{14}\text{C}$  is generally more emphatic than that labeled by the low energy beta emitter of  $^3\text{H}$ , though the resolution of former is worse than that of latter.

The lignification proceeds in three distinct stages, always preceded by deposition of carbohydrates as shown in **Fig. 7a, b and c.** The first stage lignification occurs at cell corner and middle lamella after the deposition of pectic substances has finished and  $S_1$  formation has started. The second is a slow lignification stage. During this stage, cellulose microfibrils, mannan and xylan deposit in the  $S_2$  layer forming interrupted lamella structure as proposed by Kerr and Goring<sup>42</sup>). The main lignification occurs in the third stage after the deposition of cellulose microfibrils in the  $S_3$  layer has started. Similar lignification pattern with two deposition peaks was observed in microautoradiogram of differentiating xylem of pine administered with L-phenylalanine- $[\text{G-}^3\text{H}]$ <sup>43</sup>), though L-phenylalanine is not only a precursor of lignin but also of protein.

The apparent local incorporation of radioactivity in the ray cell is due to the fact that the cell is cut longitudinally and a tangential part of the cell wall is included in the  $2\ \mu\text{m}$  thick section. This is shown by observation of cellulose microfibrils in  $S_2$  layer of this tangential part under polarization microscope (**Fig. 9.**).

The fact that deposition of lignin occurs always in the preformed carbohydrate gels seems to be one of the most important key factors creating the unique architecture of wood cell wall. It is well known that to prepare a milled wood lignin (MWL) strictly free from carbohydrate is impossible. The formation of these intimate bonds between lignin and carbohydrate is conveniently explained by the observation

that dehydrogenative polymerization of lignols occurs in thin layer of pectin or hemicellulose gels which is preformed in interrupted lamella arrangement between cellulose microfibrils.

The present observation that monolignols polymerize in pectin gel at middle lamella in the early stage of cell wall formation and in hemicellulose gel in the later stage explains also the causes of different distribution of condensed structures in different morphological regions. When dehydrogenative polymer (DHP) of coniferyl alcohol was formed in pectin or mannan gel, the product contained more condensed units than DHP prepared in the absence of the gel, and pectin was more effective for formation of condensed units than mannan<sup>31</sup>).

### Selective labeling of structural units of lignin

The results of radioassay of various xylem tissues administered with <sup>3</sup>H-labeled lignin precursors were shown in **Table 2**. The total activity of aromatic aldehydes obtained by nitrobenzene oxidation were only 8-19 % of the labeled wood

**Table 2**

Incorporation of radioactivity from labeled precursors into newly formed lignin of pine as shown by nitrobenzene oxidation

		Precursors administered			
		p-Coumaric acid- [r.-2- <sup>3</sup> H]	p-Gluco-coumaryl alcohol- [a.r.-2- <sup>3</sup> H]	Coniferin- [a.r.-2- <sup>3</sup> H]	Syringin- [a.r.-2- <sup>3</sup> H]
<sup>3</sup> H Bq*	<b>W**</b>	430	518	343	40
in	<b>Ha</b>	16	58	24	0
oxidation	<b>Va</b>	41	6	42	0
products	<b>Sa</b>	1	1	1	3

\*From 10 mg of extractive free wood meal

\*\***W**: Extractive free wood meal

**Ha**: p-hydroxybenzaldehyde, **Va**: vanillin, **Sa**: syringaldehyde

meal. This means that the information obtained by this degradative method is limited to those on a part of the lignin macromolecule. However, it is possible to estimate the selectivity of labeling by measuring the distribution of radioactivity in three kinds of aldehydes. The radioactivity of the aldehydes from the wood tissue administered with *p*-coumaric acid indicates that this acid is one of the common precursors of *p*-hydroxyphenyl, guaiacyl and syringyl lignins as expected from their biosynthetic pathway. While the radioactivity of *p*-glucocoumaryl alcohol incorporated mainly into *p*-hydroxyphenyl lignin, and only a small part into guaiacyl and syringyl lignin. A biochemical interconversions from guaiacyl units to *p*-hydroxyphenyl units occurred partly, but the conversions from guaiacyl to syringyl units and from syringyl to guaiacyl units were very small extent.

These results indicate that the biochemical interconversions between lignin precursors do not occur extensively under present experimental conditions, and the specific structural moiety is labeled selectively. Accordingly, a large part of the silver grains in the autoradiogram are assigned to the specific structural moiety corresponding to the monolignol glucoside administered.

#### **Formation and morphological distribution of condensed guaiacyl structures in pine lignin**

It has been shown by radiotracer experiments on lignification of pine that the amount of condensed guaiacyl units formed in an early stage of xylem differentiation was larger than those formed in a later stage<sup>13,44</sup>), and the factors affecting the formation of condensed structures has been studied in vitro experiments<sup>31</sup>).

This inhomogeneous formation of condensed structures can be visualized by microautoradiography employing coniferin-[arom.ring-5-<sup>3</sup>H]. As shown in Fig. 10., the <sup>3</sup>H at position 5 of guaiacyl ring of coniferyl alcohol (I) derived from coniferin is removed by formation of condensed structures (II,III,IV\*) with linkage at this position, while the <sup>3</sup>H is retained in non-condensed structures (V,VI,VII). On the other

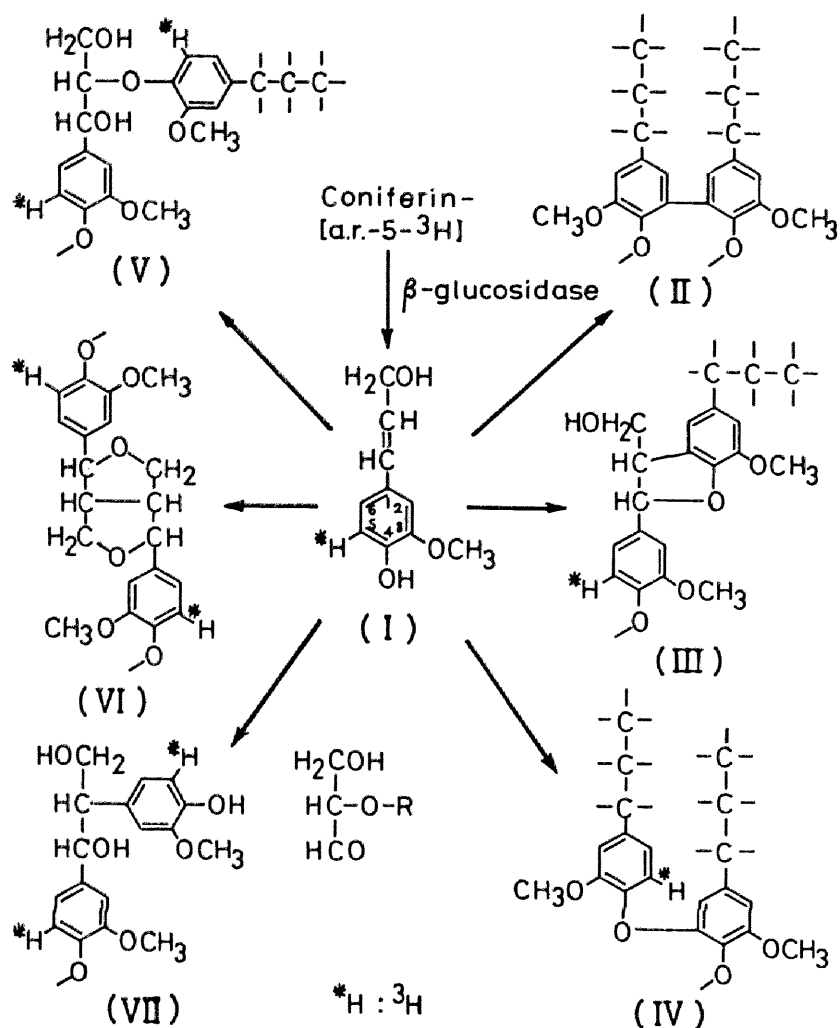


**Fig. 10.** Removal of  $^{3}\text{H}$  at position 5 of guaiacyl ring of coniferyl alcohol (I) by formation of condensed structures (II, III, IV\*) during dehydrogenative polymerization. Non-condensed structures (V, VI, VII) retain the  $^{3}\text{H}$ . If  $^{3}\text{H}$  is at position 2, no removal of  $^{3}\text{H}$  occurs.

hand, when coniferin-[arom. ring-2- $^{3}\text{H}$ ] is administered, the  $^{3}\text{H}$  at position 2 is expected to remain almost intact during the dehydrogenative polymerization, because condensed structures with bond at this position is hardly formed. Almost no elimination of  $^{3}\text{H}$  has been observed in the pine tissue administered with ferulic acid-[ring-2- $^{3}\text{H}$ ]<sup>14</sup>. (\* Strictly saying, structure IV is not a true condensed type. However, this 4-O-5 type structure is included in "condensed structures" for convenience in this thesis.)

Because the tissue section labeled by low-energy beta emitter  $^3\text{H}$  can provide a high resolution microautoradiogram, it is possible to estimate the activity semiquantitatively in different morphological regions by silver grain counting<sup>17)</sup>. And since the number of silver grains produced by the  $^3\text{H}$  at position 2 (**Fig. 11a**) and position 5 (**Fig. 11b**) are proportional to the number of total guaiacyl unit and non-condensed guaiacyl unit respectively, the difference between these two values corresponds to the number of condensed structures. The distribution of silver grains in these autoradiograms were shown in **Fig. 12c** and **d**. The difference between these two graphs indicates that the lignin formed in the middle lamella regions in an early stage of xylem differentiation contains more condensed units than that formed in a later stage in secondary wall.

One of the factors favorable to the formation of condensed guaiacyl structures may be the fact that dehydrogenative polymerization proceeds in carbohydrate gel and the kind of gel changes from pectic substances in the early stage to hemicelluloses in the later stages (**Fig. 7.** and **Fig. 8.**). One of the other factors may be the participation of *p*-coumaryl alcohol in dehydrogenative polymerization<sup>21)</sup>. Because the *p*-hydroxyphenyl unit is capable of forming condensed units with bond at 3 and 5 position of the aromatic ring with another *p*-hydroxyphenyl or guaiacyl units, the supply of *p*-coumaryl alcohol in the early stage (**Fig. 12b** and **13b**) is favorable to the formation of condensed guaiacyl structures.

It is noteworthy that the deposition of guaiacyl lignin proceeds in three distinct stages (**Fig. 12c**). The first stage lignification occurs at cell corner and compound middle lamella region after the start of deposition of carbohydrates in  $S_1$ . The second is the slow lignification stage. During this stage, the carbohydrates deposit in the  $S_2$  layer. The main lignification occurs in the third stage after the start of  $S_3$  formation. The same pattern with two lignification peaks has been observed in the microautoradiogram of pine xylem administered with coniferin- $[\beta\text{-}^{14}\text{C}]$  (**Fig. 7c**).

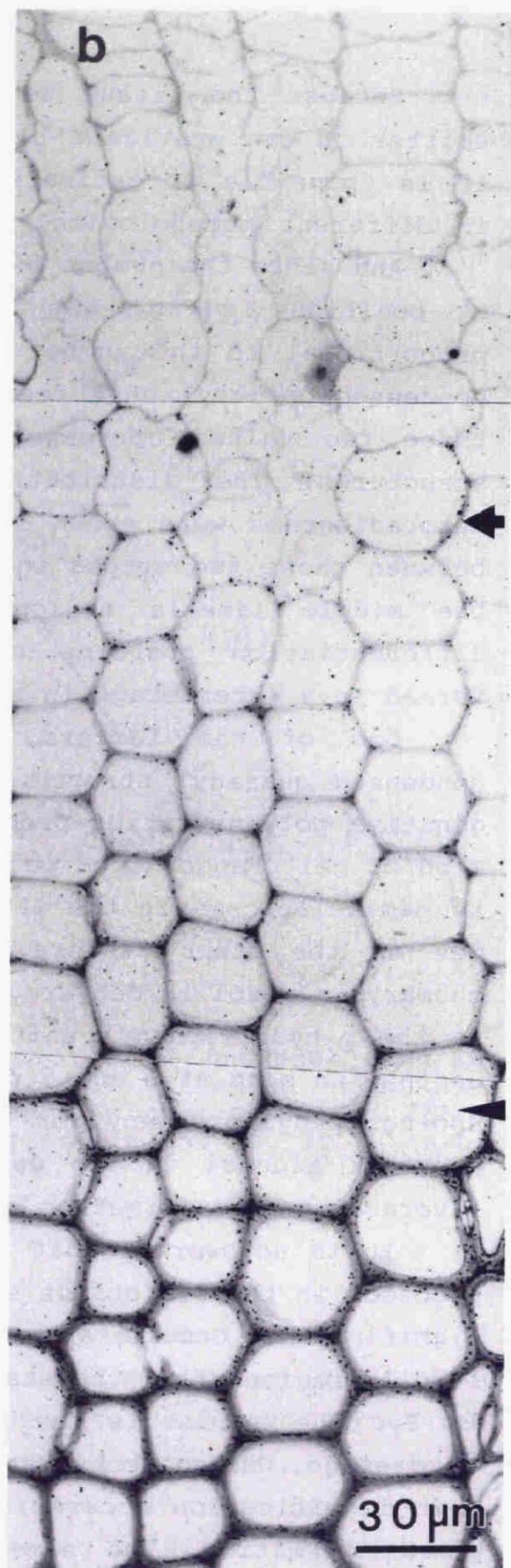
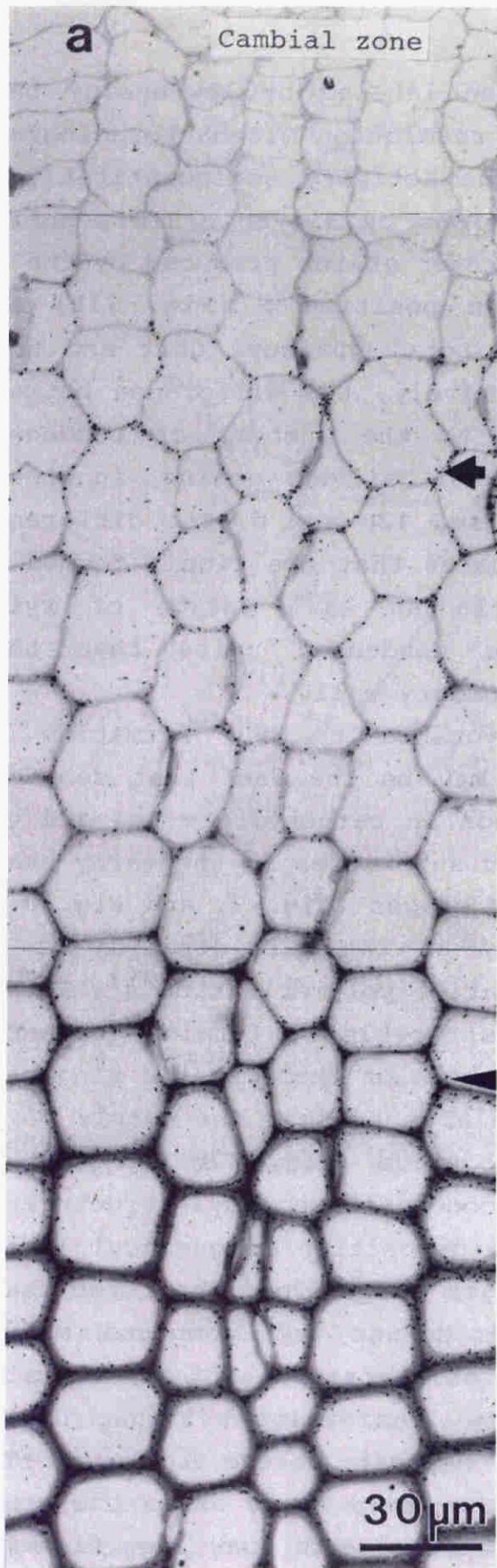


**Fig. 11a and b.** Microautoradiograms of differentiating xylem of pine administered with coniferin-[arom. ring-2-<sup>3</sup>H] (a) and coniferin-[arom. ring-5-<sup>3</sup>H] (b). Arrow and arrowhead indicate start of S<sub>1</sub> and S<sub>3</sub> formation respectively.

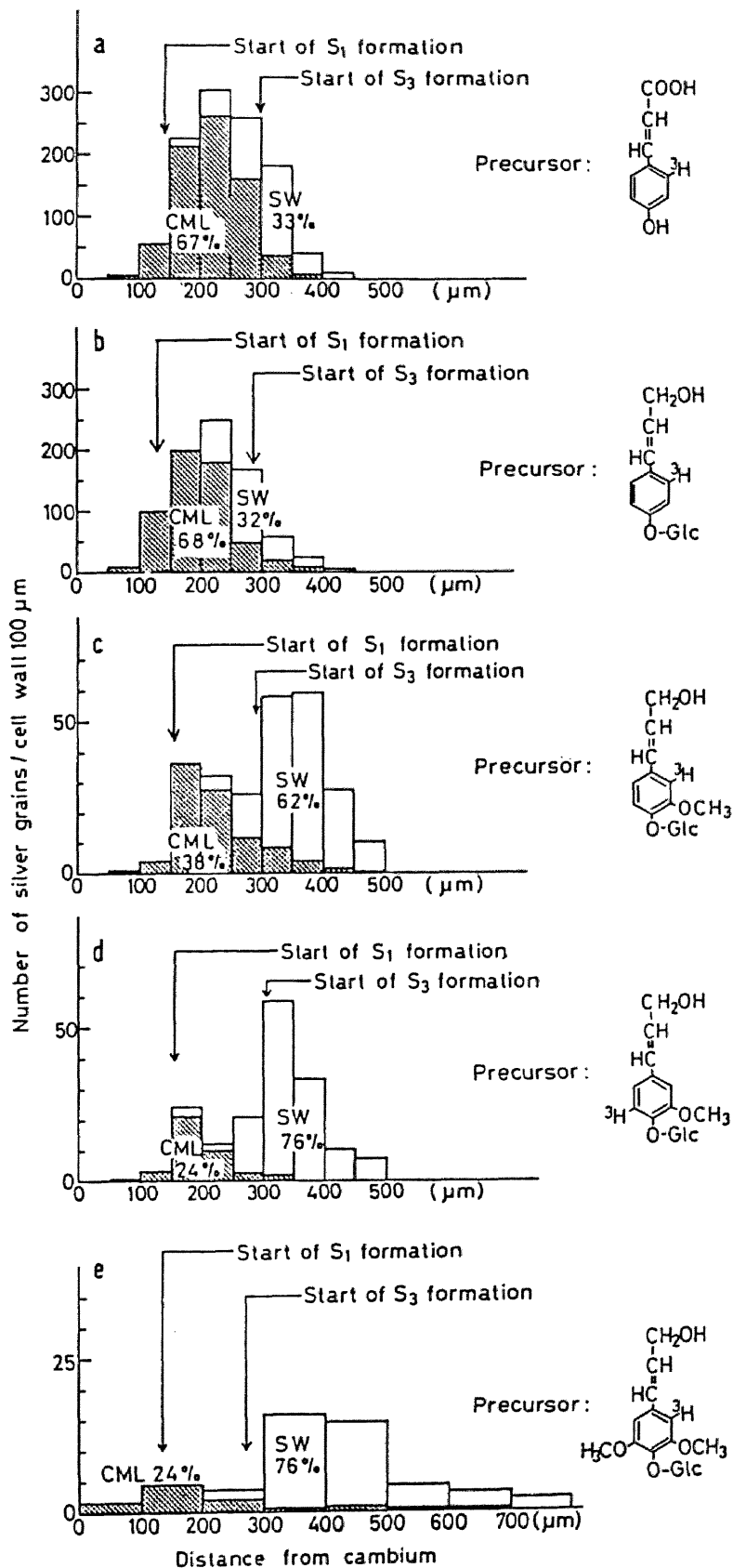


**Fig. 12.** Distribution of silver grains in microautoradiograms of pine xylem administered with p-coumaric acid-[arom. ring-2- $^3\text{H}$ ] (a), p-glucocoumaryl alcohol-[arom. ring-2- $^3\text{H}$ ] (b), coniferin-[arom. ring-2- $^3\text{H}$ ] (c), coniferin-[arom. ring-5- $^3\text{H}$ ] (d) or syringin-[arom. ring-2- $^3\text{H}$ ] (e).

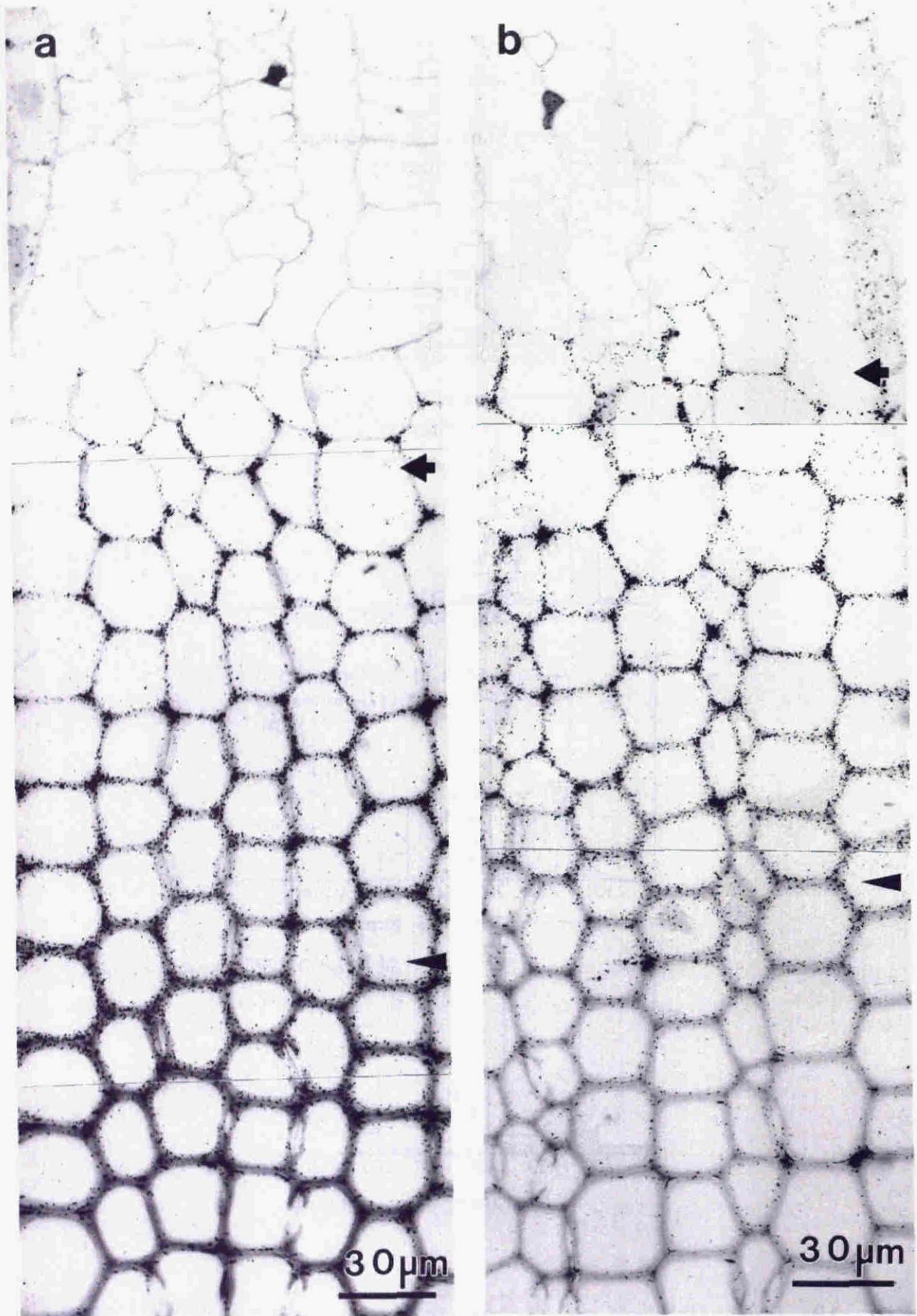


Fig. 13a and b. Microautoradiograms of differentiating xylem of pine administered with p-coumaric acid-[arom. ring-2-<sup>3</sup>H] (a) and p-glucocoumaryl alcohol-[arom. ring-2-<sup>3</sup>H] (b). Arrow and arrowhead indicate start of S<sub>1</sub> and S<sub>3</sub> formation respectively.

## Formation and morphological distribution of *p*-hydroxyphenyl and syringylpropane units

The process of formation of *p*-hydroxyphenyl and syringyl lignins were examined by administration of *p*-glucocoumaryl alcohol-[arom.ring-2-<sup>3</sup>H] and syringin-[arom.ring-2-<sup>3</sup>H] respectively. *p*-Coumaric acid-[arom.ring-2-<sup>3</sup>H] was also administered to compare its incorporation into protolignin with the other precursors. Incorporation of *p*-hydroxyphenylpropane units (**Fig. 13b.**) was observed in an earlier stage of cell wall differentiation than that of guaiacylpropane units (**Fig. 11a** and **12c**), and a large portion of *p*-hydroxyphenyl lignin was located in the compound middle lamella (**Fig. 12b**).

According to the chemical characterization of tissue fractions from middle lamella and secondary wall of black spruce tracheids by Whiting and Goring<sup>18)</sup>, the secondary wall lignin contains 1.7 times as much methoxyl per C<sub>9</sub> as the middle lamella lignin, indicating a substantial proportion of *p*-hydroxyphenylpropane residues in compound middle lamella. On the other hand, Westermarck<sup>19)</sup> reported that the content of *p*-hydroxyphenylpropane units in compound middle lamella of normal wood tracheids estimated by nitrobenzene oxidation and acidolysis was very low, while that in compression wood tracheids was high.

The present results by microautoradiography suggest that *p*-hydroxyphenylpropane unit is one of the normal building stones and may exist in substantial amount in the compound middle lamella and cell corner lignin of pine. Because the molecular weight and degree of condensation of compound middle lamella lignin is not yet high enough in the early stage of cell wall differentiation, it is possible to detect substantial amount of *p*-hydroxybenzaldehyde by nitrobenzene oxidation of the lignin at this stage as shown in **Table 2**. However, in matured cell wall, the *p*-hydroxyphenyl lignin may exist in highly condensed type with bond at 3- and/or 5-position of aromatic ring to give only a small amount of monomeric degradation products by oxidation or acidolysis.

The radioactivity from *p*-coumaric acid was incorporated in longer period than that from *p*-glucocoumaryl alcohol

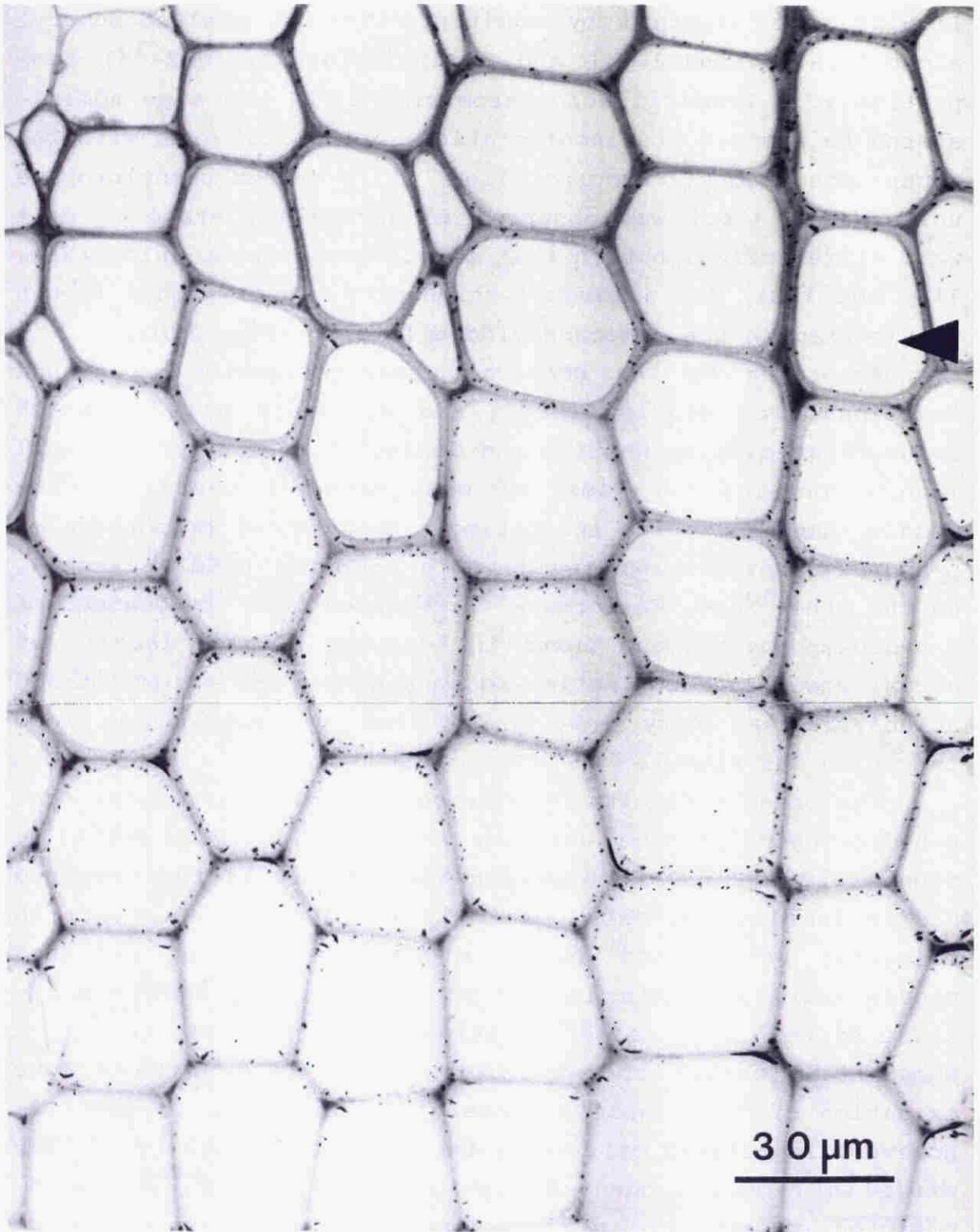


Fig. 14. Microautoradiogram of differentiating xylem of pine administered with syringin-[arom. ring-2-<sup>3</sup>H]. Arrowhead indicates start of S<sub>3</sub> formation.

(Fig. 12a, 12b, 13a and 13b). This is due to the fact that *p*-coumaric acid is a common precursor of *p*-hydroxyphenyl, guaiacyl and syringyl lignins, and a part of *p*-coumaric acid is converted into guaiacyl and syringyl units (Table 2 and Fig. 12.).

Syringyl unit was incorporated in small amount mainly in the late stage of cell wall differentiation, and its large portion was located in the inner layer of secondary wall (Fig. 14. and 12e).

The morphological distribution of three kinds of lignin moieties in matured cell wall was estimated by integration of their incorporation patterns as shown in Fig. 15. It is to be noted that *p*-coumaric acid and three kinds of monolignol glucosides are incorporated into differentiating cell wall in the same order as that of their biosynthesis. It seems natural that the kind of monolignol biosynthesized by the cell changes with its age, because lignin is a kind of secondary metabolites. These results indicate that the precursors administered are metabolized under normal biochemical regulations. One of the regulating factors may be

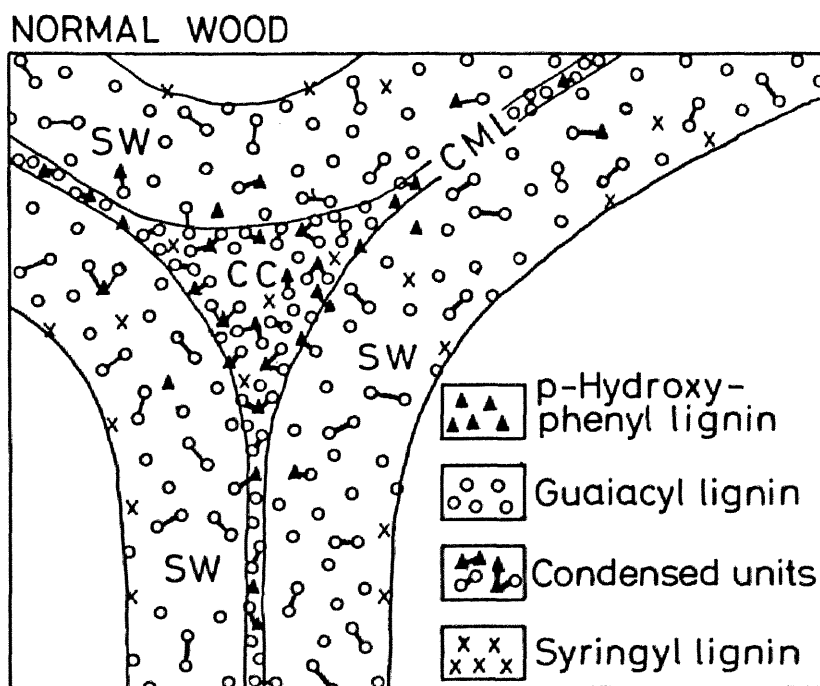


Fig. 15. A schematic representation of morphological distribution of various structural moieties in mature cell wall of pine tracheid. CC: cell corner, CML: compound middle lamella, SW: secondary wall

substrate specificity of  $\beta$ -glucosidase which catalyzes the hydrolysis of monolignol glucosides to corresponding alcohols. It has been shown that the cell-wall-bound  $\beta$ -glucosidase in spruce seedlings has different substrate specificity towards three kinds of monolignol glucosides<sup>45</sup>).

### Conclusion

The heterogeneous growing process of pine lignin macromolecule was visually demonstrated by the combination of high resolution microautoradiography and the technique of selective labeling of specific structural moieties in the lignin.

In addition, the process of deposition of carbohydrates in differentiating xylem of pine can be visualized by microautoradiography. The lignification proceeds in three distinct stage, always preceded by deposition of carbohydrates.

Lignin is a kind of secondary metabolites, and lignification is controlled fundamentally by the individual cell, and hence the mode of its biosynthesis changes with the age of the cell. It is noteworthy that the deposition of *p*-hydroxyphenyl, guaiacyl and syringyl lignins occurs in the same order as that of biosynthesis of their monolignols. Dehydrogenative polymerization of lignols proceeds in carbohydrate gels which affect the formation of condensed structure, and the kind of gel also changes with the stage of cell wall differentiation. Participation of *p*-coumaryl alcohol in polymerization also increases the content of condensed structures. As a result, a highly condensed *p*-hydroxyphenyl lignin and condensed guaiacyl structure is formed mainly in cell corner and compound middle lamella in the early stage of cell wall differentiation, while the syringyl lignin is formed in the late stage mainly in the inner layer of secondary wall.

These observations indicate that a lignin molecule grows up in the differentiating cell wall under the rigid biochemical control to a macromolecule which is heterogeneous in structure specific to morphological regions. The origin of the heterogeneity of lignin structure is understood well based on the biogenesis of protolignin in the cell wall.

### 3.2. Pine compression wood

The characteristic features of compression wood and its chemical components have been discussed in detail by Timell (46). It has been shown by degradative analysis that the structure of lignin in compression wood is different from that of lignin in normal wood. In addition, the pattern of lignification in pine compression wood is considered to be different from that in normal wood; lignification of secondary wall occurred after the start of  $S_3$  (inner layer of secondary wall) formation in normal wood<sup>43,47</sup>). But  $S_3$  layer does not exist in the compression wood of pine. Fujita et al.<sup>48,49</sup>) showed by UV-microscopic and autoradiographic methods that the lignin content of pine compression wood was extremely high in outer layer of  $S_2$  ( ${}_0S_2$ ) and the lignification proceeded from outer to inner layer of cell wall. However, formation and distribution of the various structural units of lignin in the cell wall of compression wood have not been studied.

This chapter deals with the growing process of lignin macromolecule in compression wood of pine visualized by microautoradiography, and heterogeneous feature of the macromolecular structure compared with those of normal wood lignin. The precursors of lignin, *p*-glucocoumaryl alcohol-[arom. ring-2-<sup>3</sup>H] (H-b), coniferin-[arom. ring-2-<sup>3</sup>H] (G-a), coniferin-[arom. ring-5-<sup>3</sup>H] (G-b) and syringin-[arom. ring-2-<sup>3</sup>H] (S-a) were shown in Fig. 16.

The structure of cell wall layer and process of xylem differentiation in compression wood are different from those in normal wood. Therefore, it is difficult to choose shoots which are similar in degree of growth. In this experiment, the upper and under parts of a inclined shoot were employed to make a strict comparison between compression and opposite woods which are in the same degree of xylem growth (Fig. 17). It has been shown that the selective labeling of *p*-hydroxyphenyl, guaiacyl and syringyl units in the lignin of pine

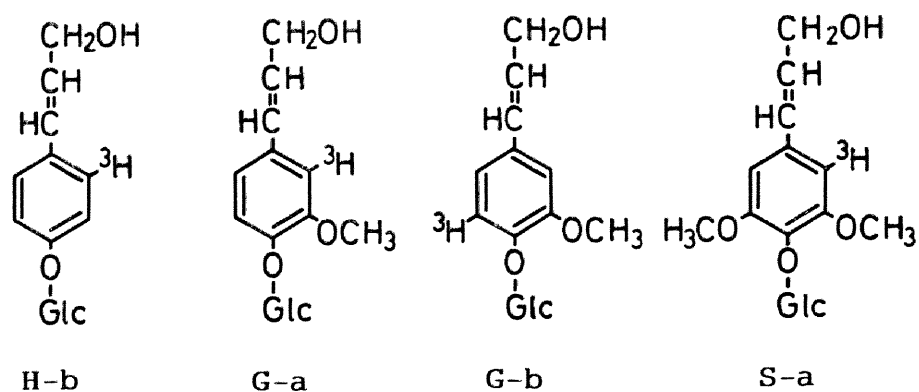


**Fig. 16.** Precursors used for labeling of lignin in pine opposite and compression wood lignin.

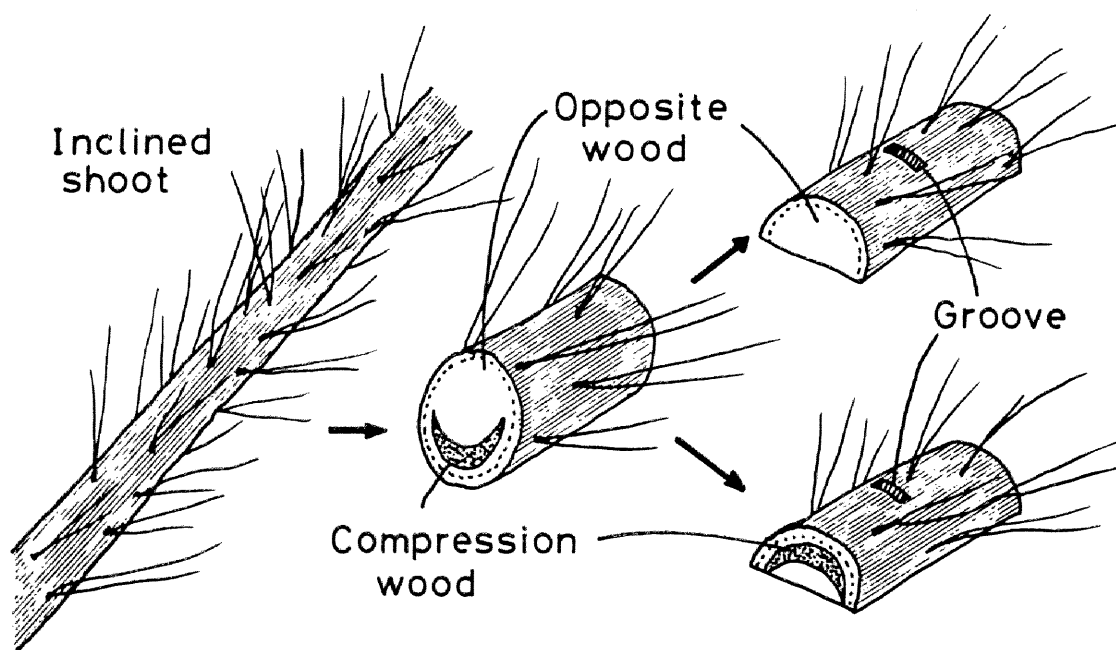


**Fig. 17.** Preparation of plant materials and administration of labeled precursors of lignin to differentiating xylem of pine opposite and compression wood.

normal wood is achieved by the administration of tritiated *p*-glucocoumaryl alcohol, coniferin and syringin (3.1.). In this work, the silver grains in the microautoradiograms were assigned to *p*-hydroxyphenyl, guaiacyl, non-condensed guaiacyl and syringyl units corresponding to the precursors administered. The distribution of the labeled units in differentiating xylem was shown in Fig. 18.

As shown in Fig. 18a and Fig. 19a, *p*-hydroxyphenyl units were incorporated in the early stage of lignification mainly in the compound middle lamella of the newly formed xylem of opposite wood tissue. This result is similar to that observed in normal wood of pine (3.1.). By the chemical analysis of the tissue fraction of spruce which mainly consists of compound middle lamella, Whiting and Goring<sup>18)</sup> indicated that *p*-hydroxyphenyl units were contained in the compound middle lamella lignin. In contrast to these results observed in opposite and normal wood, *p*-hydroxyphenyl units were mainly incorporated into secondary wall in differentiating xylem of compression wood (Fig. 18a and Fig. 19b, c). The incorporation was most active during the formation of  ${}_0S_2$ .

Guaiacyl units were mainly incorporated into secondary wall in compression (Fig. 20a) and in opposite wood (Fig. 21a). The incorporation was most active in the late stage of lignification. In opposite wood, the incorporation of guaiacyl units into secondary wall occurs just after the start of  $S_3$  formation in rather short period (Fig. 18b and Fig. 21a). On the other hand, in compression wood, deposition of guaiacyl units occurs during long period from the start of formation of  ${}_0S_2$  to the formation of inner layer of  $S_2$  ( ${}_iS_2$ ) (Fig. 18b and Fig. 20a, c). And the lignification proceeds from outer side to inner side of cell wall (Fig. 20c). Fujita et al. (48,49) observed a similar lignification process in compression wood of Cryptomeria by UV microscope and by autoradiography administered with [<sup>3</sup>H]-phenylalanine. Guaiacyl units also deposits in compound middle lamella during the early stage of xylem differentiation in both compression (Fig. 18b and Fig. 20a, c) and opposite wood (Fig. 18b and Fig. 21a).

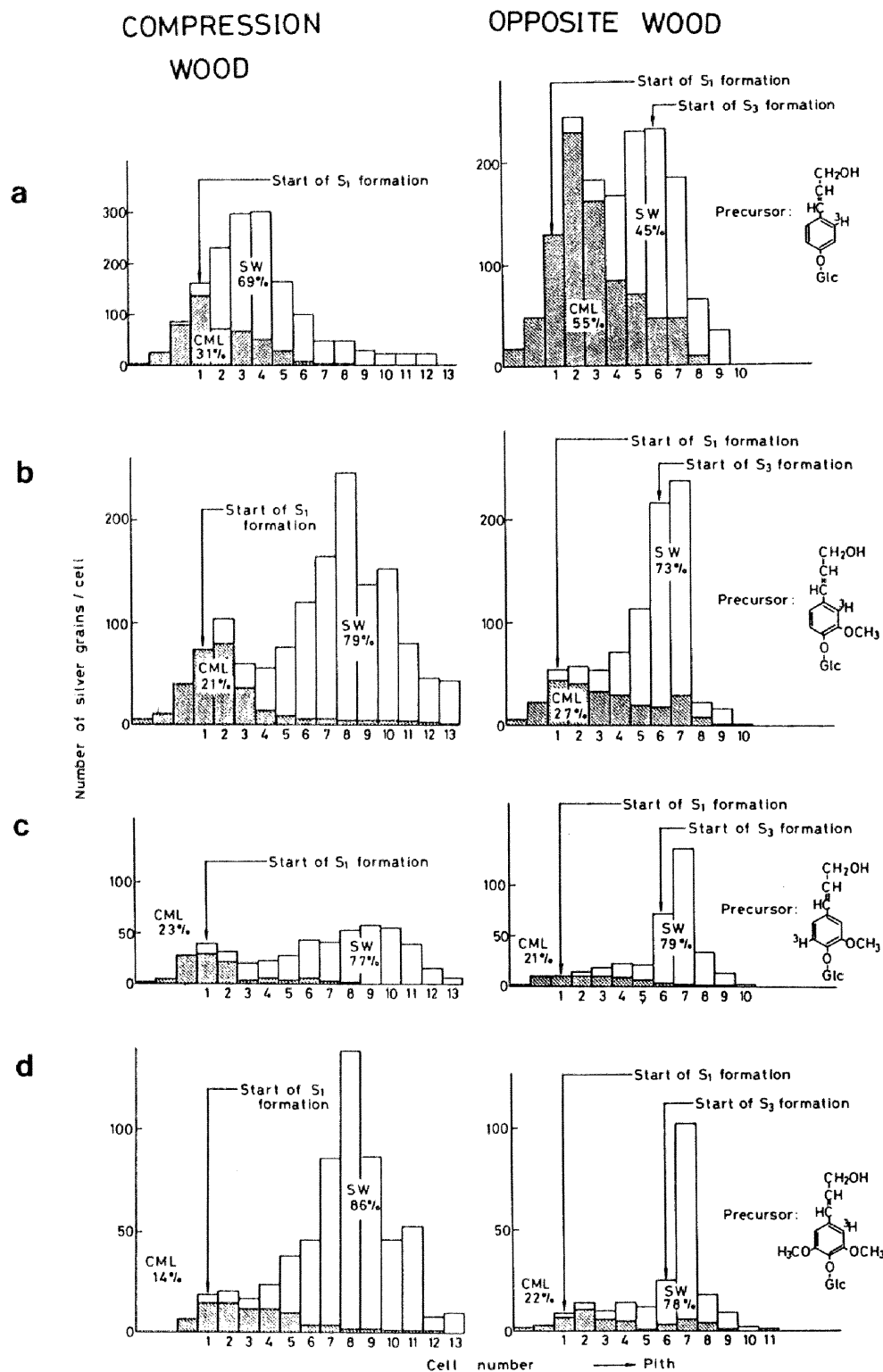


**Fig. 18.** Distribution of silver grains in microautoradiograms of pine xylem of compression wood (left) and opposite wood (right) administered with *p*-gluco coumaryl alcohol-[arom. ring-2- $^3$ H] (a), coniferin-[arom. ring-2- $^3$ H] (b), coniferin-[arom. ring-5- $^3$ H] (c) or syringin-[arom. ring-2- $^3$ H] (d).

\* The cell number shows the order of cell counted from the cell in which formation of  $S_1$  layer started.

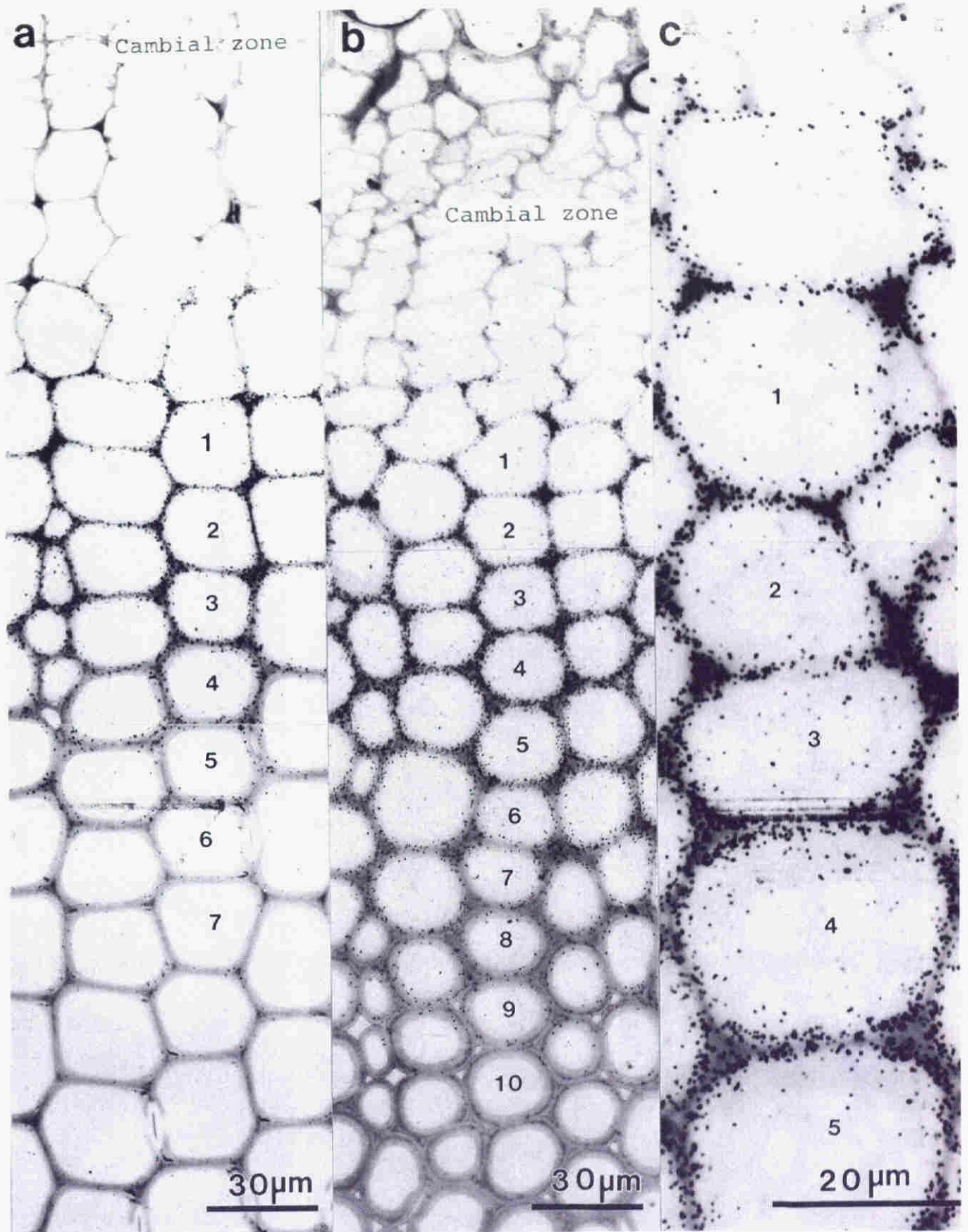


**Fig. 19a.** Microautoradiogram of differentiating xylem of pine opposite wood administered with *p*-glucocoumaryl alcohol-[arom. ring-2-<sup>3</sup>H], **b** and **c**: Microautoradiograms of differentiating xylem of pine compression wood administered with *p*-glucocoumaryl alcohol-[arom. ring-2-<sup>3</sup>H]. The number in autoradiograms corresponds to the cell number in Fig. 18.

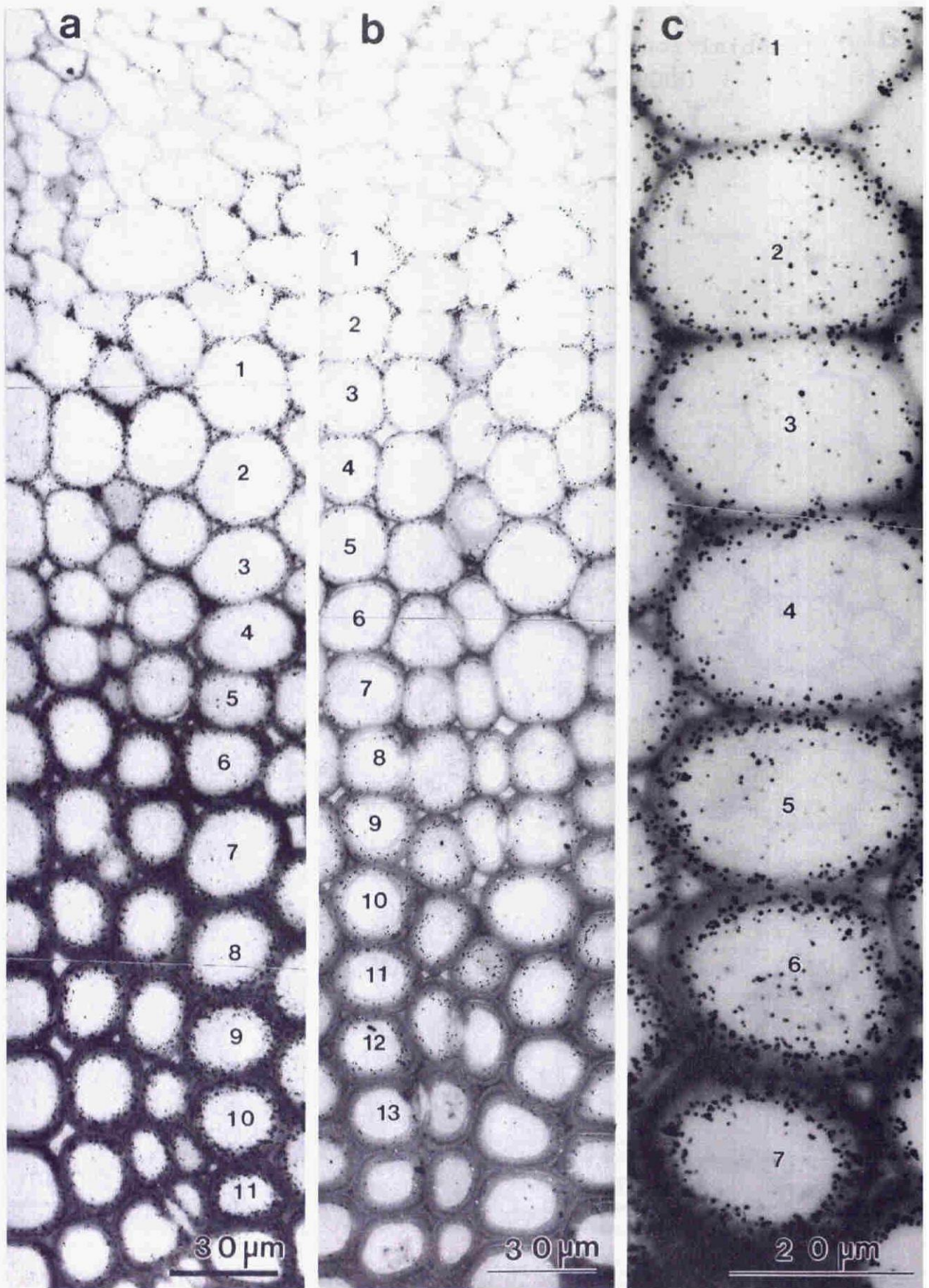


Fig. 20a and c. Microautoradiograms of differentiating xylem of pine compression wood administered with coniferin-[arom. ring-2-<sup>3</sup>H], b : Microautoradiogram of differentiating xylem of pine compression wood administered with coniferin-[arom. ring-5-<sup>3</sup>H]. The number in autoradiograms corresponds to the cell number in Fig. 18.

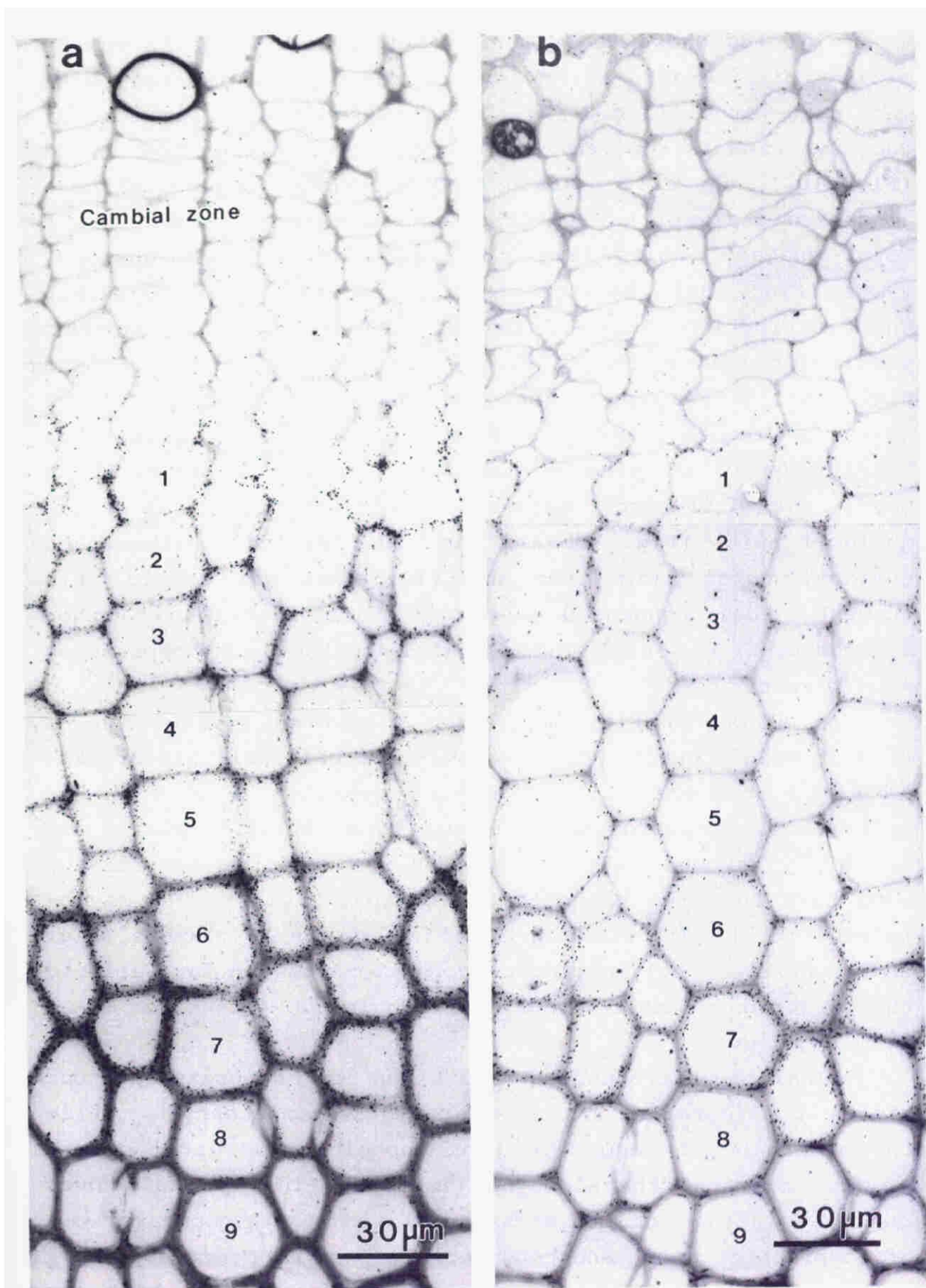


Fig. 21. Microautoradiograms of differentiating xylem of pine opposite wood administered with coniferin-[arom. ring-2-<sup>3</sup>H] (a) and coniferin-[arom. ring-5-<sup>3</sup>H] (b). The number in autoradiograms corresponds to the cell number in Fig. 18.

**Fig. 18c** shows the distribution of silver grains on the microautoradiograms of xylem of pine administered with coniferin-[arom. ring-5-<sup>3</sup>H]. Because the <sup>3</sup>H at position 5 of guaiacyl ring is removed when condensed structures are formed (**Fig. 10.**), the silver grains indicated the presence of non-condensed guaiacyl units. Difference between distribution of total guaiacyl units (**Fig. 18b**) and non-condensed guaiacyl units (**Fig. 18c**) indicates distribution of condensed units. The distribution of non-condensed guaiacyl units in compound middle lamella is low (21%) in opposite wood (**Fig. 18c** and **Fig. 21b**). This suggests that condensed structure of guaiacyl units is rich in compound middle lamella. Similar result has been observed in pine normal wood (3.1.). In compression wood, the difference between the distribution of total guaiacyl units (**Fig. 18b** and **Fig. 20a, c**) and non-condensed guaiacyl units (**Fig. 18c** and **Fig. 20b**) was small. This suggests that condensed guaiacyl units distribute rather homogeneously in all morphological regions of compression wood tissue.

As shown in **Fig. 18d, 22a, b** and **c**, syringyl units deposit mainly during the late stage of cell wall differentiation in compression wood and in opposite wood. This is similar to that observed in normal wood (3.1.). Lapierre and Rolando<sup>50)</sup> showed that syringyl units of pine compression wood have few free phenolic end groups. Their result may be related to the distribution of this unit in <sub>1</sub>S<sub>2</sub> layers (**Fig. 22c**), where the polymerization conditions may be favorable to the formation of endwise polymer rich in β-O-4 linkage<sup>31)</sup>.

Alkaline nitrobenzene oxidation of compression wood yields considerable amount of *p*-hydroxybenzaldehyde, while the oxidation of normal wood or opposite wood gives only a slight amount of the aldehyde (**Table 3**). This probably dues to the existence of *p*-hydroxyphenyl units in secondary wall of compression wood, and considerable part of *p*-hydroxyphenyl units in secondary wall may be non-condensed type which can afford aldehyde on alkaline nitrobenzene oxidation. And it should be emphasized that *p*-hydroxyphenyl units in compound

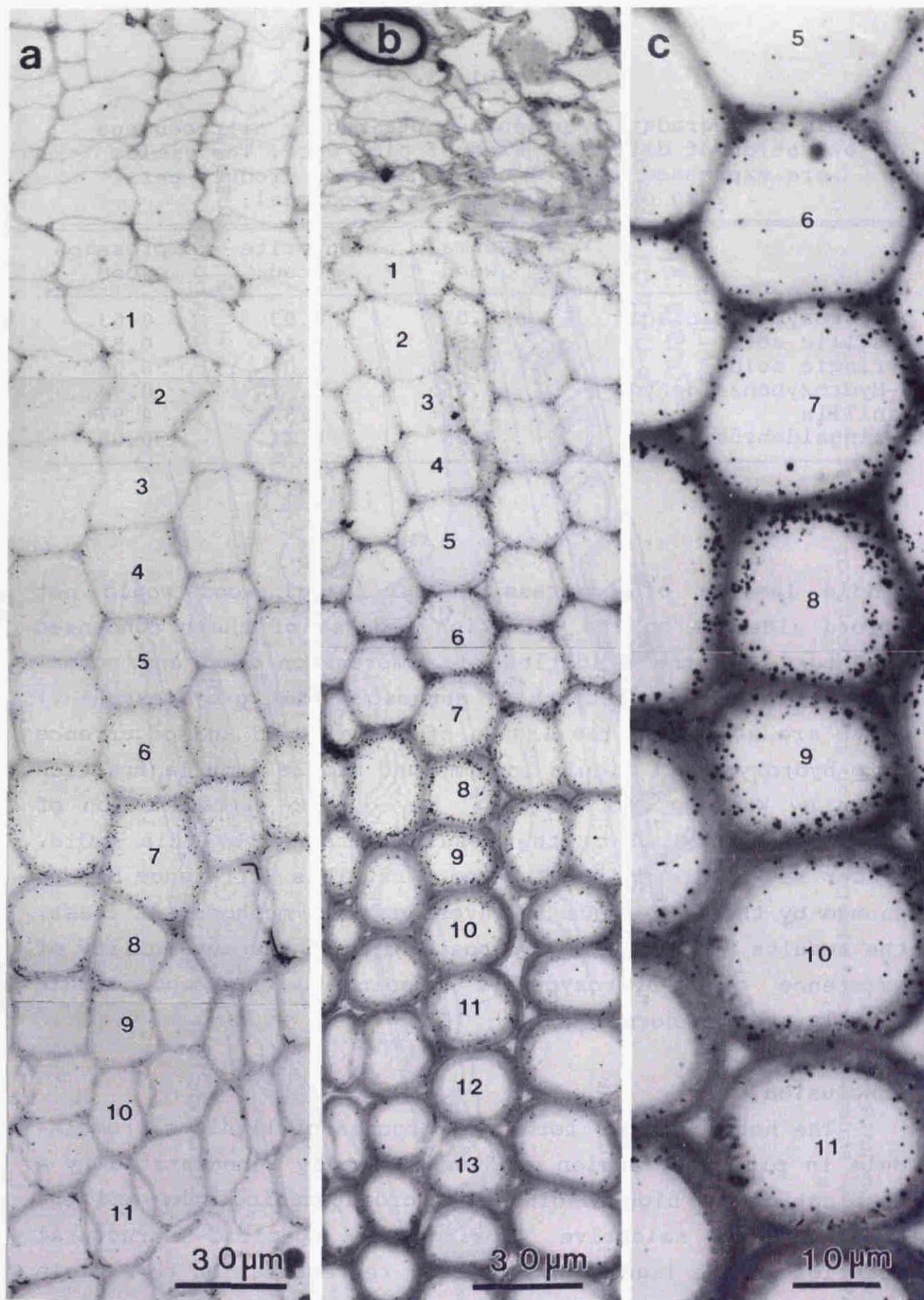


Fig. 22a. Microautoradiogram of differentiating xylem of pine opposite wood administered with syringin-[arom. ring-2-<sup>3</sup>H], b and c: Microautoradiograms of differentiating xylem of pine compression wood administered with syringin-[arom. ring-2-<sup>3</sup>H]. The number in autoradiograms corresponds to the cell number in Fig. 18.

**Table 3**

Yield of degradation products obtained by nitrobenzene oxidation of different kind of pine wood. The yields are expressed as  $\mu\text{mol}$  of degradation product per 20mg of extractive free wood meal.

	Normal wood	Opposite wood	Compression wood
p-Hydroxybenzoic acid	0.04	0.03	0.03
Vanillic acid	1.50	0.40	0.51
Syringic acid	0.04	0.03	0.05
p-Hydroxybenzaldehyde	0.05	0.11	0.94
Vanillin	5.23	3.52	4.97
Syringaldehyde	0.26	0.11	0.05

middle lamella of compression and normal wood would not afford aldehyde on the oxidation because of their condensed structure. By the oxidation of compression wood and normal wood of spruce, Westermark<sup>19)</sup> suggested that p-hydroxyphenyl units are absent in the lignin of normal wood and occurrence of p-hydroxyphenyl lignin in compound middle lamella fraction shown by Whiting and Goring<sup>18)</sup> may due to contamination of compression wood. But, the results obtained by this radio-tracer method are different from hers. This difference may be caused by the difference in investigating methods. At least, the results by biogenetic approach suggest the possibility of existence of p-hydroxyphenyl lignin in compound middle lamella even in normal wood.

### Conclusion

The heterogeneous formation process of lignin macromolecule in pine compression wood was visually demonstrated by a combination of high-resolution microautoradiography and the technique of selective labeling of specific structural moieties in the lignin. A schematic representation to explain the process of deposition of three structural units in compression wood was shown in **Fig. 23**. In compression wood, the order of deposition of lignin building stones,

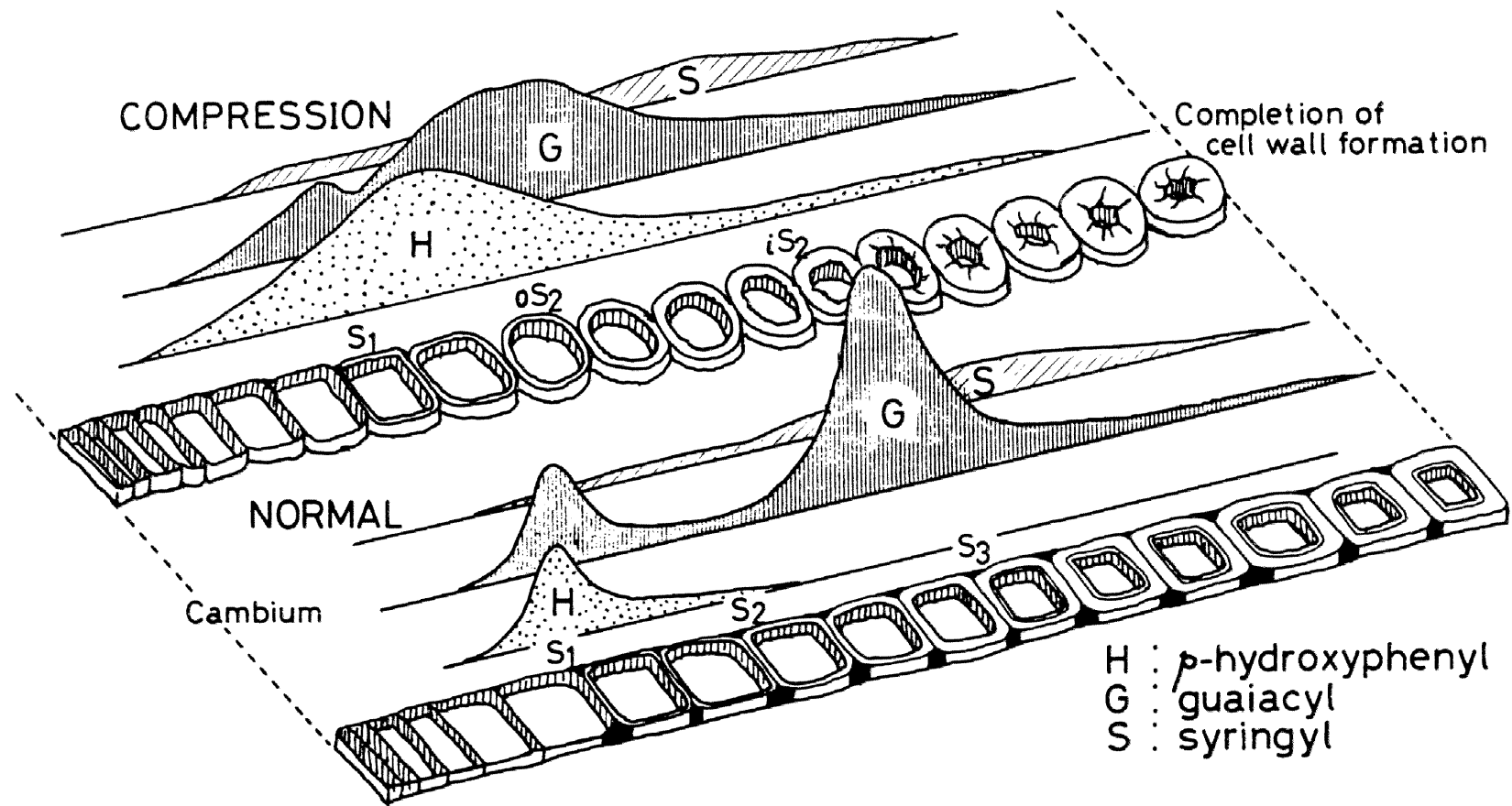
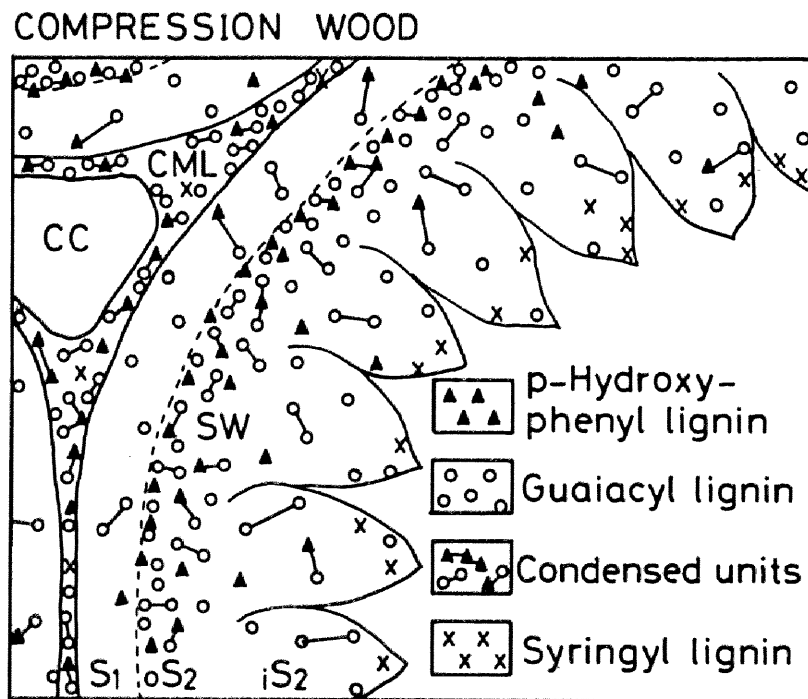


Fig. 23. A schematic representation of the process of deposition of three kinds of lignin structural units.

p-hydroxyphenyl, guaiacyl and syringyl units, during the formation of cell wall was same as those in normal wood, but their deposition pattern with regard to the differentiation stage, morphological region and period, was quite different from that in normal wood. The process of lignification in differentiating xylem of opposite wood was similar to those observed in normal wood. The characteristic features of the formation of compression wood lignin are (1) the period of lignification in secondary wall is long, (2) the most active lignification occurs in  $\text{oS}_2$  layer and (3) p-hydroxyphenyl units distribute mainly in secondary wall.

The morphological distribution of three kinds of lignin moiety in mature cell wall of compression wood was estimated by integration of their incorporation patterns, as shown in Fig. 24.



**Fig. 24.** A schematic representation of morphological distribution of various structural moieties in mature cell wall of pine tracheid of compression wood.

CC: cell corner, CML: compound middle lamella, SW: Secondary wall

### 3.3. Ginkgo

Ginkgo biloba is one of the oldest still living trees on the earth. The vascular tissue of this tree is very similar to that of conifers. The wood is also similar to that of conifers except for the irregularity in size and shape of tracheids<sup>51</sup>). The chemical properties of the ginkgo wood is also similar to that of the coniferous wood<sup>46</sup>), and the ginkgo lignin is a guaiacyl type. But the pattern of fertilization of ginkgo tree is different from that of conifers. It is very interesting to investigate the formation and structure of ginkgo lignin to elucidate the relation between lignin structure and evolution of woody plant lignins.

This chapter deals with the process of formation of protolignin macromolecule in ginkgo visualized by microautoradiography. The deposition pattern of *p*-hydroxyphenyl, guaiacyl and syringyl moieties in the cell wall of differentiating xylem was examined, and heterogeneous distribution of condensed structures in *p*-hydroxyphenyl and guaiacyl lignin was estimated in ginkgo xylem. Labeled precursors for specific labeling of each units of lignin were shown in **Fig. 25**.

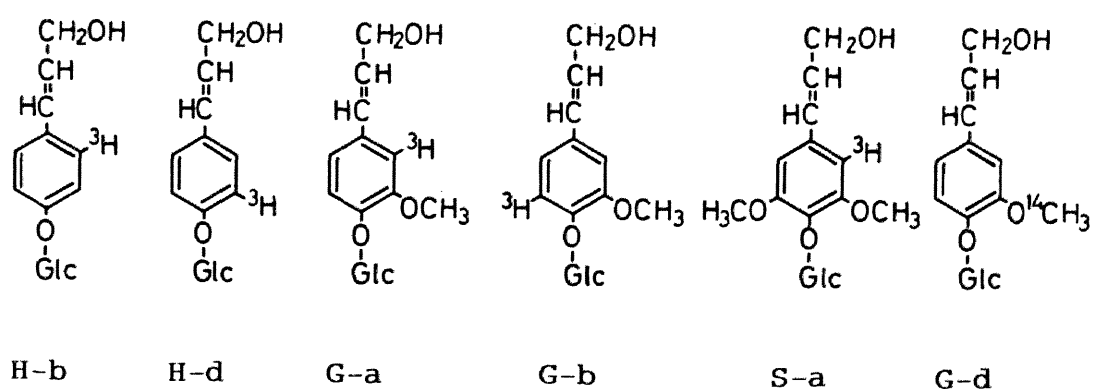


**Fig. 25.** Precursors used for labeling of ginkgo lignin.

### Selectivity of labeling

The radioactivity of each fraction prepared from the specifically labeled wood meal according to Fig. 26. is shown in Table 4. The majority of the radioactivity were in the E fraction (61.1-80.0%) and the radioactivity in the wood residues (fraction A) was very low (0.5-2.0%) in every sample. This is because of the fact that the radioactivity incorporated exclusively into lignin from labeled precursors (H-b - S-a). In the samples administered with precursor H-b and H-d, 20.2% and 27.6% of radioactivity were in p-hydroxybenzaldehyde respectively. The difference between two samples is ascribed to the partial removal of  $^3\text{H}$  at position 3 of aromatic ring of precursor H-d. When condensed structures are formed or the methoxylation is occurred at position 3 or/and 5 of p-hydroxyphenyl unit, the  $^3\text{H}$  is removed.

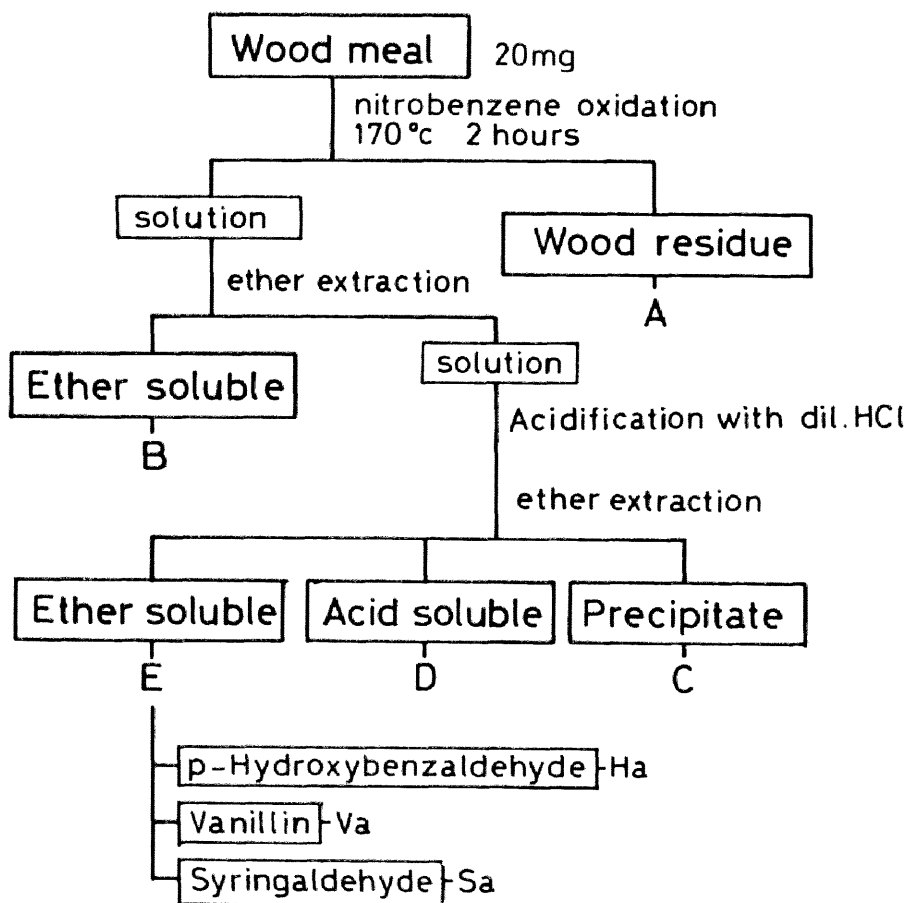


Fig. 26. Fractionation of oxidation products of ginkgo wood.

**Table 4**

Distribution of radioactivity in nitrobenzene oxidation products from specifically labeled ginkgo wood (20mg)

Fractions in Fig.26.	Incorporation of radioactivity ( $^3\text{H} \times 10^3\text{Bq}$ )					
	Precursors administered					
	H-b	H-d	G-a	G-b	S-a	
Total (Wood meal)	3.58( 100)*	5.89( 100)	20.6( 100)	4.79( 100)	4.06( 100)	
A	0.03( 0.9)	0.11( 2.0)	0.11( 0.5)	0.06( 1.3)	0.06( 1.5)	
B	0.01( 0.2)	0.02( 0.3)	0.04( 0.2)	0.01( 0.2)	0.01( 0.1)	
C	0.20( 5.7)	0.27( 4.5)	1.32( 6.4)	0.15( 3.1)	0.13( 3.2)	
D	0.58(16.3)	1.18(20.1)	5.79(28.1)	1.48(30.8)	1.35(33.3)	
E	2.76(80.0)	4.31(73.1)	13.37(64.8)	3.10(64.7)	2.51(61.1)	
E {	Ha	0.72(20.2)	1.63(27.6)	0.02( 0.5)	0.01( 0.3)	0.00( 0.1)
	Va	0.21( 5.8)	0.27( 4.6)	4.91(23.8)	2.92(61.0)	0.01( 0.2)
	Sa	0.03( 0.9)	0.09( 1.5)	0.12( 3.0)	0.08( 1.6)	1.19(29.2)

\* Percent of total activity in wood meal

The radioactivity in wood meal administered with precursor **G-a** ( $20.6 \times 10^3 \text{Bq}$ ) for labeling of guaiacyl type lignins was much higher than that administered with precursor **G-b** ( $4.79 \times 10^3 \text{Bq}$ ). The sample administered with precursor **G-a** gave vanillin which carried 23.8% of radioactivity. While, in the sample administered with precursor **G-b**, 61.0% of radioactivity was found in vanillin. These differences are reasonable results because  $^3\text{H}$  at position 5 of aromatic ring of precursor **G-b** is removed by the formation of condensed structure with bond at this position<sup>21</sup>). Thus the sample in which only non-condensed guaiacyl units were labeled by administration of precursor **G-b** gives vanillin in high yield of 61.0% by the oxidation.

The wood meal obtained from the xylem administered with precursor **S-a** gave syringaldehyde with 29.2% of radioactivity. This shows that syringyl moieties in lignin do not afford syringaldehyde in quantitative yield by the alkaline nitrobenzene oxidation. The radioactivity in acid soluble fraction (**D**) from the sample administered with precursor **S-a** was the highest among 5 samples and that administered with **H-b** was lowest. It is interesting that acid soluble lignin fragments are derived in larger amount from non-condensed type lignin than from condensed type lignin.

Distribution of radioactivity in the aromatic aldehydes (**Ha**, **Va** and **Sa**) were shown in **Fig. 27**. to give the degree of selectivity of labeling from each labeled precursor. Except for the *p*-hydroxyphenyl units (precursor **H-b** and **H-d**), the selectivity of labeling the structural units corresponding to the administered precursors was high enough. *p*-Glucocoumaryl alcohol-[arom. ring-2- $^3\text{H}$ ] (**H-b**) and -[arom. ring-3- $^3\text{H}$ ] (**H-d**) administered to the differentiating xylem were partly converted to guaiacyl units as shown by the partial incorporation of radioactivity into vanillin (**Va**). The apparent reduction of the interconversion seen in the sample administered with precursor **H-d** would be due to the removal of  $^3\text{H}$  at position 3 of aromatic ring by the methoxylation at this position, which results in the low radioactivity in guaiacyl units.

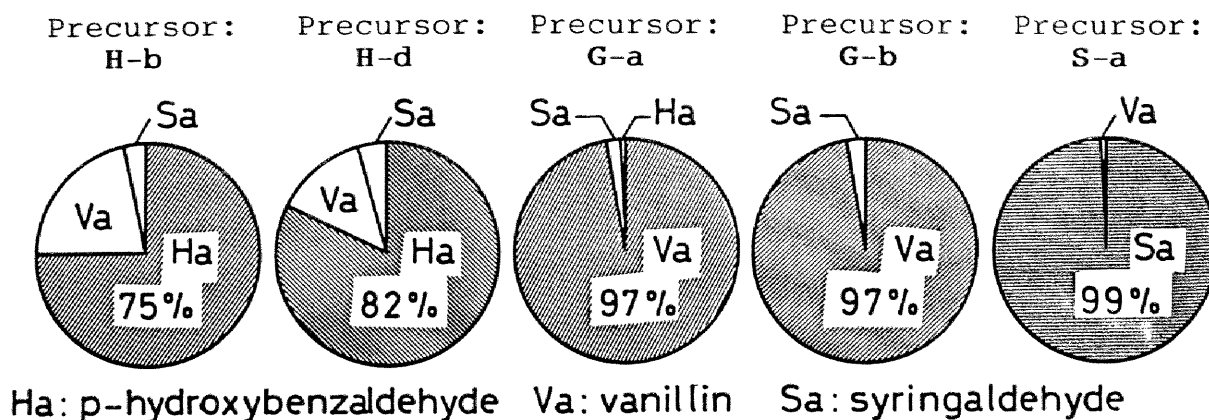


Fig. 27. Distribution of radioactivity in the aromatic aldehydes derived from specifically labeled ginkgo wood by nitrobenzene oxidation.

#### Microautoradiography

Fig. 28. shows the microautoradiogram of newly formed ginkgo xylem administered with coniferin-[OMe- $^{14}\text{C}$ ] (G-d). The microautoradiogram of  $^{14}\text{C}$ -labeled sample is usually emphasized in contrast because  $^{14}\text{C}$  is higher energy emitter than  $^3\text{H}$ . So,  $^{14}\text{C}$ -labeling is suitable to visualize a general incorporation pattern of the precursor. Coniferin is a specific precursor of guaiacyl units in ginkgo lignin as shown in Table 4, and the methoxyl groups are retained during the polymerization<sup>12)</sup>. From these results, it is considered that silver grains in Fig. 28. indicate the deposition of guaiacyl units. There are two peaks of deposition, the first peak is at the cell corner and compound middle lamella just after the formation of primary wall has finished and formation of outer layer of secondary wall ( $S_1$ ) has started. The second peak appears after the deposition of cellulose microfibrils has started in inner layer of secondary wall ( $S_3$ ). Main lignification occurs in this stage. Similar lignification pattern with two deposition peaks has been observed in the microautoradiograms of differentiating xylem of pine administered with coniferin-[ $\beta$ - $^{14}\text{C}$ ] (3.1.) and L-phenylalanine-[G- $^3\text{H}$ ]<sup>43)</sup>. The incorporation of this precursor in the tracheids was not in uniform manner in the later stage. This suggests that the lignin contents and/or structure in these

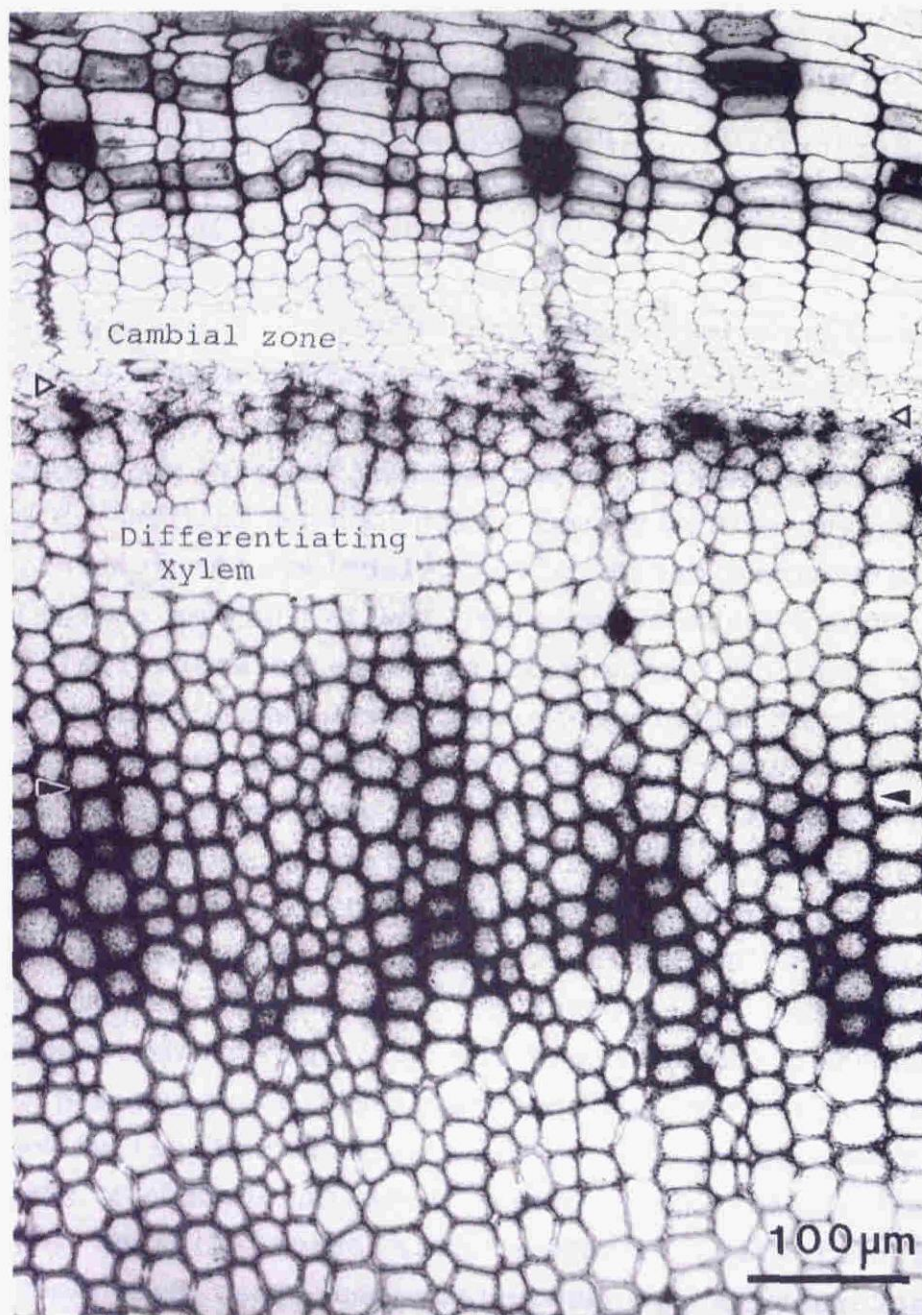


Fig. 28. Microautoradiogram of differentiating xylem of Ginkgo biloba administered with coniferin-[OMe- $^{14}$ C].

▷ Start of S<sub>1</sub> formation. ▶ Start of S<sub>3</sub> formation.

tracheids may not be uniform. This is perhaps due to the fact that ginkgo xylem contains different kind of tracheids<sup>51)</sup> which individually control the lignification.

Because the tissue section labeled by low-energy beta emitter  $^3\text{H}$  can provide a high resolution microautoradiogram, it is possible to estimate semiquantitatively the activity in different morphological regions by silver grain counting (3.1. and 3.2.). The process of formation and morphological distribution was examined by administration of *p*-glucocoumaryl alcohol-[arom. ring-2- $^3\text{H}$ ] (H-b) and -[arom. ring-3- $^3\text{H}$ ] (H-d). Incorporation of *p*-hydroxyphenyl units (Fig. 29a) could be observed mostly in an early stage of cell wall differentiation, and a large portion of *p*-hydroxyphenyl lignin was located in the compound middle lamella (Fig. 30, Fig. 31a). Similar results have been obtained in the microautoradiographic studies of differentiating xylem of pine (3.1.). The deposition of "non-condensed" *p*-hydroxyphenyl units which have no carbon-carbon bonds at the labeled position 3 of the aromatic ring (but they may have at position 5) are shown in Fig. 31b. Only 33% of "non-condensed" structures were distributed in compound middle lamella, while 61% of total *p*-hydroxyphenyl units was located in this region. This difference is due to the removal of  $^3\text{H}$  at position 3 by the formation of condensed *p*-hydroxyphenyl units which are rich in the compound middle lamella region of ginkgo wood. By means of the analysis of methoxyl content Whiting and Goring<sup>18)</sup> indicated that the tissue fraction from middle lamella of spruce wood contained considerable amount of *p*-hydroxyphenyl units. But it was shown that *p*-hydroxybenzaldehyde and *p*-hydroxybenzoic acid found only trace amount in the oxidation products of middle lamella fraction<sup>19)</sup>. This contradiction may be explained by the high condensation of *p*-hydroxyphenyl units in the compound middle lamella lignin, which can not give corresponding monomeric aldehyde and acid on oxidation.

Fig. 29b shows a microautoradiogram of the ginkgo xylem administered with coniferin-[arom. ring-2- $^3\text{H}$ ]. It is obvious that the deposition of guaiacyl lignin proceeds in three

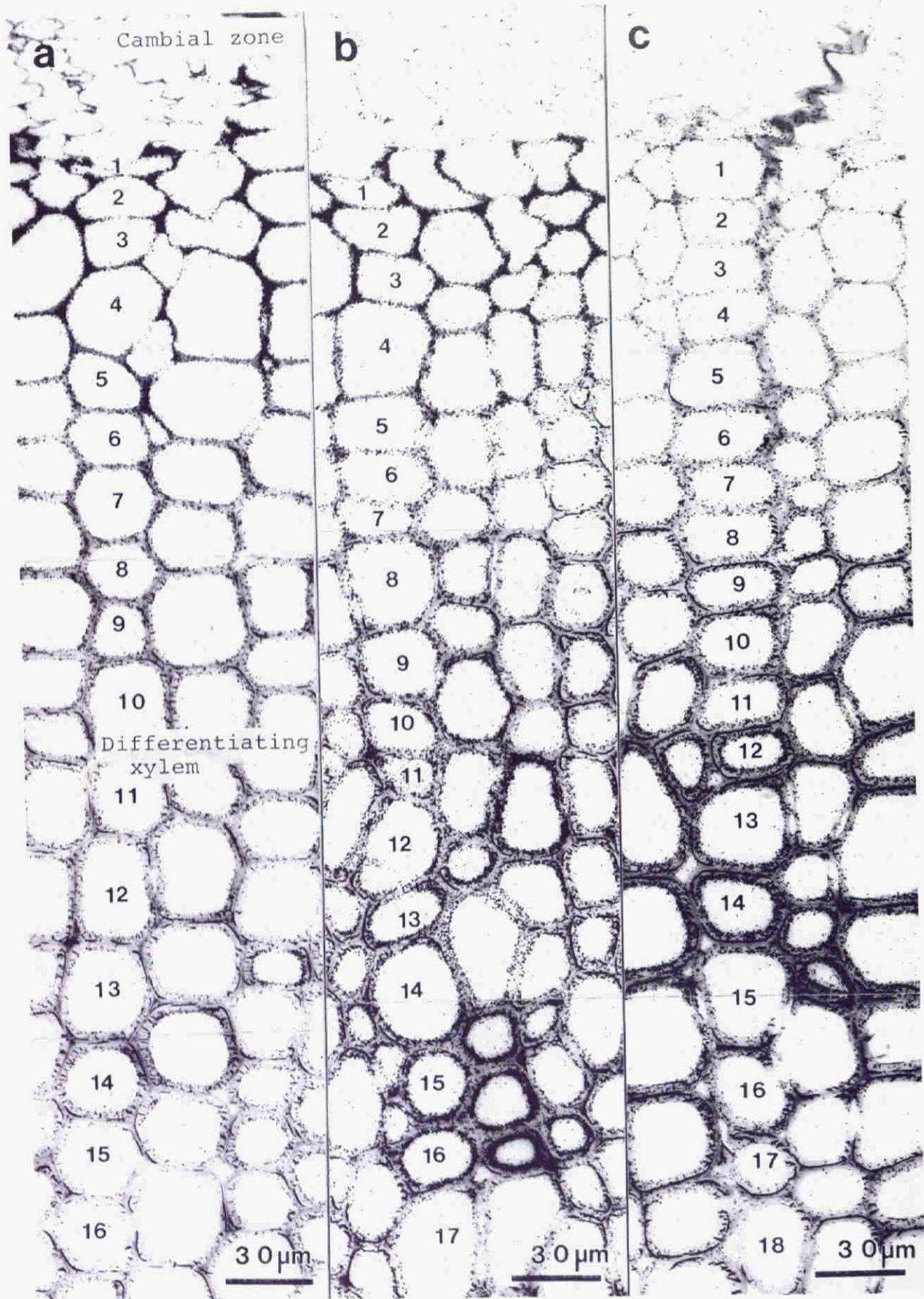


Fig. 29. Microautoradiogram of differentiating xylem of *Ginkgo biloba* administered with p-glucocoumaryl alcohol-[arom. ring-2- $^3\text{H}$ ] (a), coniferin-[arom. ring-2- $^3\text{H}$ ] (b) and coniferin-[arom. ring-5- $^3\text{H}$ ] (c). The number in microautoradiograms shows the order of cell counted from the cell in which formation of  $\text{S}_1$  started.

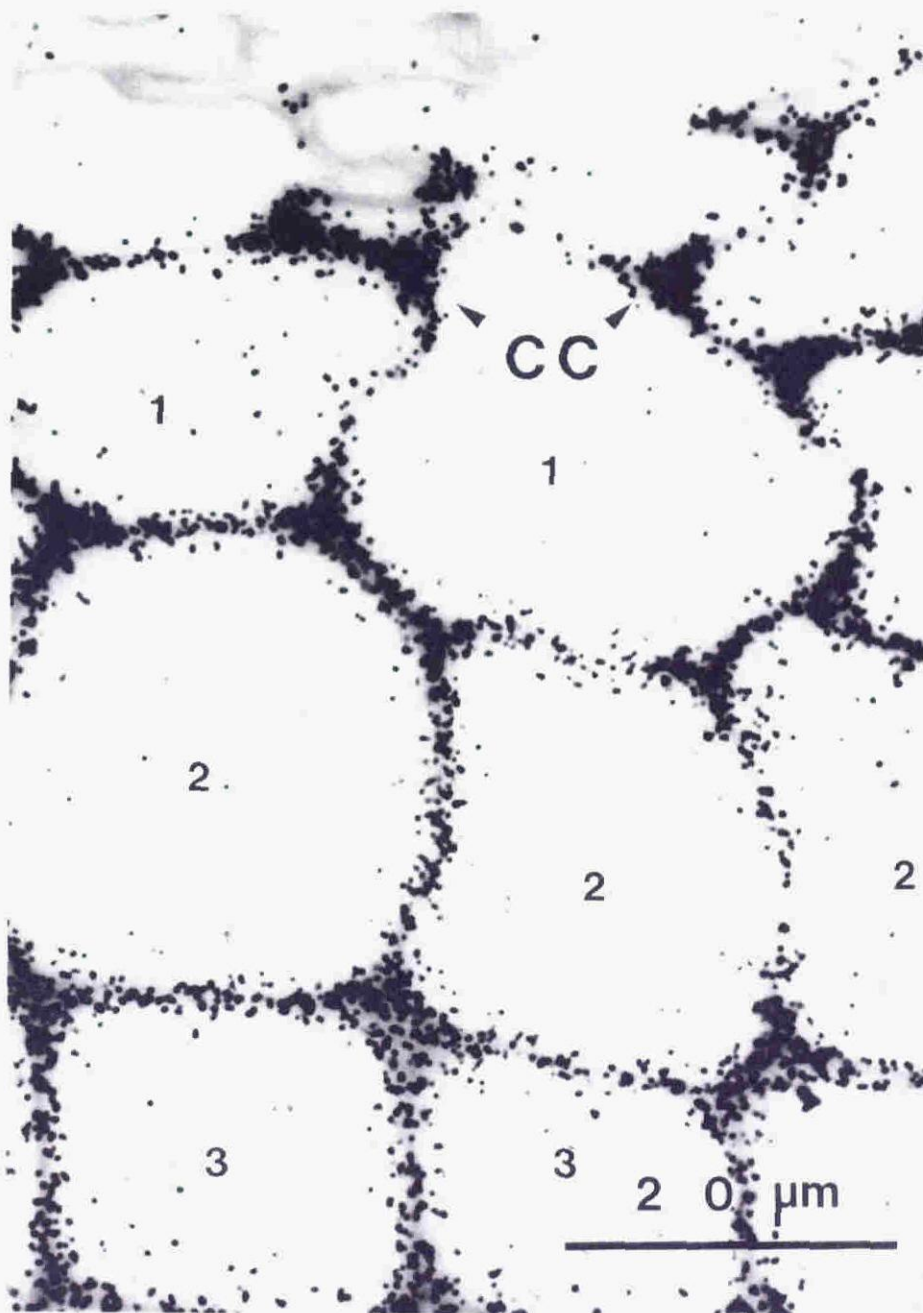
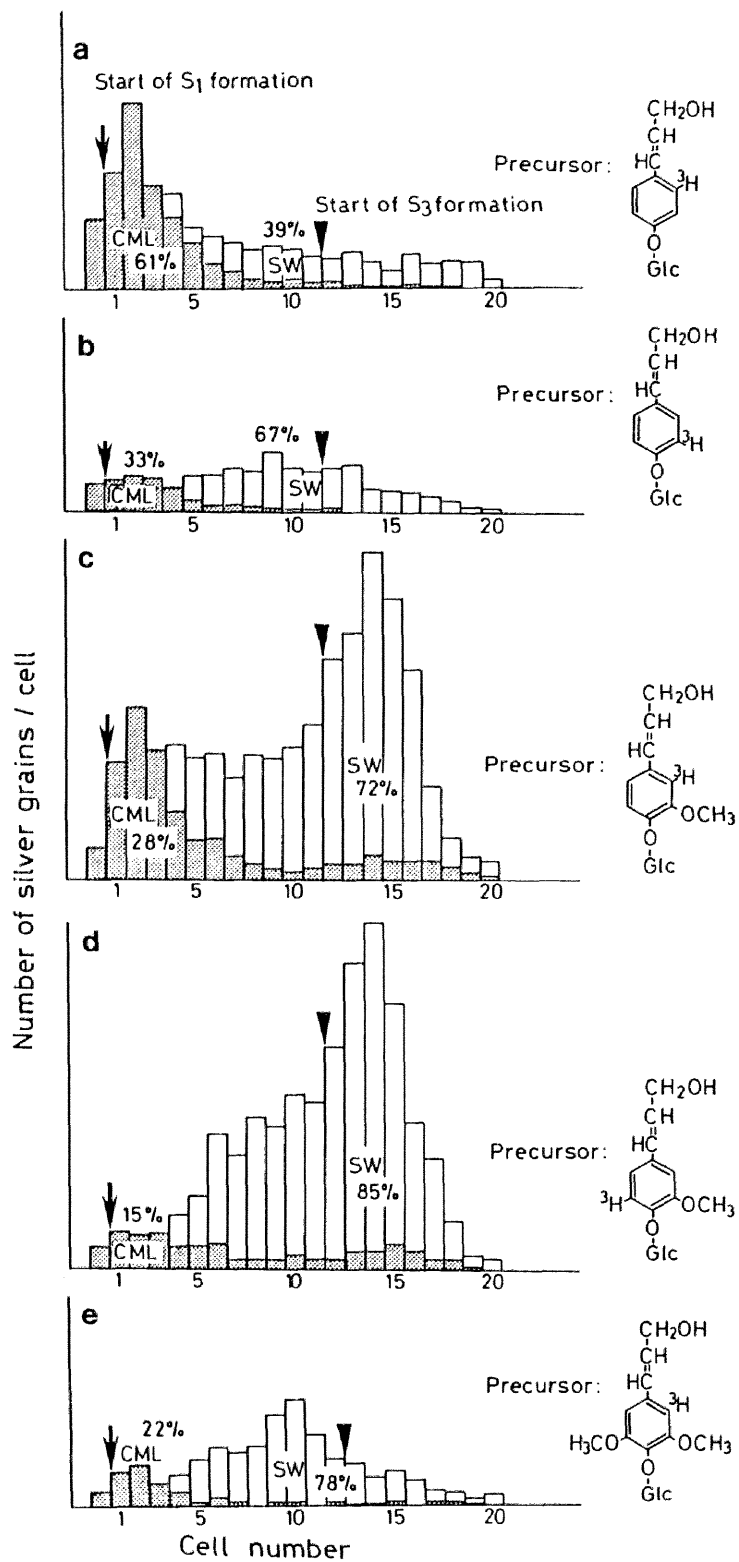


Fig. 30. Microautoradiogram of differentiating xylem of *Ginkgo biloba* administered with *p*-glucocoumaryl alcohol-[arom. ring-2-<sup>3</sup>H]. The number in microautoradiograms shows the order of cell counted from the cell in which formation of S<sub>1</sub> started.  
CC: cell corner



**Fig. 31.** Distributions of silver grains in microautoradiograms of ginkgo xylem administered with labeled precursors. The cell number shows the order of cell counted from the cell in which formation of S<sub>1</sub> started.

distinct stage. The first stage occurs at the cell corners and in the compound middle lamella region after the start of deposition of carbohydrates in  $S_1$ . The second is the slow lignification stage. During this phase, the carbohydrates are deposited in the  $S_2$  layer. The main lignification occurs in the third stage after the start of  $S_3$  formation. Similar result has been shown in the microautoradiogram of pine (3.1.).

It has been shown that the amount of condensed guaiacyl units of pine formed in an early stage of xylem differentiation is larger than those formed in a later stage<sup>13)</sup>. In this study, the removal of  $^3\text{H}$  at position 5 of guaiacyl ring during the formation of condensed structure has been determined to estimate the formation of condensed guaiacyl units in ginkgo wood. The deposition of all guaiacyl units (precursor: coniferin-[arom. ring-2- $^3\text{H}$ ]) and non-condensed guaiacyl units (precursor: coniferin-[arom. ring-5- $^3\text{H}$ ]) were shown in **Fig. 29b** and **c**. Since the number of silver grains owing to the  $^3\text{H}$  at position 2 and position 5 of guaiacyl ring is proportional to the amount of newly formed total and non-condensed guaiacyl units, respectively, the difference between these two values corresponds to the amount of condensed structures. The difference in the distribution of silver grains between two microautoradiograms (**Fig. 31c** and **d**) indicates that the lignin formed in the compound middle lamella regions at an early stage of xylem differentiation contains much more condensed units than that formed at a later stage in secondary wall. These results are similar to those observed in the microautoradiograms of pine normal wood (3.1.). The factors being favorable to the formation of condensed guaiacyl structures have been discussed in 3.1..

The process of formation of syringyl lignin was examined by administration of syringin-[arom. ring-2- $^3\text{H}$ ] to the ginkgo xylem. This was largely incorporated in the cytoplasm inside the cell wall at the middle stage of xylem differentiation (**Fig. 32**, arrow). This indicates that the incorporation may not be related to the biosynthesis of the ginkgo lignin. The distribution of syringyl units were shown in **Fig. 31e**. The

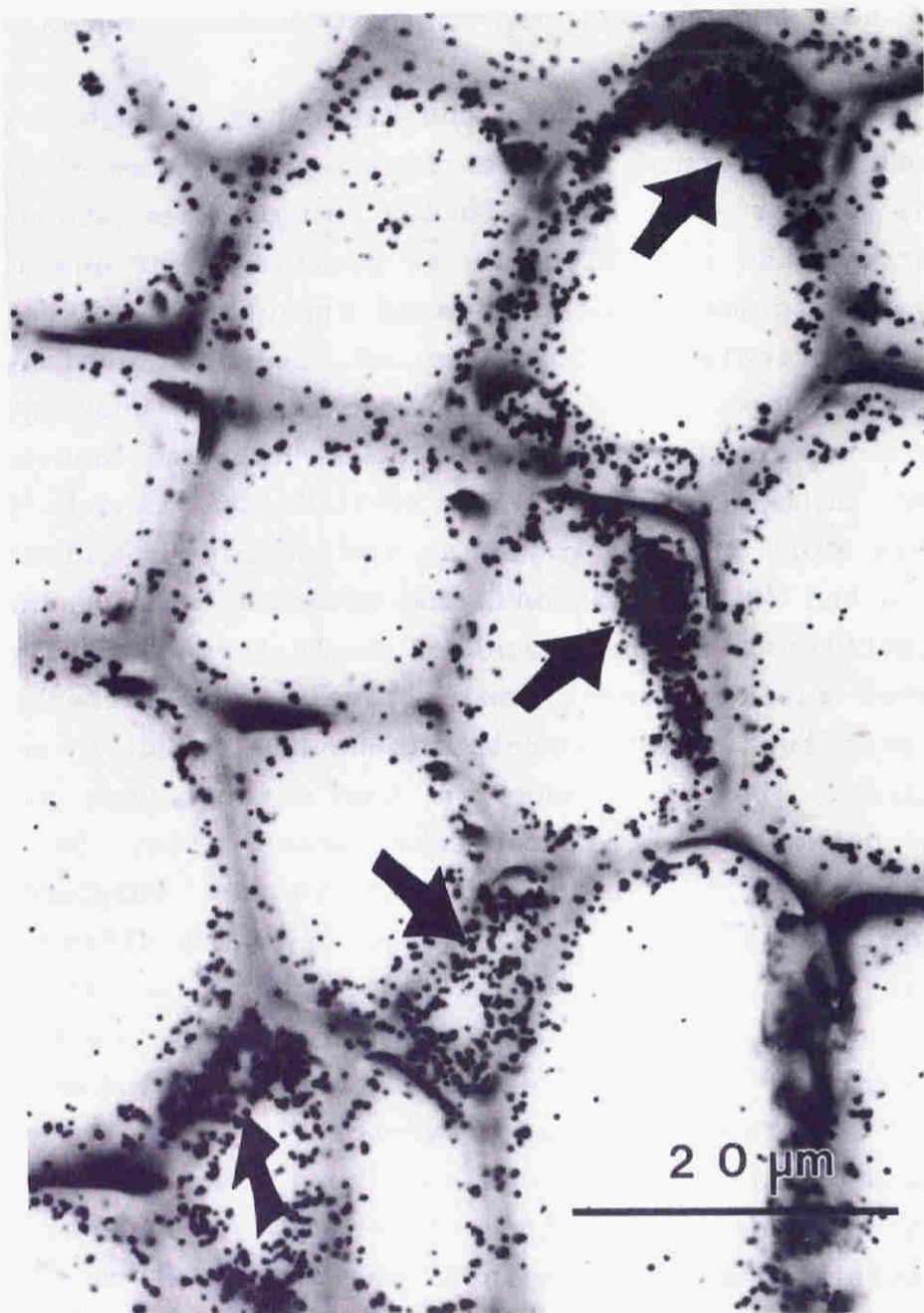


Fig. 32. Microautoradiogram of differentiating xylem of *Ginkgo biloba* administered with syringin-[arom. ring-2-<sup>3</sup>H].

period of its main deposition was different from that of guaiacyl units. This result suggests that syringyl units do not belong to the main part of ginkgo lignin.

The reason why each labeled precursor was incorporated into specific morphological regions may be explained by the substrate specificity of  $\beta$ -glucosidase which catalyzes the hydrolysis of monolignol glucosides to corresponding alcohols. It has been shown that the cell-wall-bound  $\beta$ -glucosidase in spruce seedlings has different substrate specificity towards the three kinds of monolignol glucosides<sup>45</sup>). It has been shown in a series of autoradiographic studies that each precursor monolignol was incorporated into the specific morphological region in a conifer, pine normal- (3.1.), opposite- and compression wood (3.2.). These results indicate that the deposition of *p*-hydroxyphenyl, guaiacyl and syringyl lignins occurs in the same order as in the biosynthesis of the corresponding monolignols. Considering the process of evolution of plant kingdom, it is obvious that biogenetic pattern and fundamental structure of wood lignin had been already established at the time the oldest tree species, genus *Ginkgo* appeared on the earth, back to 210 million years from the present<sup>46</sup>).

#### **Analysis of degradation products**

HPLC profile of the degradation products of ginkgo xylem by alkaline nitrobenzene oxidation was shown in **Fig 33a** and **b**. To compare the normal wood with the compression wood, two samples obtained from the same tree were subjected to the oxidation. In both chromatograms, the peaks of *p*-hydroxybenzoic acid, vanillic acid, *p*-hydroxybenzaldehyde and vanillin could be observed. The amount of *p*-hydroxybenzaldehyde in the compression wood sample was over tree times as large as that in the normal wood sample, while the amounts of other compounds were almost equal (**Table 5**). However, this difference between normal and compression wood of ginkgo is much smaller than that of coniferous woods<sup>19</sup>) (**Table 3**). The compression wood of ginkgo is not a typical one with respect

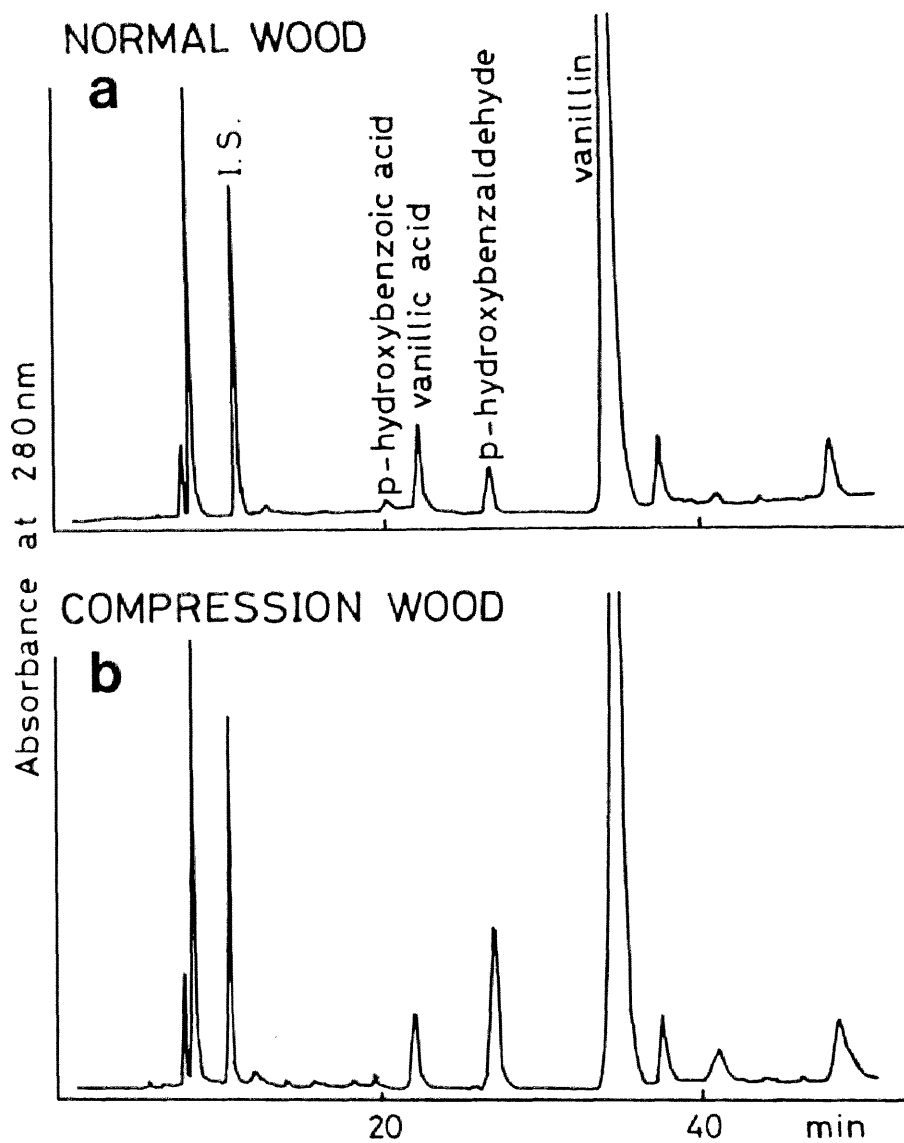


**Fig. 33.** HPLC profiles of products from nitrobenzene oxidation of ginkgo normal wood (a) and compression wood (b). I.S. : Internal standard, 3,5-dihydroxybenzoic acid.

**Table 5**

Yield of degradation products obtained by nitrobenzene oxidation of ginkgo wood. The yields are expressed as  $\mu\text{mol}$  of product per 20mg of extractive free wood meal.

	Normal wood	Compression wood
p-Hydroxybenzoic acid	0.12( $\mu\text{mol}$ )	0.12( $\mu\text{mol}$ )
Vanillic acid	0.70	0.63
Syringic acid	-	-
p-Hydroxybenzaldehyde	0.16	0.55
Vanillin	7.24	6.97
Syringaldehyde	0.11	0.06

to the morphological aspects, because ginkgo compression wood does not have the helical cavities in the cell wall of tracheid<sup>52</sup>). This characteristic feature in morphology of ginkgo compression wood may related to the low content of p-hydroxyphenyl units in the lignin. In addition, it is also noted that the ginkgo normal wood gave a high amount of p-hydroxybenzoic acid and p-hydroxybenzaldehyde by the oxidation. The amount of these two compounds was 3.5% of the total amount of 6 compounds. This value is much higher than that observed in the oxidation products of spruce wood, which gives these p-hydroxyphenyl-related-compounds in trace amount (19,53). Erickson and Miksche<sup>54</sup>) indicated the similar result by permanganate oxidation. They suggested that the ginkgo normal wood sample used in their experiment would contain a part of the compression wood. However, the tissue used in this work as a normal wood did not contain any part of compression wood; this was confirmed by the light-microscopic and polarization-microscopic observation.

The amounts of syringic acid and syringaldehyde were very low (Table 5). Obst and Landucci<sup>55</sup>) indicated by pyrolysis-gas chromatography that syringyl content of ginkgo wood was much lower than that of Norway spruce or red pine wood. It seems that syringyl units is not one of the main components of ginkgo lignin.

## Conclusion

The heterogeneous formation process of the ginkgo lignin macromolecule was demonstrated by a combination of high-resolution microautoradiography and the technique of selective labeling of specific structural moieties in the lignin. The lignification process of ginkgo is very similar to that of conifers. *p*-Hydroxyphenyl lignin was formed in the cell corner and compound middle lamella at the initial stage of lignification just after the  $S_1$  formation started. Guaiacyl lignin was formed in compound middle lamella at an early stage and in the secondary wall at a later stage when the  $S_3$  layer was formed. The lignin deposited in the compound middle lamella was highly condensed compared with that in the secondary wall both in the cases of *p*-hydroxyphenyl and guaiacyl units. Syringyl lignin was considered not to be main part of ginkgo lignin.

These observations indicate that lignin develops in the differentiating cell wall under definite biochemical controls to a macromolecule which is heterogeneous in structure and specific to different morphological regions.

## CHAPTER 4

### Formation and Structure of Lignin in Angiosperms

Angiosperm lignins consist mainly of syringylpropane units and guaiacylpropane units. It has been shown that the ratios of syringyl to guaiacyl units vary in different morphological regions<sup>1,2,5</sup>). It is very important to reveal the localization of syringyl and guaiacyl units. But most papers dealing with hardwood lignin do not pay much attention to *p*-hydroxyphenylpropane units in lignin. Most hardwood lignins give a small amount of compounds derived from *p*-hydroxyphenylpropane units by oxidative degradation. But they do not provide conclusive proof that *p*-hydroxyphenyl unit is not one of the important building stones of angiosperm lignins. However, it has been shown that *p*-hydroxyphenyl units in lignin can not be estimated quantitatively by degradative method<sup>20,21</sup>). Therefore, it is expected that *p*-hydroxyphenylpropane units exists also in hardwood as one of the main building stones.

In this study, *p*-glucocoumaryl alcohol-[arom. ring-2-<sup>3</sup>H] (H-b), coniferin-[arom. ring-2-<sup>3</sup>H] (G-a), -[β-<sup>14</sup>C] (G-c) and syringin-[arom. ring-2-<sup>3</sup>H] (S-a), -[β-<sup>14</sup>C] (S-b) was administered to differentiating xylem of magnolia (4.1.), lilac (4.2.), beech (4.3.) or poplar (4.4.), and the incorporation of each units into cell wall lignin were visualized by microautoradiography. In addition, the process of deposition of <sup>14</sup>C-labeled carbohydrates into the differentiating xylem was examined.

#### 4.1. Magnolia

It is considered that *p*-glucocoumaryl alcohol, coniferin and syringin were suitable precursors of *p*-hydroxyphenyl, guaiacyl and syringyl propane units in magnolia lignin

respectively. Because coniferin and syringin were detected in the cambial sap of magnolia<sup>25)</sup> and in gymnosperms (Chapter 3) selective radio-labeling of each units of lignin was attained by administration of these tritiated glucosides.

### Selectivity in labeling guaiacyl and syringyl moieties

**Table 6** shows the incorporation of radioactivity from syringin-[arom. ring-2-<sup>3</sup>H] or coniferin-[arom. ring-2-<sup>3</sup>H] into syringyl or guaiacyl moieties of the lignin in newly formed xylem as determined by nitrobenzene oxidation. While the molar **Sa/Va** ratio of wood tissues administered with labeled coniferin and syringin were 1.74 (molar **Va/Sa** ratio: 0.57) and 1.66 respectively, the <sup>3</sup>H-**Va/Sa** ratio of the former and <sup>3</sup>H-**Sa/Va** ratio of the latter were high value of 8.69 and 115, respectively. This indicates that the rate of interconversion between guaiacyl and syringyl units during 3 hours metabolism was appreciably low, although a small part of guaiacyl units was converted to syringyl units. Thus, 90 and 99% of radioactivities in the wood tissues administered with labeled coniferin and syringin respectively were attributed to the corresponding structural moieties.

**Table 6**

Selectivity in labeling of syringyl and guaiacyl units based on the specific radioactivity of syringaldehyde (**Sa**) and vanillin (**Va**) by nitrobenzene oxidation

Precursor	Coniferin-[a.r-2- <sup>3</sup> H]		Syringin-[a.r-2- <sup>3</sup> H]	
	Sa	Va	Sa	Va
Aldehyde				
μmol <sup>1)</sup>	2.30	1.32	2.26	1.36
molar ratio	<b>Va/Sa:0.57(Sa/Va:1.74)</b>		<b>Sa/Va:1.66</b>	
<sup>3</sup> H Bq <sup>1)</sup>	2.0	17.2	78.5	0.7
<sup>3</sup> H-ratio	<b>Va/Sa:8.69</b>		<b>Sa/Va:115</b>	
<sup>3</sup> H-distribution %	10	90	99	1

1) Values from 10mg of extractive free wood meal

### Visualization of formation of lignin

The localization of radio-labeled lignin was visualized by silver grains on the microautoradiogram. The silver grains in **Fig. 34a, b** and **c** shows the deposition of *p*-hydroxyphenyl, guaiacyl and syringyl moieties of protolignin in the cell wall respectively. The microautoradiogram of differentiating xylem of magnolia administered with *p*-glucocoumaryl alcohol-[arom.ring-2-<sup>3</sup>H] (**Fig. 34a**) showed that the deposition of *p*-hydroxyphenyl units of lignin in differentiating xylem occurred mainly during the formation of S<sub>1</sub> layer. The *p*-hydroxyphenyl units distributed mostly in the compound middle lamella region of vessels and fibers (**Fig. 35**). **Fig. 34b** is a microautoradiogram of differentiating xylem of magnolia administered with coniferin-[β-<sup>14</sup>C]. It shows the deposition of guaiacyl units. It is noticeable that deposition of guaiacyl lignin occurred in two peaks. The first deposition of guaiacyl lignin occurred during the formation of S<sub>1</sub> layer (outer layer of secondary wall) and the later deposition occurred after the start of S<sub>3</sub> layer (inner layer of secondary wall) formation. The similar lignification pattern has been observed in microautoradiograms of pine administered with coniferin-[β-<sup>14</sup>C] (3.1.), pine administered with phenylalanine-[G-<sup>3</sup>H]<sup>43</sup>) and also ginkgo administered with coniferin-[OMe-<sup>14</sup>C] (3.3.). The early stage deposition mainly corresponds to the formation of the compound middle lamella lignin. The lignification during this period was remarkable at the cell corners of vessel and fiber. The later deposition mainly corresponds to the formation of secondary wall lignin. The period of lignification of the secondary wall is longer than that of the lignification of the compound middle lamella (**Fig. 34b**). **Fig. 34c** shows a microautoradiogram of differentiating xylem of magnolia administered with syringin-[β-<sup>14</sup>C]. The silver grains indicate the deposition of syringyl units. Syringyl lignin was mostly formed at the late stage of cell wall differentiation (**Fig. 34c**).

To obtain more detailed information about the deposition of guaiacyl and syringyl lignin, <sup>3</sup>H-labeled tissue sections

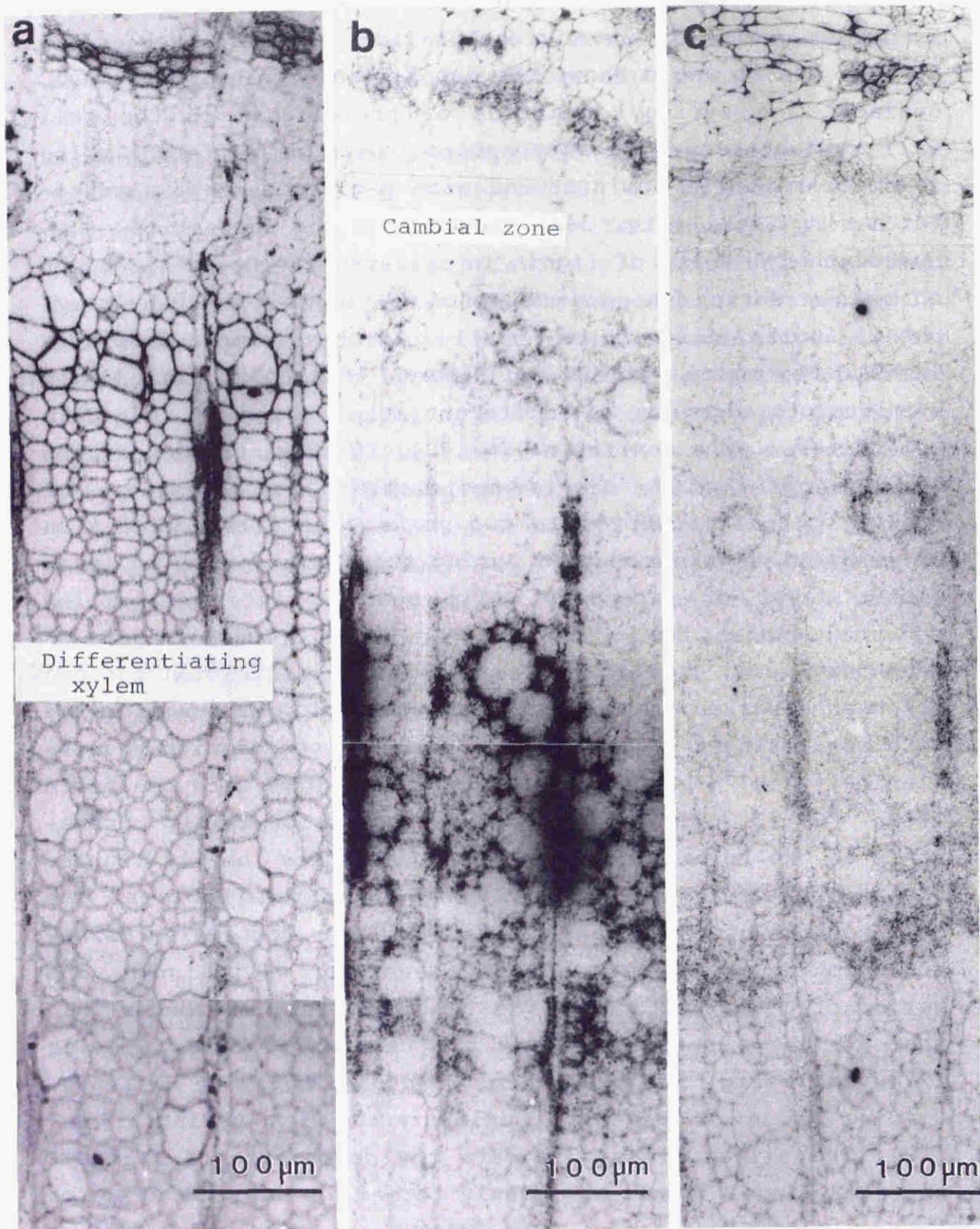


Fig. 34. Microautoradiograms of differentiating xylem of magnolia administered with a: p-glucocoumaryl alcohol-[arom. ring-2- $^3\text{H}$ ], b: coniferin-[ $\beta$ - $^{14}\text{C}$ ] or c: syringin-[ $\beta$ - $^{14}\text{C}$ ].

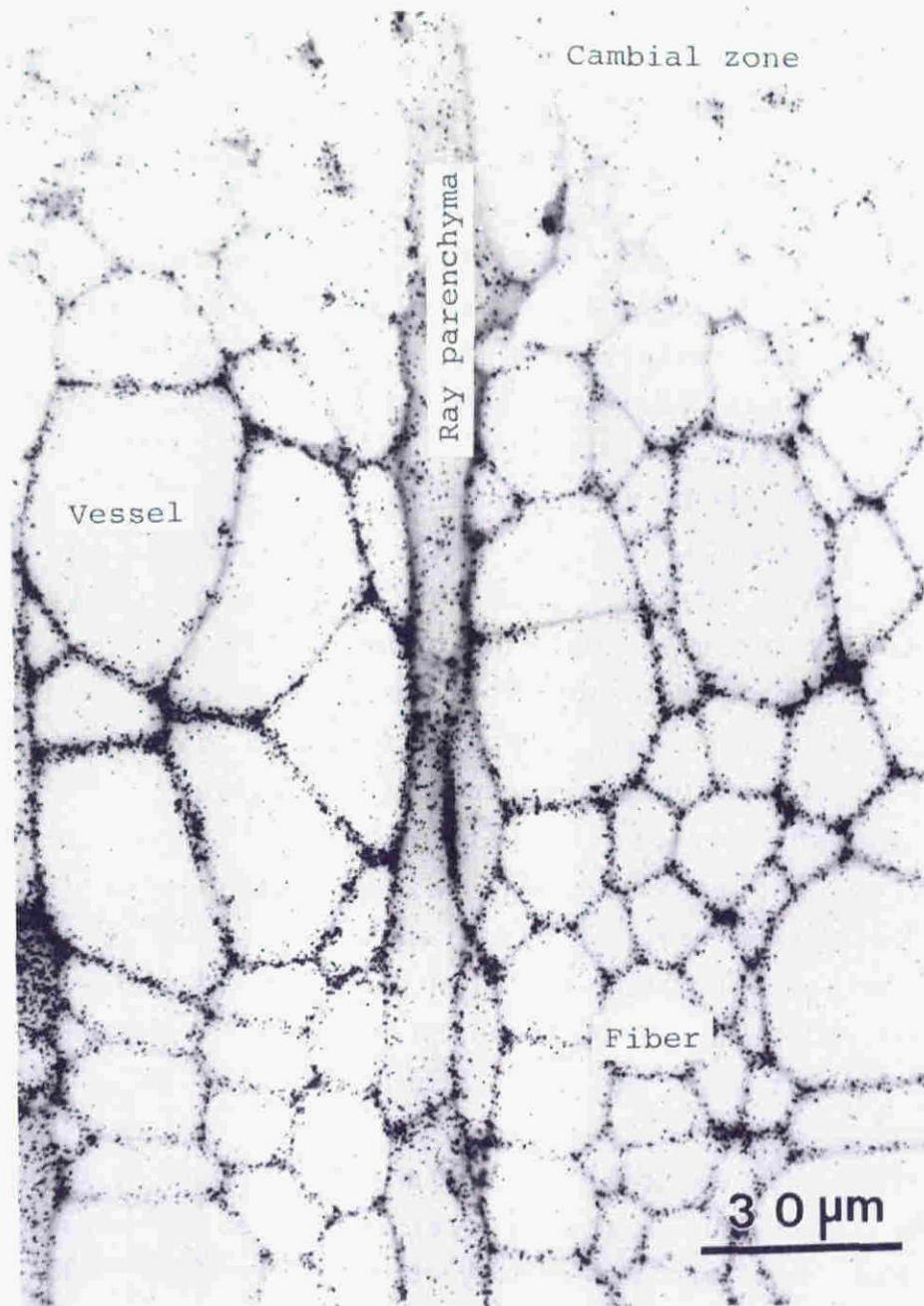


Fig. 35. Microautoradiogram of differentiating xylem at the initial stage of lignification of magnolia administered with *p*-glucocoumaryl alcohol-[arom. ring-2-<sup>3</sup>H]

were also investigated. The radioactivity from coniferin-[arom. ring-2-<sup>3</sup>H] was incorporated into newly formed vessel walls and cell corners in the early stage of xylem differentiation and slightly later in compound middle lamella of fiber (**Fig. 36a** and **Fig. 37. left**). At almost the same stage, formation of outer layer of secondary wall (S<sub>1</sub>) was observed by polarization photomicrograph (**Fig. 37. right**). Moderate incorporation into secondary wall of fiber was observed in the middle stage of xylem differentiation, and also in the late stage (Arrows in **Fig. 36a**). In contrast, the radioactivity from syringin-[arom. ring-2-<sup>3</sup>H] was incorporated significantly into secondary wall of fiber and slightly into vessel wall in the middle stage of xylem differentiation (**Fig. 36b** and **Fig. 38. Left**). The formation of the inner layer of secondary wall (S<sub>3</sub>) started in the middle stage of lignin deposition (**Fig. 38. right**).

The apparent high density incorporation into the ray cell wall is due to the fact that the ray cell wall was tangentially cut into a 2 μm thick section (**Fig. 36**). This was confirmed also by the observation of the sections on polarization microscope. Therefore, the semiquantitative estimation of the lignin deposition based on the silver grain density is not applicable to the ray cells.

The characteristic pattern of incorporation of radioactivity in magnolia was similar to those observed in microautoradiograms of differentiating xylem of poplar which was administered with labeled ferulic acid and sinapic acid in the dark<sup>17</sup>). These results also indicate that coniferin and syringin act as good lignin precursors as ferulic and sinapic acids.

The high selectivity in labeling magnolia lignin enabled us to locate guaiacyl and syringyl moieties more distinctly, and the use of low-energy beta emitter <sup>3</sup>H has provided microautoradiograms of high resolution which permitted semiquantitative measurement of radioactivity by counting the silver grains in different morphological regions (**Fig. 37** and **Fig. 38**). The deposition of guaiacyl and syringyl moieties of magnolia lignin was shown semiquantitatively in **Fig. 39** and

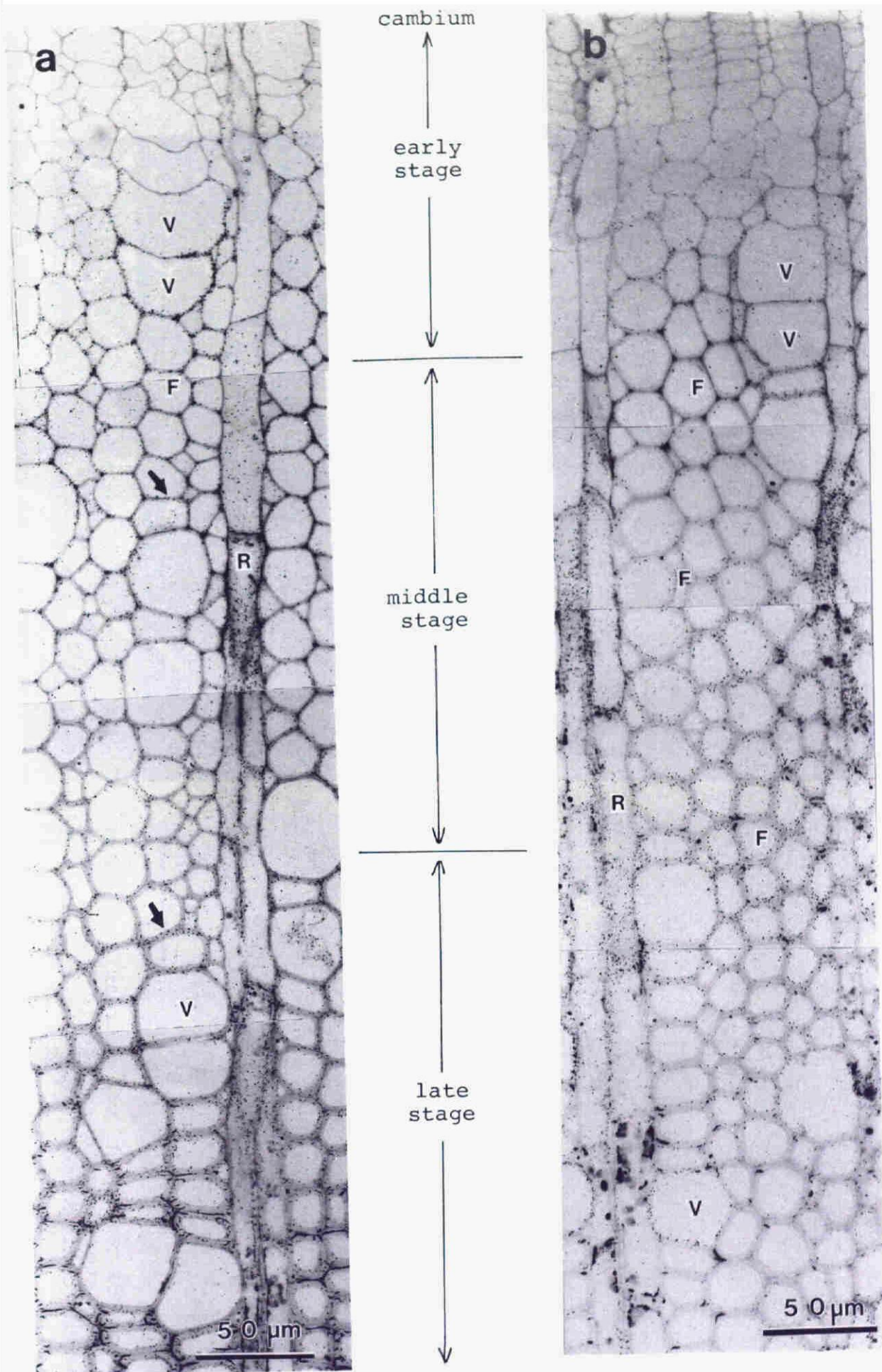
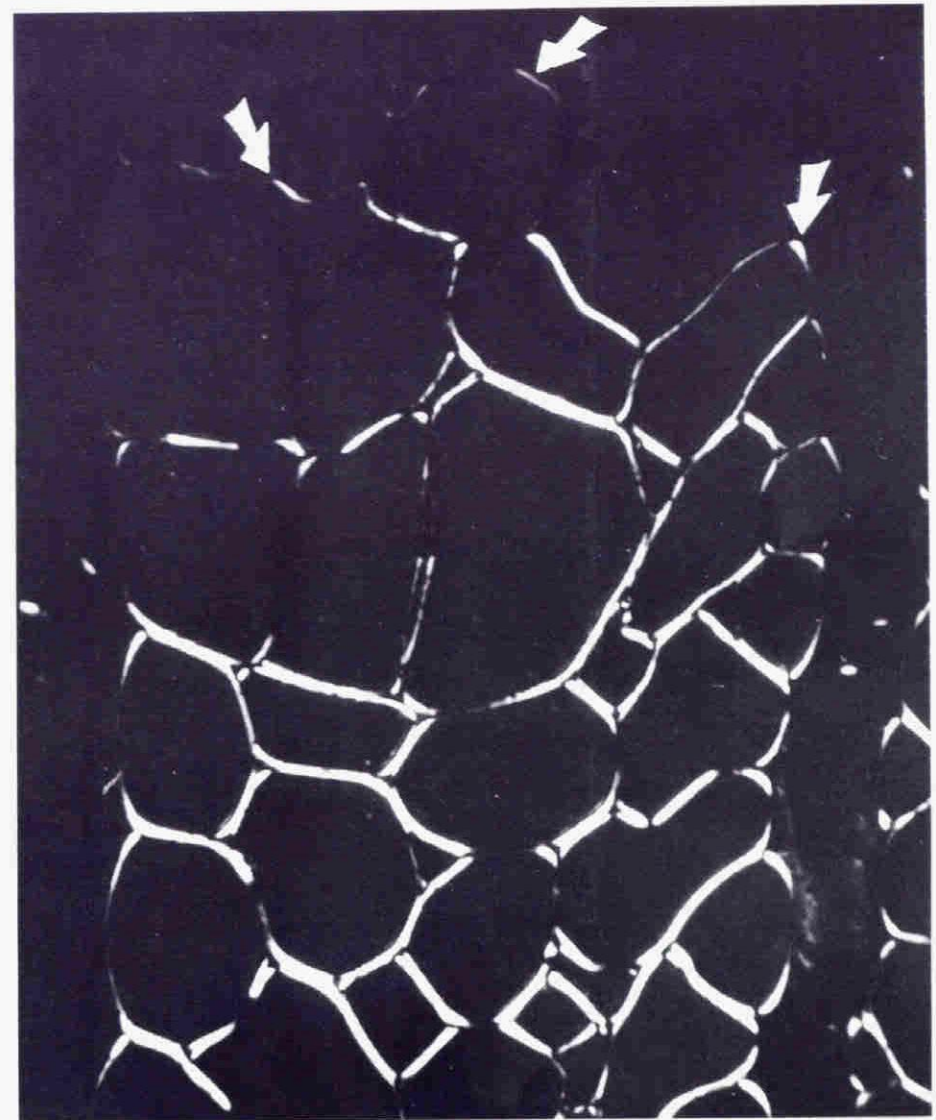
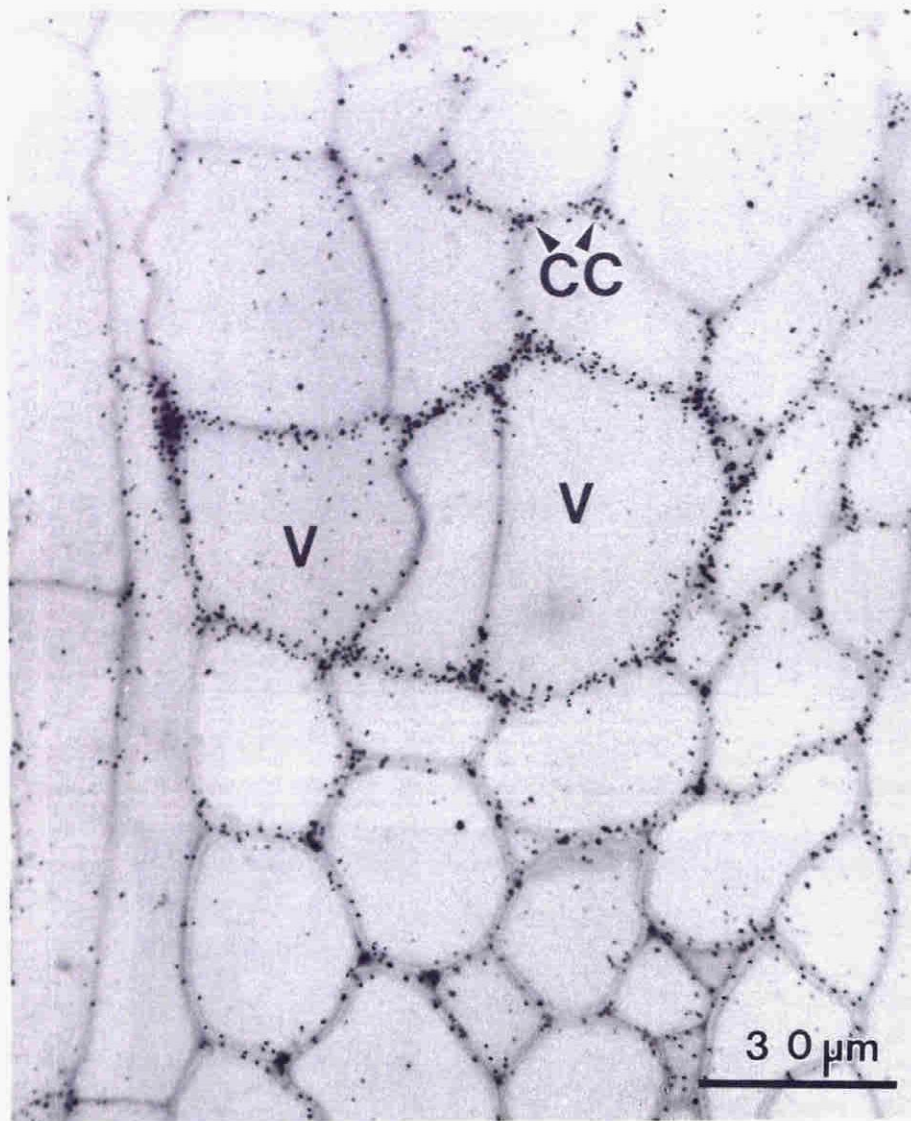
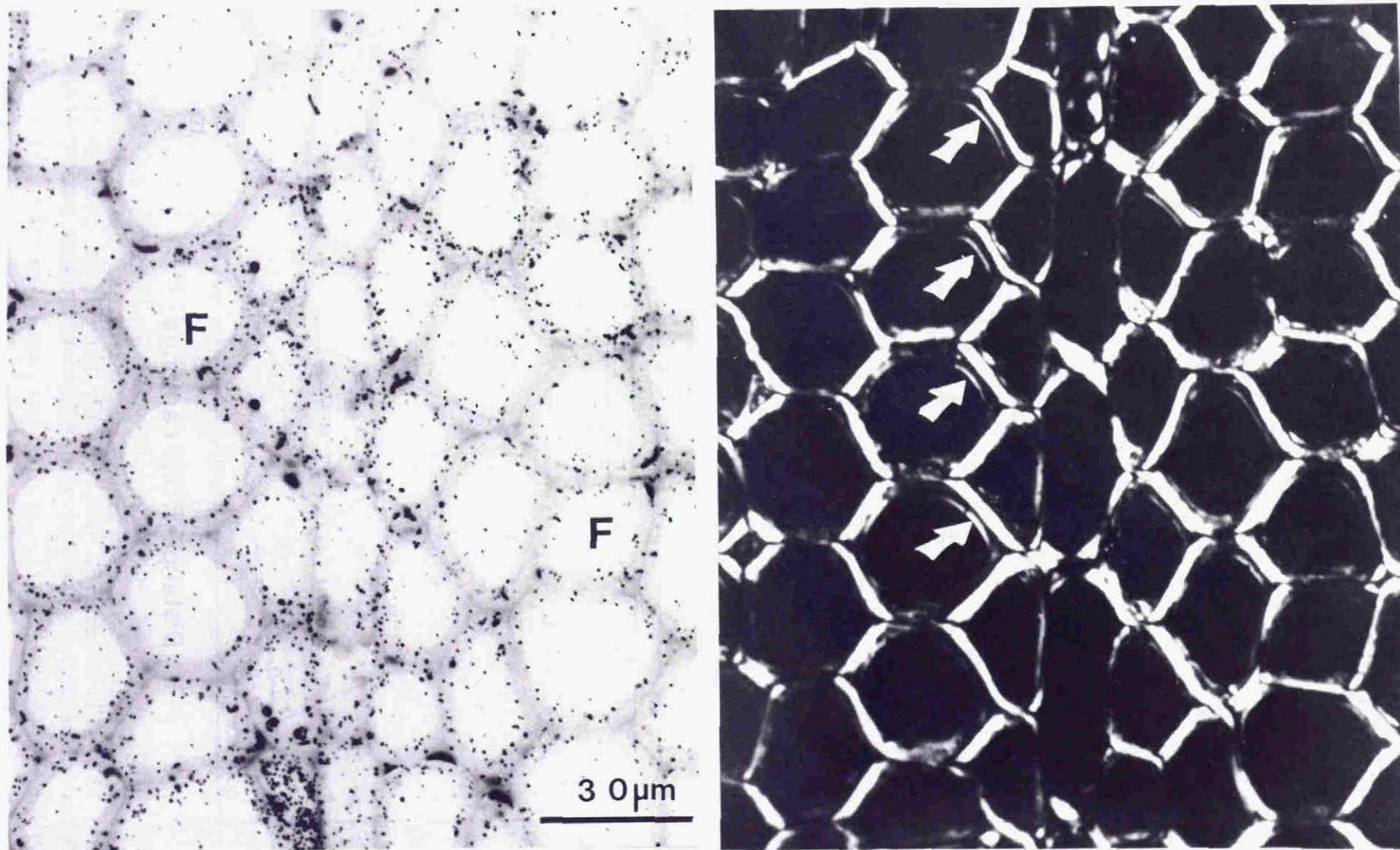


Fig. 36. Microautoradiograms of differentiating xylem of magnolia administered with coniferin-[arom. ring-2-<sup>3</sup>H] (a) and syringin-[arom. ring-2-<sup>3</sup>H] (b). V: vessel, F: fiber, R: ray cell



**Fig. 37.** A part of microautoradiogram of differentiating xylem in early stage administered with coniferin-[arom. ring-2-<sup>3</sup>H] (left). Silver grains in vessel (V) wall, cell corner (CC), and compound middle lamella indicate deposition of guaiacyl units. Polarization photomicrograph of the same section (right) indicate that



**Fig. 38.** A part of microautoradiogram of differentiating xylem in early stage administered with syringin-[arom. ring-2-<sup>3</sup>H] (left). Distribution of silver grains indicate that syringyl units deposit mainly in secondary wall of fiber (F). Polarization photomicrograph of the same section (right) indicate that inner layer of secondary wall (S<sub>3</sub>, arrow) of fiber is formed at this stage.

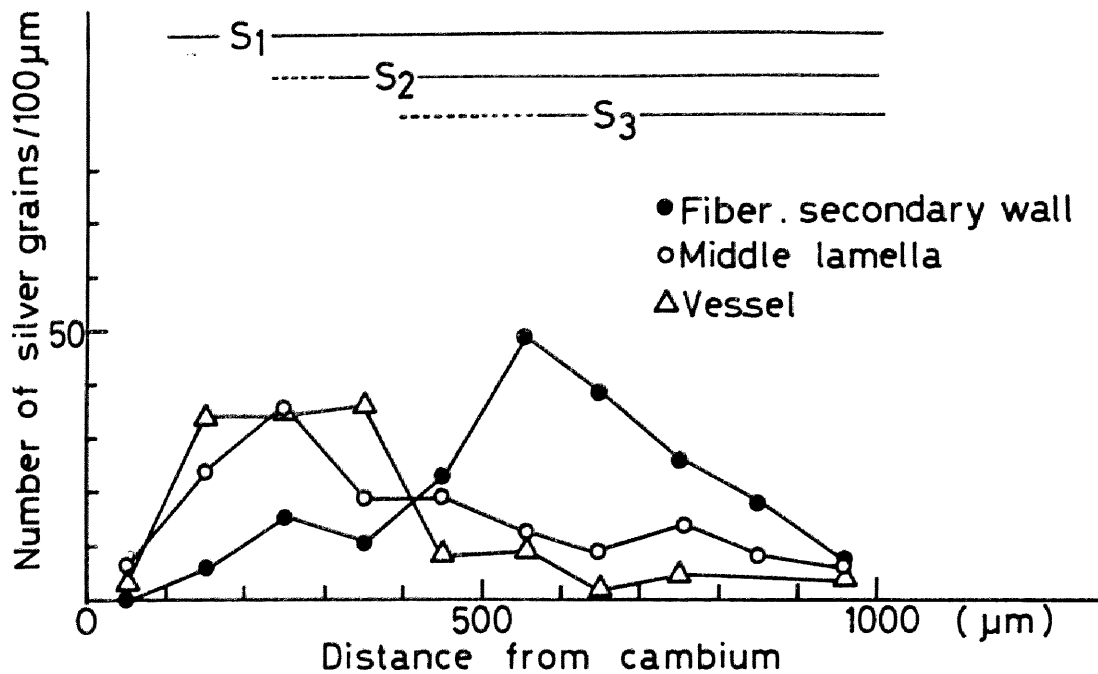


Fig. 39. Deposition of guaiacyl lignin as determined by counting the silver grains per 100 µm length of cell wall in the differentiating xylem of magnolia which was administered with labeled coniferin.

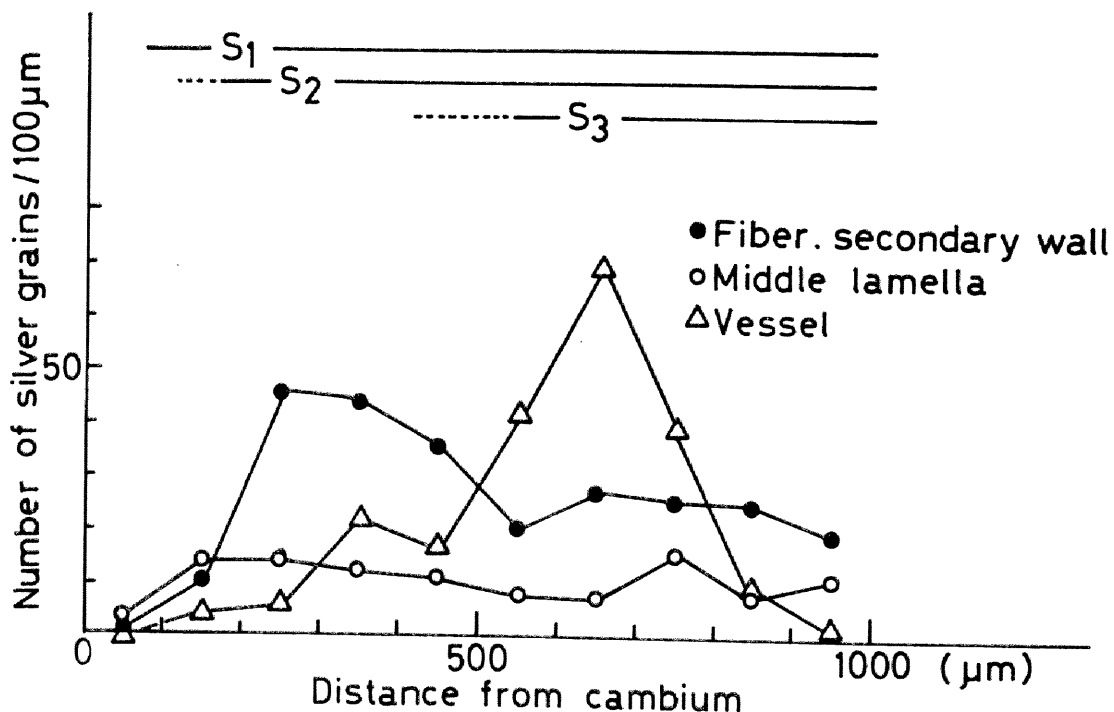


Fig. 40. Deposition of syringyl lignin as determined by counting the silver grains per 100 µm length of cell wall in the differentiating xylem of magnolia which was administered with labeled syringin.

**Fig. 40.** The number of silver grains per 100  $\mu\text{m}$  cell wall is considered to be proportional to the amount of lignin formed during the 3 hours metabolism.

The deposition patterns of three units shown in these microautoradiograms indicate that the compound middle lamella lignin mainly consists of *p*-hydroxyphenyl and guaiacylpropane units and that the secondary wall lignin mainly consists of guaiacyl and syringylpropane units. However, the exact content of three units could not be estimated by this method. These microautoradiograms suggest that at least more than two kinds of isozymes of  $\beta$ -glucosidase are present in differentiating xylem. The isozyme(s) existed in the early stage ( $S_1$  formation stage) is/are able to hydrolyse *p*-glucocoumaryl alcohol and coniferin, and another isozyme(s) produced in the later stage (after the start of  $S_3$  formation) is/are able to hydrolyse coniferin and syringin. In other words, the cell in differentiating xylem may produce isoenzymes of different substrate specificity depending on the age and kind of the cell. It has been known that hydrolytic activities of  $\beta$ -glucosidase for *p*-glucocoumaryl alcohol, coniferin and syringin vary widely with the sources of the enzyme<sup>45,56</sup>). However, it is open to further research whether substrate specificity of the enzyme plays an important role in heterogeneous deposition of *p*-hydroxyphenyl, guaiacyl and syringyl moieties in magnolia.

**Fig. 41.** shows HPLC profile of nitrobenzene oxidation products from magnolia xylem. In addition to the compounds derived from guaiacyl and syringyl units, a peak corresponding to *p*-hydroxybenzaldehyde can be seen. However, the amount of this compound is very low. The yields and their molar ratios are shown in **Table 7**. The total amount of *p*-hydroxybenzaldehyde and *p*-hydroxybenzoic acid was only 0.06  $\mu\text{mol}$  from 20mg of wood meal, and the molar content was only 0.8%. On the other hand, **Fig. 34a** and **35** suggests that *p*-hydroxyphenylpropane units are one of the main components of compound middle lamella lignin. If *p*-hydroxyphenylpropane

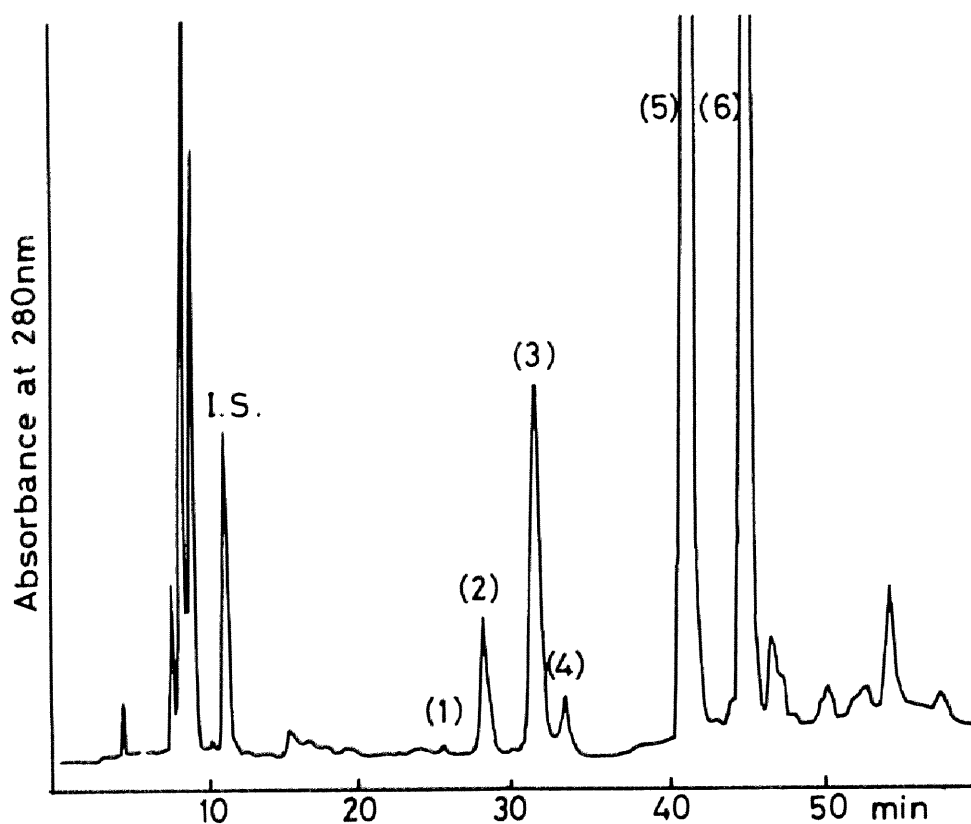


Fig. 41. HPLC profile of products from nitrobenzene oxidation of xylem of magnolia. (1): *p*-Hydroxybenzoic acid, (2): Vanillic acid, (3): Syringic acid, (4): *p*-Hydroxybenzaldehyde, (5): Vanillin, (6) Syringaldehyde, I.S.: Internal standard, 3,5-dihydroxybenzoic acid

**Table 7**

Yield\* of degradation products obtained by nitrobenzene oxidation of magnolia wood.

Compounds	$\mu\text{mol}$	% (mol)**
<i>p</i> -Hydroxybenzoic acid(HA)	0.02	
Vanillic acid(VA)	0.30	
Syringic acid(SA)	0.45	
<i>p</i> -Hydroxybenzaldehyde(Ha)	0.04	
Vanillin(Va)	2.39	
Syringaldehyde(Sa)	4.56	
HA+Ha	0.06	0.8
VA+Va	2.69	34.7
SA+Sa	5.01	64.5

\* Yields are expressed as  $\mu\text{mol}$  of degradation product per 20mg of extracted free wood meal.

\*\* Based on the total yield of six compounds.

**Table 8**

Yield\* of *p*-hydroxybenzoic acid and *p*-hydroxybenzaldehyde from L-tyrosine and albumin obtained by alkaline nitrobenzene Oxidation.

	L-Tyrosine	Albumin
<i>p</i> -Hydroxybenzoic acid(HA)	1.1(%)	0.2(%)
<i>p</i> -Hydroxybenzaldehyde(Ha)	3.3	0.1
(HA)+(Ha)	4.4	0.3

\* Yields are given as a weight percent of L-tyrosine or albumin

units are of highly condensed, they will give low yield of *p*-hydroxybenzaldehyde on oxidation. This suggestion is supported by the facts that nitrobenzene oxidation of birch gave *p*-hydroxybenzaldehyde from only the differentiating xylem in the initial stage of lignification, but mature wood did not give<sup>24</sup>).

It should be considered that proteins contained in the cell wall may give rise to *p*-hydroxybenzaldehyde and *p*-hydroxybenzoic acid on oxidation. **Table 8.** shows the yields of the acid and aldehyde produced from tyrosine and albumin by alkaline nitrobenzene oxidation. Total amount of the products from tyrosine was 4.4%. But free tyrosine has not been found in xylem tissue of angiosperms and gymnosperms. A kind of protein, albumin, gave only very small amount of these compounds on oxidation. Nitrogen content of magnolia wood used in this experiment was only 0.17%. From the nitrogen content, this sample contained only a small amount of protein, about 1.06% calculated using the factor 6.25 for converting nitrogen to protein<sup>57</sup>). This suggests that *p*-hydroxybenzaldehyde and *p*-hydroxybenzoic acid from magnolia wood on oxidation are not produced from protein. If total amount (0.06  $\mu$ mol) of these compounds were derived from proteins in the wood tissue, 2.7mg (calculated as albumin) of protein must exist in 20mg of magnolia wood. This value

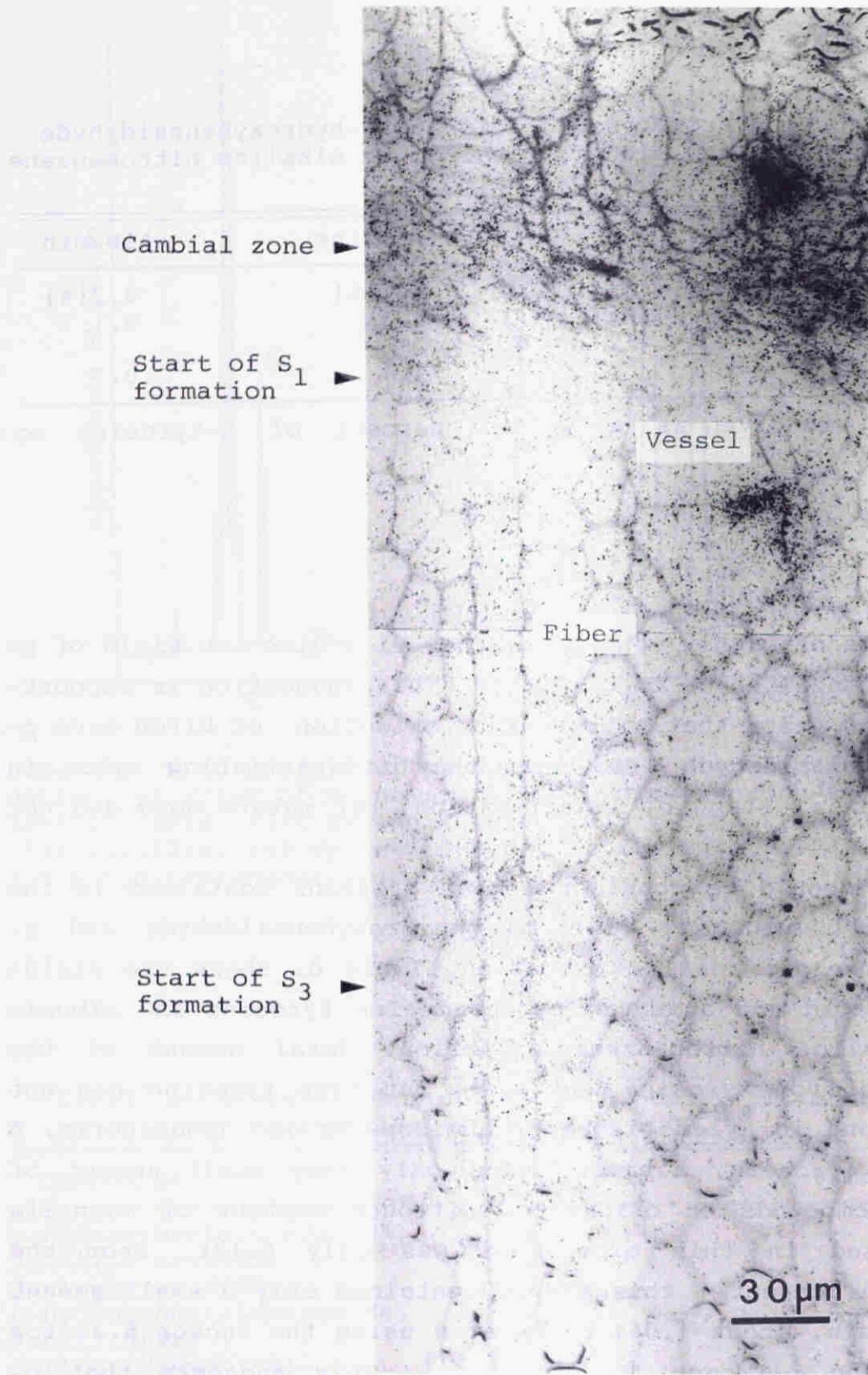


**Fig. 42.** Microautoradiogram of differentiating xylem of magnolia administered with UDP-glucuronic acid-[glucuronyl- $U-^{14}C$ ].

corresponds to the nitrogen content of more than 2%, ten times more of actual content. Only a very small part of *p*-hydroxybenzaldehyde and *p*-hydroxybenzoic acid may be derived from proteins in xylem tissue.

**Fig. 42.** is a microautoradiogram of newly formed xylem of magnolia administered with UDP-glucuronic acid-[glucuronyl-U-<sup>14</sup>C]. It is known that UDP-glucuronic acid is the common precursors of pectic substance and xylan in woody plant<sup>39</sup>). Two peaks of incorporation of radioactivity in the xylem can be seen at the earliest stage of cell wall formation and at the stage of secondary wall formation. The former incorporation is considered to be the deposition of pectic substance, and the latter is that of xylan. This result is similar to those observed in the case of pine (3.1., Fig. 7). It is very interesting that lignification is always occurred after the deposition of carbohydrates. It seems that compound middle lamella lignin is formed in pectin gel and secondary wall lignin is formed in xylan gel.

It is well known that the structure of compound middle lamella lignin is different from secondary wall lignin. This can be explained by the fact that the lignification in the compound middle lamella and secondary wall proceeds under different conditions. Each lignification gives rise to different *p*-hydroxyphenyl to guaiacyl and syringyl to guaiacyl ratios of lignin. In addition to the ratios, bonding patterns of each unit will be different between in the early stage lignification and the late stage lignification. This is supported by the results of dehydrogenative polymerization of coniferyl alcohol under different conditions, in which more condensed structures were formed in pectin gel than in xylan gel<sup>31</sup>).

#### 4.2. Lilac

Coniferin and syringin have been found in the cambial sap of lilac<sup>25</sup>). But the glucoside of *p*-coumaryl alcohol has never been detected.

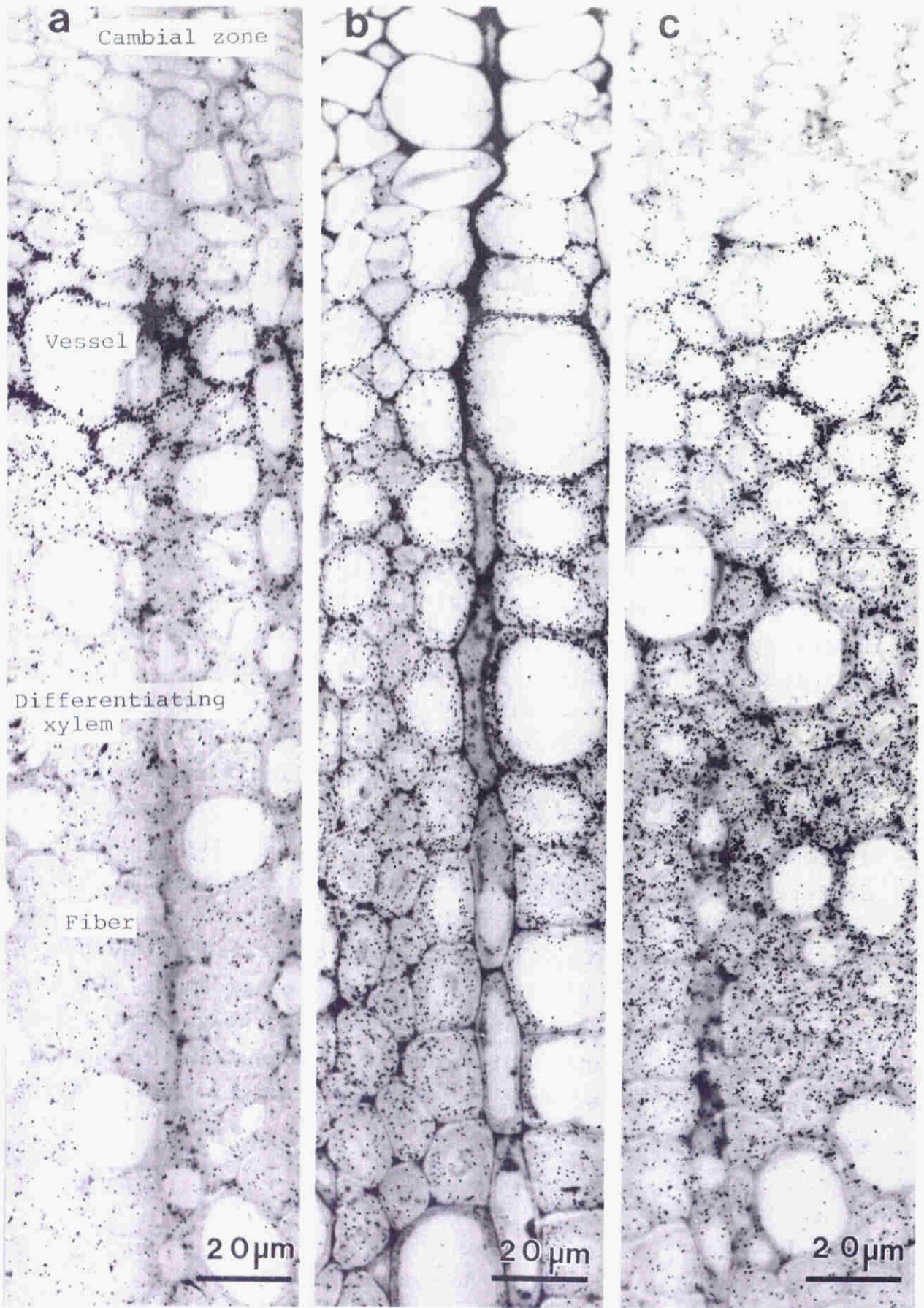
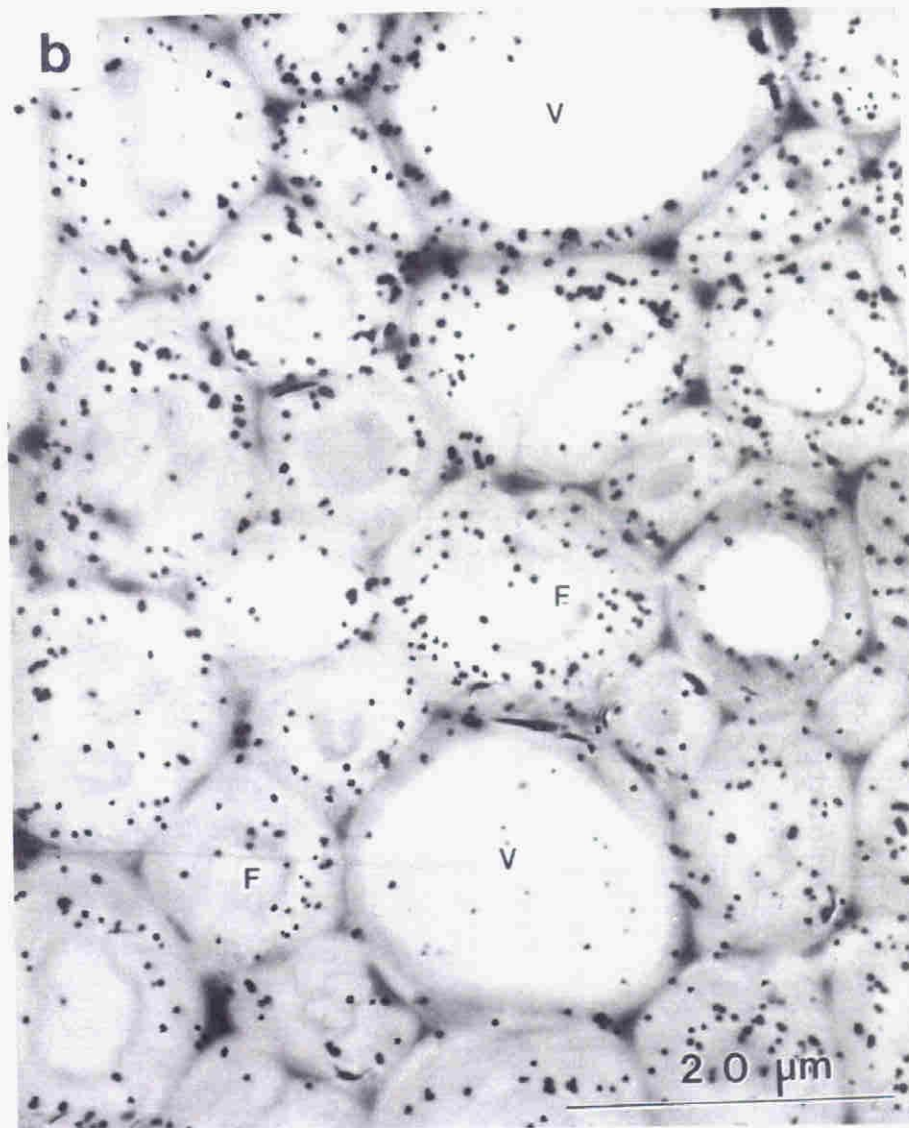
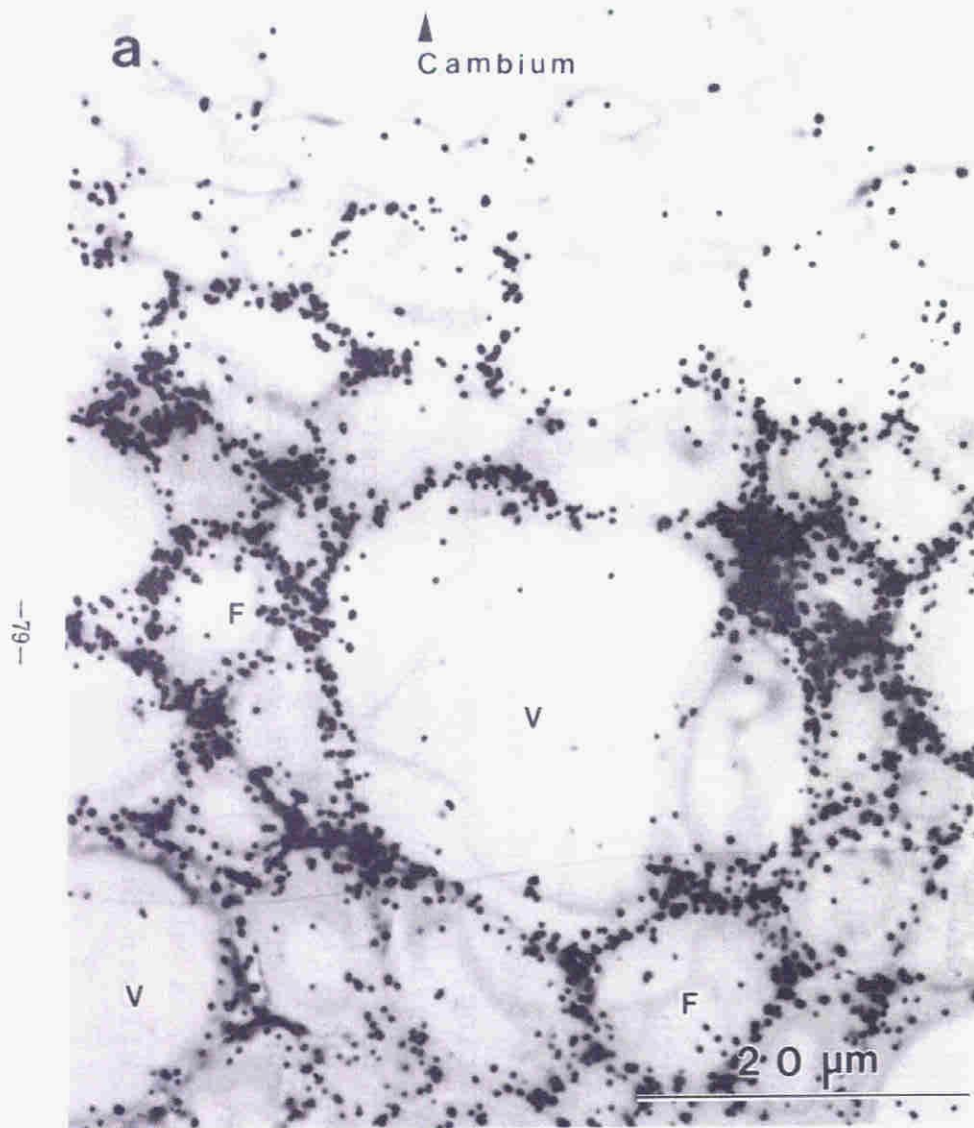


Fig. 43. Microautoradiograms of differentiating xylem of lilac administered with **a**: p-glucocoumaryl alcohol-[arom. ring-2-<sup>3</sup>H], **b**: coniferin-[arom. ring-2-<sup>3</sup>H] or **c**: syringin-[arom. ring-2-<sup>3</sup>H].



**Fig. 44.** A part of microautoradiograms of differentiating xylem of lilac administered with *p*-glucocoumaryl alcohol-[arom. ring-2-<sup>3</sup>H] (a) and syringin-[arom. ring-2-<sup>3</sup>H] (b).  
V: vessel, F: fiber

When a growing stem of lilac was administered the  $^3\text{H}$ -labeled monolignol glucosides, each lignin precursor was efficiently incorporated into the newly formed xylem at different stages of cell wall formation as revealed by microautoradiography (Fig. 43). Fig. 43a shows the microautoradiogram of newly formed xylem of lilac administered with *p*-glucocoumaryl alcohol-[arom. ring-2- $^3\text{H}$ ]. The radioactivity is incorporated only during the early stages of cell wall development. Fig. 44a shows an enlarged photograph of a part of this microautoradiogram. As can be seen, the distribution of silver grains indicates that *p*-hydroxyphenyl lignin components were deposited mainly in the compound middle lamella regions during the formation of  $S_1$  layer, and were not present in the secondary wall. This incorporation is not an artifact, because the incorporation pattern is quite different from those of other units. Guaiacyl lignin formed continuously from the early to later stages, and in both the vessels and fiber walls (Fig. 43b). Interestingly, syringyl lignin was deposited mostly in the secondary wall of fibers, although a small amount was also incorporated to form compound middle lamella lignin (Fig. 43c and Fig. 44b).

These results indicates the presence of isozymes which regulate the lignification. Perhaps they will be  $\beta$ -glucosidases.

#### 4.3. Beech

Fig. 45a shows the microautoradiogram of newly formed xylem of beech administered with *p*-glucocoumaryl alcohol-[arom. ring-2- $^3\text{H}$ ]. This visualizes the localization of newly formed *p*-hydroxyphenylpropane units of lignin. It is seen that *p*-hydroxyphenylpropane units deposit in the early stage of lignification. Remarkable incorporation can be seen in the cell corner of fiber and vessel wall during the formation of  $S_1$  layer. But after this stage, no incorporation was observed. Fig. 45b, a microautoradiogram of beech xylem administered with coniferin-[arom. ring-2- $^3\text{H}$ ], shows the localization of

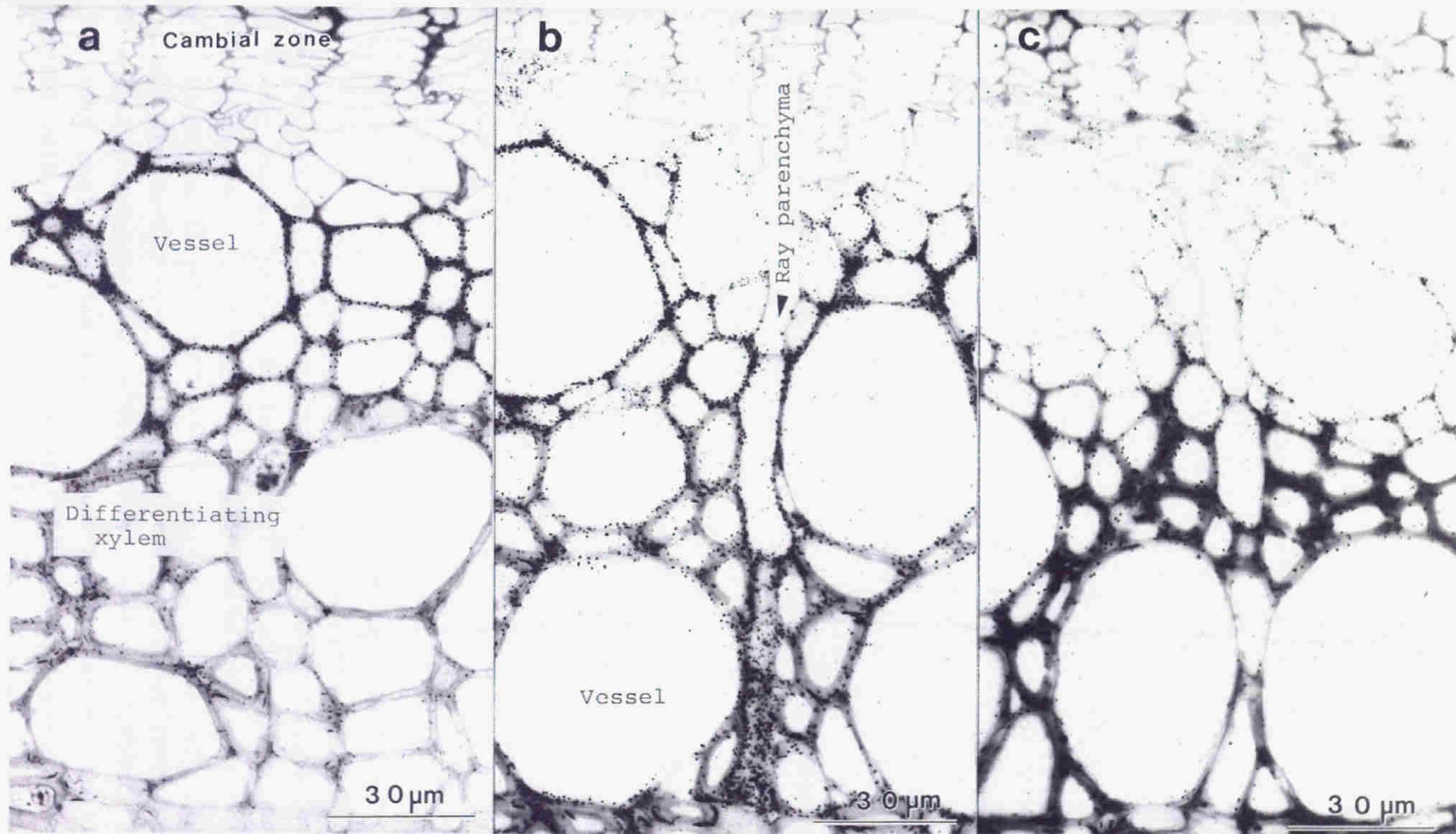


Fig. 45. Microautoradiograms of differentiating xylem of beech administered with a: p-glucocoumaryl alcohol-[arom. ring-2-<sup>3</sup>H], b: coniferin-[arom. ring-2-<sup>3</sup>H], c: syringin-[arom. ring-2-<sup>3</sup>H].

newly formed guaiacyl units of lignin. As can be seen from this microautoradiogram, guaiacylpropane units deposit in the cell corner and the compound middle lamella of vessel and fiber walls during the formation of  $S_1$  layer. And the deposition in the secondary wall of vessel and fiber walls can be seen in the late stage of lignification. Guaiacylpropane units deposit also in ray parenchyma wall in the later period than that in other kind of cell. **Fig. 45c** shows a microautoradiogram of beech xylem administered with syringin-[arom. ring-2- $^3\text{H}$ ]. Syringyl units mainly deposit in the secondary wall of fiber, but the amount of deposition in the cell corner and the compound middle lamella is lower than those of other units. These results are similar to those observed in magnolia and lilac.

#### 4.4. Poplar

**Fig. 46a** shows the microautoradiogram of newly formed xylem of poplar administered with UDP-glucuronic acid-[glucuronyl-U- $^{14}\text{C}$ ]. The radioactivity was mainly incorporated in the cell wall of cambial zone. Glucuronic acid may be converted to pectic substance and deposited in primary cell wall. Small amount of radioactivities were incorporated during the formation of secondary wall. These results were similar to that observed in magnolia (**Fig. 42**). Perhaps the latter incorporation would indicate the deposition of xylan.

**Fig. 46b** shows the microautoradiogram of poplar xylem administered with *p*-glucocoumaryl alcohol-[arom. ring-2- $^3\text{H}$ ]. The incorporation of activity from this precursor can be seen in the early stage ( $S_1$  formation) of lignification. This is similar to those observed in other hardwood (magnolia and lilac). The silver grains would indicate location of *p*-hydroxyphenylpropane units. In poplar, *p*-hydroxyphenylpropane units deposits almost exclusively into vessel wall, and lignification of vessel wall occurs earlier than that of fiber. Guaiacylpropane units in vessel wall are also formed

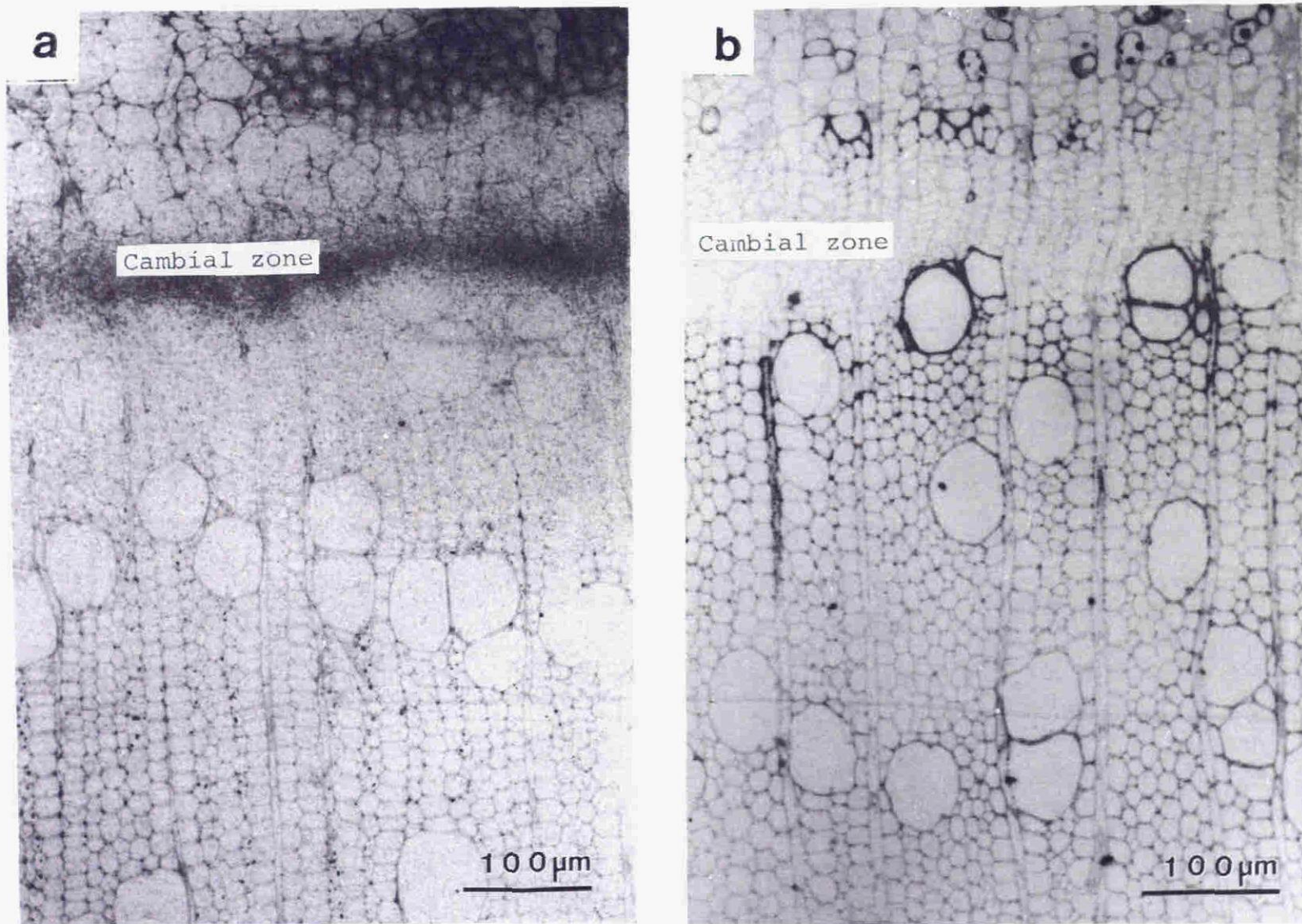


Fig. 46. Microautoradiograms of differentiating xylem of poplar administered with UDP-glucuronic acid-[glucuronyl-U-<sup>14</sup>C] (a) and p-glucocoumaryl alcohol-[arom. ring-2-<sup>3</sup>H] (b).

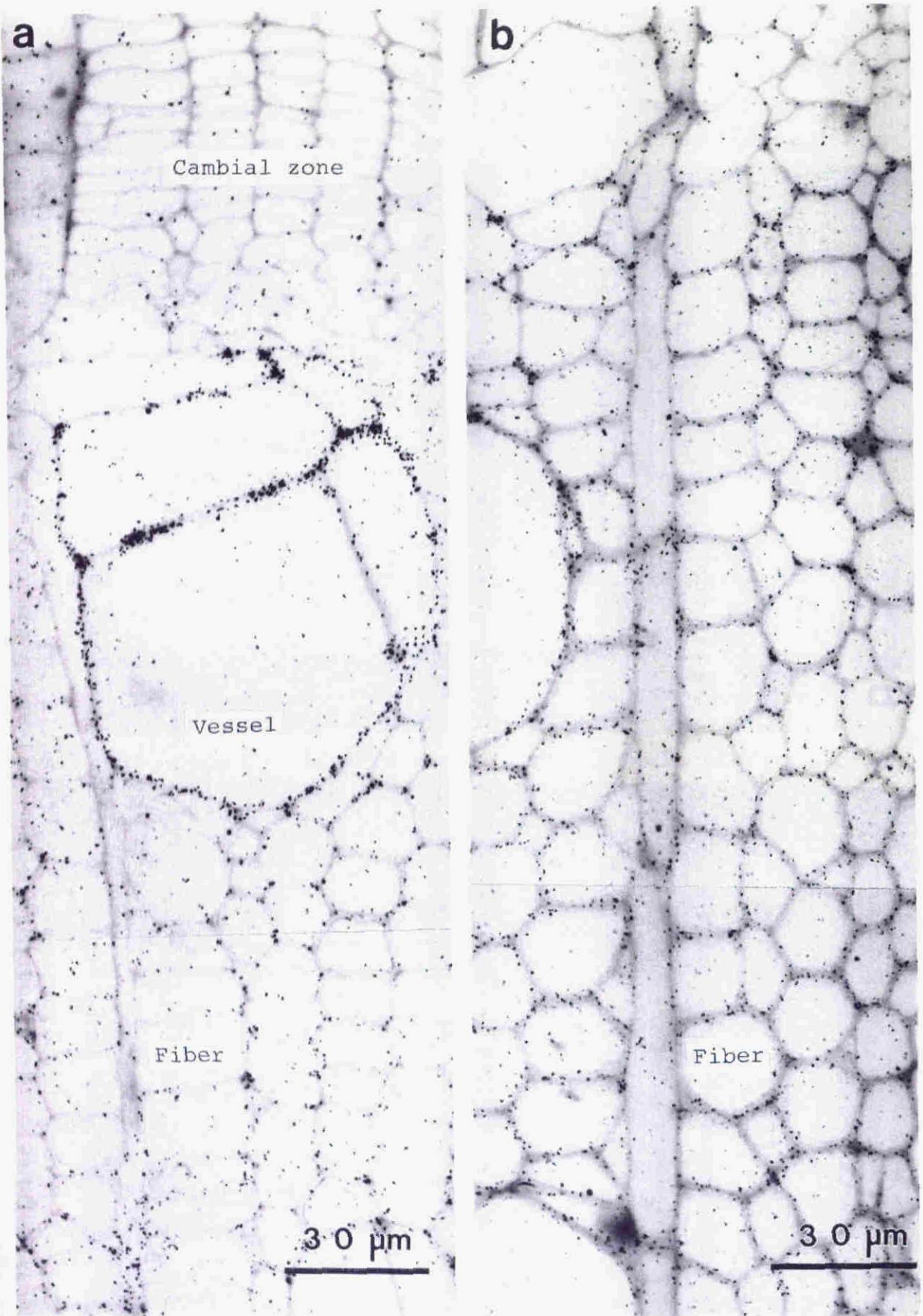
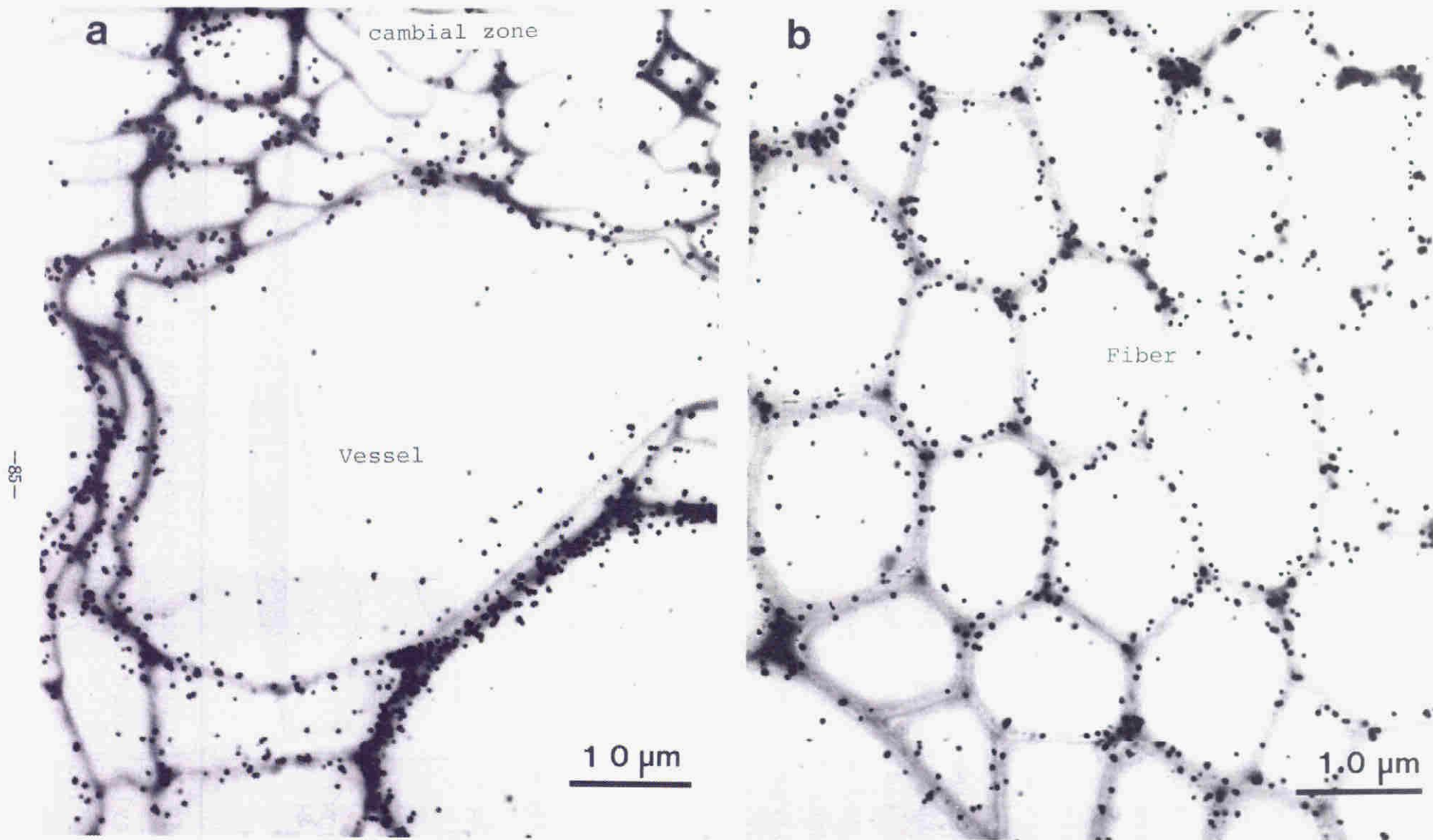


Fig 47. Microautoradiograms of differentiating xylem of poplar administered with  $^3\text{H}$ : a: coniferin-[arom. ring-2- $^3\text{H}$ ], b: syringin-[arom. ring-2- $^3\text{H}$ ].



**Fig. 48.** Microautoradiograms of differentiating xylem of poplar administered with *p*-hydroxybenzoic acid-[arom. ring-2-<sup>3</sup>H]. **a:** Initial stage (formation of S<sub>1</sub> layer) of lignification. **b:** Late stage of (after the start of S<sub>3</sub> formation) of lignification.

earlier than in fiber (Fig. 47a). The similar pattern has been observed in the newly formed xylem of poplar administered with ferulic acid- $[\beta\text{-}^{14}\text{C}]^{17}$ ). Syringylpropane units mainly deposits in the secondary wall of fiber (Fig. 47b). These results are similar to the case of magnolia, lilac or beech.

It is well known that poplar xylem contains *p*-hydroxybenzoic acid esterified to cell wall. Fig. 48a and b show the microautoradiograms of xylem of poplar administered with *p*-hydroxybenzoic acid-[arom. ring-2- $^3\text{H}$ ]. The radioactivities from this precursor were incorporated both in compound middle lamella and secondary wall of differentiating xylem. These deposition patterns are quite different from that observed in the microautoradiogram of poplar xylem administered with *p*-glucocoumaryl alcohol-[arom. ring-2- $^3\text{H}$ ]. This may be due to the fact that this *p*-hydroxybenzoic acid is formed via *p*-coumaric acid, and an intermediate located in the latest stage of shikimic acid pathway in poplar lignin biosynthesis<sup>58</sup>). This suggests that the radioactivity observed in Fig. 46b would not largely be due to that of esterified *p*-hydroxybenzoic acid. The distributions of two kinds of *p*-hydroxyphenyl units are summarized in Fig. 49.

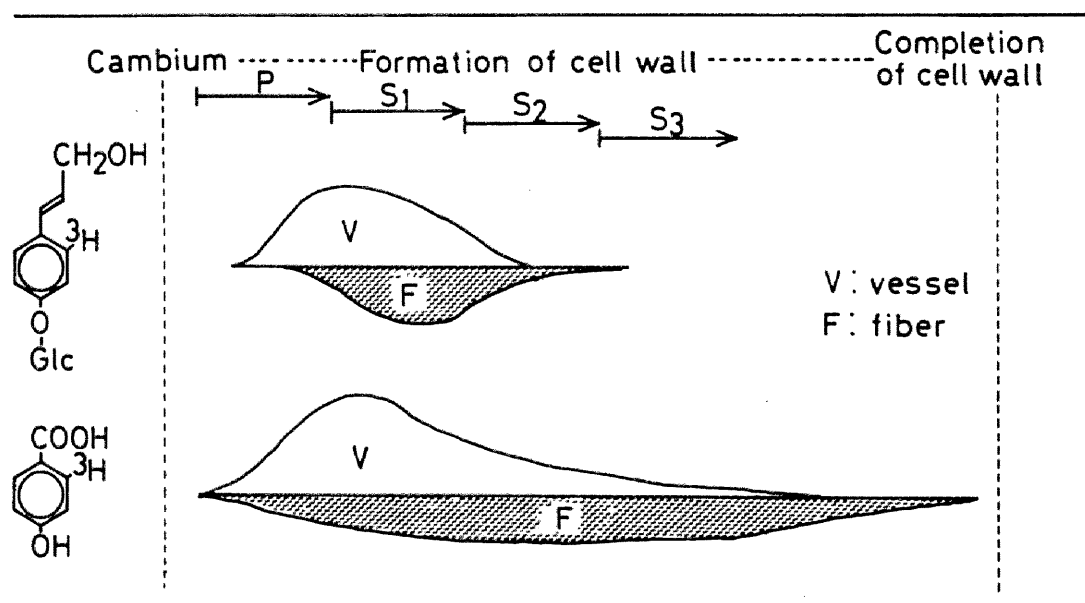


Fig. 49. Distribution of silver grains in microautoradiograms of differentiating xylem of poplar administered with *p*-glucocoumaryl alcohol-[arom. ring-2- $^3\text{H}$ ] and *p*-hydroxybenzoic acid-[arom. ring-2- $^3\text{H}$ ]. P, primary wall; S<sub>1</sub>, S<sub>2</sub> and S<sub>3</sub>, outer, middle and inner layer of secondary wall.

## Conclusion

p-Glucocoumaryl alcohol, the effective precursor of p-hydroxyphenyl lignin, was radio-labeled and administered to differentiating xylem of three hardwoods, magnolia, beech, lilac and poplar. The distribution of radioactivity in various morphological regions was visualized by microautoradiography. It was shown that p-hydroxyphenylpropane units are formed in compound middle lamella during the formation of S<sub>1</sub> layer. These results strongly suggest that p-hydroxyphenylpropane units also exist in hardwood lignin as one of the main building stones of compound middle lamella lignin. The p-hydroxyphenyl lignin is formed after the deposition of carbohydrate, perhaps pectic substance, in the early stage of cell wall formation. Thus, p-coumaryl alcohol polymerizes in pectin gel to form highly condensed structures which is hardly degraded by nitrobenzene oxidation.

## CHAPTER 5

### Summary

The growing process of macromolecular protolignin in the cell wall was visually traced by microautoradiography. The results indicate that the structure of protolignin macromolecule is heterogeneous with respect to monomer composition, distribution of interunit linkage (to form condensed substructures), and association with carbohydrates. However, protolignin is not a disordered copolymer of various monolignols, but a macromolecule formed under a rigid biochemical regulations. The heterogeneous nature of protolignin is a natural and inevitable consequence of the unique mechanism of its biogenesis. **Fig. 50.** illustrates the successive deposition of cell wall components and their irreversible assembly to form a lignified cell wall in tree xylem. The causes of the heterogeneity of protolignin structure may be explained by **Fig. 50.** as follows.

1. The process of lignification is fundamentally controlled by the individual cell.
2. Lignification is preceded always by deposition of cell wall polysaccharides, and polymerization of monolignol occurs in the carbohydrate gel, which affects the structure of poly-lignol. The kind of carbohydrate changes with the stage of cell wall development, i.e., formation of cell wall layers, as shown in **Fig. 50..** Polymerization of lignol in pectic substances in the earliest stage may be one of the reasons for that the compound middle lamella and cell corner lignin contains more condensed substructures than the secondary wall lignin.
3. The monolignol utilized varies with type and age of the cell. Indeed, incorporation of monolignols into protolignin occurs in the same order as their biosynthesis, namely p-coumaryl, coniferyl and finally sinapyl alcohols are

deposited successively (**Fig. 50**). *p*-Hydroxyphenylpropane unit is able to form interunit linkage at both C-3 and C-5 of the aromatic ring, and the participation of *p*-coumaryl alcohol in the earliest stage will be another reason for the fact that middle lamella lignin is rich in condensed units.

The various factors regulating lignification are closely correlated with each other.

It is to be noted that there is a common feature in biogeneses between gymnosperm and angiosperm lignins. The differences in properties between softwood lignin and hardwood lignin will be thoroughly understood by more detailed studies on biosynthesis of three kind of cell wall polymers, cellulose, hemicellulose and lignin, and their assembly to form lignified cell wall.

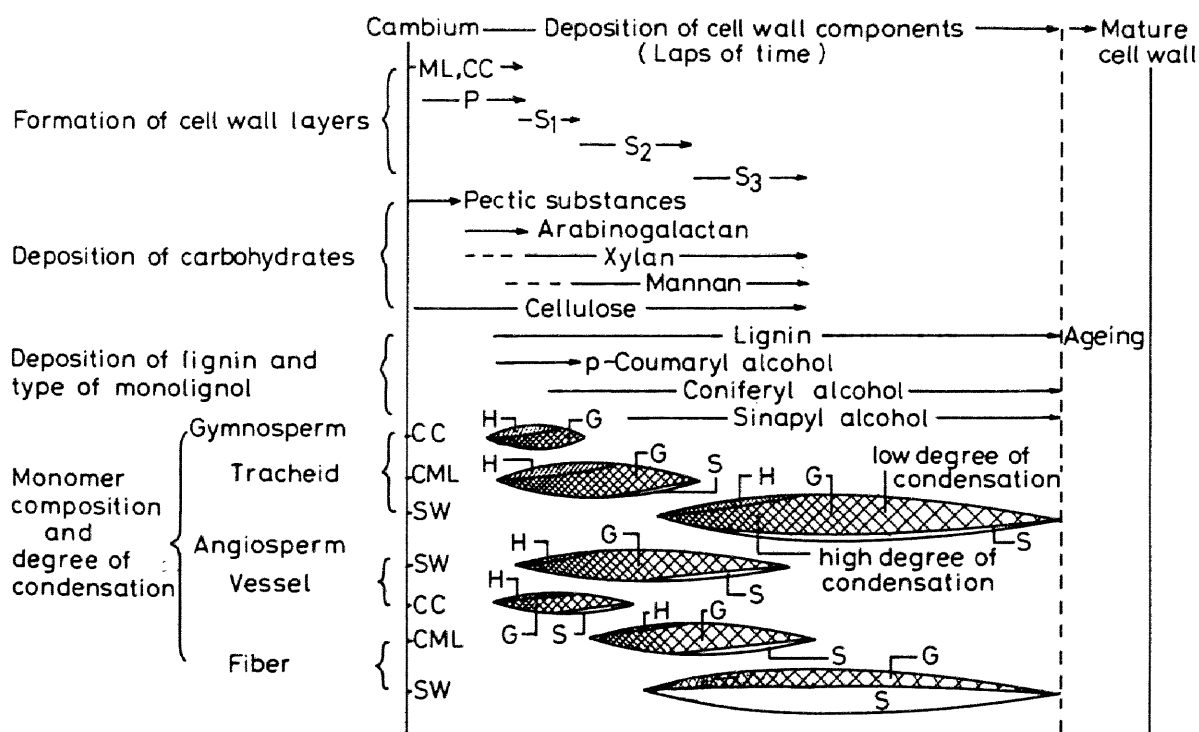


**Fig. 50.** A schematic representation of the process of deposition of cell wall components and the heterogeneous formation of protolignin macromolecule. **ML**: middle lamella, **CC**: cell corner, **P**: primary wall, **CML**: compound middle lamella, **S<sub>1</sub>**, **S<sub>2</sub>** and **S<sub>3</sub>**: outer, middle and inner layer of secondary wall, **H**, **G** and **S**: *p*-hydroxyphenyl-, guaiacyl- and syringylpropane units.

## References

- 1) B. J. Fergus and D. A. I. Goring, *Holzforschung*, 24, 113 (1970).
- 2) B. J. Fergus and D. A. I. Goring, *Holzforschung*, 24, 118 (1970).
- 3) Y. Musha and D. A. I. Goring, *Wood Sci. Technol.*, 9, 45 (1975).
- 4) S. Saka, R. J. Thomas and J. S. Gratzl, *Proc. ISWPC, Stockholm, Sweden, Vol. 1, SPCI Report 38*, p. 35 (1981)
- 5) S. Saka and D. A. I. Goring, In: "Biosynthesis and Biodegradation of Wood Components", T. Higuchi ed. Academic Press Inc., New York, 1985; p. 51.
- 6) W. F. Manders, *Holzforschung*, 41, 13 (1987)
- 7) N. Cyr, R. M. Elofson, J. A. Ripmeester and G. W. Mathison *J. Agric. Food. Chem.*, 36, 1197 (1988)
- 8) D. J. Gardner, G. D. McGinnis and L. W. Amos, *J. Wood Chem. Technol.*, 9, 219 (1989)
- 9) R. H. Atalla and U. P. Agarwal, *Science*, 227, 636 (1985)
- 10) R. H. Atalla and U. P. Agarwal, *J. Raman Spectroscopy*, 17, 229, (1986)
- 11) N. Terashima, M. Okada and Y. Tomimura, *Mokuzai Gakkaishi*, 25, 422 (1979)
- 12) Y. Tomimura and N. Terashima, *Mokuzai Gakkaishi*, 25, 427 (1979)
- 13) N. Terashima, Y. Tomimura and H. Araki, *Mokuzai Gakkaishi*, 25, 595 (1979)
- 14) Y. Tomimura, T. Yokoi and N. Terashima, *Mokuzai Gakkaishi*, 25, 427 (1979)
- 15) Y. Tomimura, T. Yokoi and N. Terashima, *Mokuzai Gakkaishi*, 26, 37 (1980)
- 16) Y. Tomimura, Y. Sasao, T. Yokoi and N. Terashima, *Mokuzai Gakkaishi*, 26, 558 (1980)
- 17) N. Terashima, K. Fukushima, S. Tsuchiya and K. Takabe, *J. Wood Chem. Technol.*, 6, 495 (1986)
- 18) P. Whiting and D. A. I. Goring, *Wood Sci. Technol.*, 16, 261 (1982).
- 19) U. Westermark, *Wood Sci. Technol.*, 19, 223 (1985)

- 20) V. O. Faix and W. Schweers, *Holzforschung*, 29, 48 (1975)
- 21) N. Terashima, In "Plant Cell Wall Polymers", N. G. Lewis and M. G. Paice, ed. ACS Symposium Series, 399, 1989, p.148. American Chemical Society, Washington, DC.
- 22) N. S. Cho, L. Y. Lee, G. Meshitsuka and J. Nakano, *Mokuzai Gakkaishi*, 26, 527 (1980)
- 23) H. -L. Hardell, G. J. Leary, M. Stoll and U. Westermark, *Svensk Papperstidn.*, 83, 71 (1980)
- 24) T. J. Eon, G. Meshitsuka and J. Nakano, *Mokuzai Gakkaishi*, 33, 576 (1987)
- 25) M. Terazawa, H. Okuyama and M. Miyake, *Mokuzai Gakkaishi*, 30, 322 (1984)
- 26) K. Freudenberg and J. M. Harkin, *Phytochem.*, 2, 189 (1963)
- 27) R. K. Ibrahim, *Z. Pflazenphysiol.*, 85, 253 (1977)
- 28) K. Freudenberg, H. Reznik, W. Fuchs and M. Richert, *Naturwissenschaften*, 42, 29 (1955)
- 29) A. Björkman, *Svensk Papperstidn.*, 60, 243 (1957)
- 30) T. Koshijima, T. Watanabe and J. Azuma, *Chemistry Letters*, 1984, 1737, (1984)
- 31) N. Terashima and Y. Seguchi, *Cell. Chem. Technol.*, 22, 147 (1988).
- 32) C. F. Koelsch, *J. Am. Chem. Soc.*, 61, 969 (1939)
- 33) Hodgson and Jenkinson, *J. Chem. Soc.*, 1927, 3041 (1927)
- 34) K. Kratzl and G. Billek, *Holzforschung*, 7, 66 (1953)
- 35) W. Fuchs, *Chem. Ber.*, 88, 1825 (1955)
- 36) I. A. Pearl, *Organic Syntheses*, 30, 101 (1950)
- 37) H. E. Helferich, H. E. Scheiber, R. Streck and F. Vorsats, *Ann*, 518, 211 (1935)
- 38) L. He and N. Terashima, *Mokuzai Gakkaishi*, 35, 116 (1989)
- 39) G. Dalessandro and D. H. Northcote, *Planta*, 151, 61(1981)
- 40) K. Kratzl and H. Faigle, *Monatsh. Chem.* 89, 768 (1959)
- 41) K. Freudenberg, *Biochemische Vorgänge bei der Holzbildung*, In: "Biochemistry of Wood" (Eds. K. Kratzl and G. Billek), Pergmon Press, London, p. 121 (1959)

- 42) A. J. Kerr and D. A. I. Goring, Cellulose Chem. Technol., 9, 563 (1975)
- 43) K. Takabe, M. Fujita, H. Harada and H. Saiki, Mokuzai Gakkaishi, 27, 813 (1981)
- 44) K. Fukushima, Formation and Structure of Lignin, Master Thesis, Nagoya University (1987)
- 45) S. Marcinowski and H. Grisebach, Eur. J. Biochem., 87 37 (1978)
- 46) T. E. Timell, Origin and evolution of compression wood, In: "Compression Wood in Gymnosperms Vol. 1", Springer-Verlag, Berlin, p. 597 (1986)
- 47) K. Takabe, M. Fujita, H. Harada and H. Saiki, Mokuzai Gakkaishi, 31, 613 (1985)
- 48) M. Fujita, H. Saiki and H. Harada, Mokuzai Gakkaishi, 24, 158 (1978)
- 49) M. Fujita and H. Harada, Mokuzai Gakkaishi, 25, 89 (1979)
- 50) C. Lapierre and C. Roland, Holzforschung, 42, 1 (1988)
- 51) T. E. Timell, Holzforschung, 37, 1 (1983)
- 52) T. E. Timell, Wood Sci. Technol. 12, 89 (1978)
- 53) J. Sorvari, E. Sjöström, A. Klemola and J. E. Laine, Wood. Sci. Technol. 20, 35 (1986)
- 54) V. M. Erickson and G. E. Miksche, Holzforschung, 28, 135 (1974)
- 55) J. R. Obst and L. L. Landucci, J. Wood Chem. Technol., 6, 495 (1986)
- 56) W. Hösel, E. Surholt and E. Borgmann, Eur. J. Biochem., 84, 487 (1978)
- 57) U. Westermarck, H. -L. Hardell and T. Iversen, Holzforschung, 40, 65 (1986)
- 58) N. Terashima, I. Mori and T. Kanda, Phytochem., 14, 1991 (1975)

## Acknowledgement

The works dealt in this thesis were carried out under the guidance of Professor N. Terashima during the period from 1984 to 1989 in the Laboratory of Chemistry of Forest Products, Department of Forest Products, Faculty of Agriculture, Nagoya University. The author tenders his cordial and sincere thanks to Professor N. Terashima for his valuable guidance and helpful cooperation throughout this study.

The author is grateful to Associate Professor S. Yasuda, Associate Professor H. Kawakami and Dr. T. Fukuda for their helpful advice and constructive criticism.

The author wants to express his sincere thanks to Associate Professor M. Fujita and Dr. K. Takabe, Faculty of Agriculture, Kyoto University, for technical support in microautoradiography.

The author is also thankful to Mr. S. Kitamura for elemental analysis and to Miss L. He, Mr. Y. Seguchi, Mr. Y. Sano, Mr. I. Henmi, Mr. Y. Uchida, Mrs. M. Kitamura and all members of the Laboratory of Chemistry of Forest Products for their help and cooperation in this study.

## List of Publications Concerning the Thesis

1. Heterogeneity in formation of lignin. VII.  
An autoradiographic study on the formation of guaiacyl and syringyl lignin in poplar.  
N. Terashima, K. Fukushima, S. Tsuchiya and K. Takabe  
J. Wood Chem. Technol., 6, 495-504 (1986)
2. Heterogeneity in formation of lignin. VIII.  
An autoradiographic study on the formation of guaiacyl and syringyl lignin in Magnolia kobus DC.  
N. Terashima, K. Fukushima and K. Takabe  
Holzforschung, 40 Suppl., 101-105 (1986)
3. Heterogeneity in formation of lignin. X.  
Visualization of lignification process in differentiating xylem of pine by microautoradiography.  
N. Terashima, K. Fukushima, Y. Sano and K. Takabe  
Holzforschung, 42, 347-350 (1988)
4. Heterogeneity in formation of lignin. XI.  
An autoradiographic study of the heterogenous formation and structure of pine lignin.  
N. Terashima and K. Fukushima  
Wood Sci. Technol., 22, 259-270 (1988)
5. Biogenesis and structure of macromolecular lignin in the cell wall of tree xylem as studied by microautoradiography.  
N. Terashima and K. Fukushima  
In "Plant Cell Wall Polymers, Biogenesis and Biodegradation" N. G. Lewis and M. G. Paice eds., ACS Symposium Series 399, American Chemical Society, Washington D.C., p.160-168 (1989)
6. Heterogeneity in formation of lignin. XIII.  
Formation and structure of p-hydroxyphenyl lignin in various hardwoods visualized by microautoradiography.  
K. Fukushima and N. Terashima  
J. Wood Chem. Technol., submitted
7. Heterogeneity in formation of lignin. XIV.  
Formation and structure of lignin in differentiating xylem of Ginkgo biloba.  
K. Fukushima and N. Terashima  
Holzforschung, submitted
8. Heterogeneity in formation of lignin. XV.  
Formation and structure of lignin in compression wood of pine studied by microautoradiography.  
K. Fukushima and N. Terashima  
Wood Sci. Technol., submitted